

# Sculpting the Standard Model from low-scale Gauge-Higgs-Matter $E_8$ Grand Unification in ten dimensions

Alfredo Aranda,<sup>1,2,\*</sup> Francisco J. de Anda,<sup>3,2,†</sup>  
António P. Morais,<sup>4,5,6,‡</sup> and Roman Pasechnik<sup>6,§</sup>

<sup>1</sup>*Facultad de Ciencias-CUICBAS, Universidad de Colima,  
C.P.28045, Colima, México 01000, México*

<sup>2</sup>*Dual CP Institute of High Energy Physics, C.P. 28045, Colima, México*

<sup>3</sup>*Tepatlán's Institute for Theoretical Studies, C.P. 47600, Jalisco, México*

<sup>4</sup>*Departamento de Física, Universidade de Aveiro,  
Campus de Santiago, 3810-183 Aveiro, Portugal*

<sup>5</sup>*Centre for Research and Development in Mathematics and Applications (CIDMA),  
Campus de Santiago, 3810-183 Aveiro, Portugal*

<sup>6</sup>*Department of Astronomy and Theoretical Physics,  
Lund University, 221 00 Lund, Sweden*

## Abstract

A model with complete supersymmetric unification of the Standard Model matter content, interactions and families replication into a single  $E_8$  gauge superfield in ten dimensions is presented. The gauge and extended Poincaré symmetries are broken through compactification of the  $\mathbb{T}^6/(\mathbb{Z}_3 \times \mathbb{Z}_3)$  orbifold with Wilson lines, which reduces the original symmetry and matter content into those of the Standard Model. Proton decay is strongly suppressed automatically, while the unification scale is required to be as low as  $10^6 - 10^9$  GeV so that the corresponding physics may be potentially accessible and testable by future collider measurements. Such a low-scale Grand Unification concept yields a highly-constrained and predictive New Physics framework in a minimal and phenomenologically testable and consistent way.

---

\* [fefo@ucol.mx](mailto:fefo@ucol.mx)

† [fran@tepaitis.mx](mailto:fran@tepaitis.mx)

‡ [aapmorais@ua.pt](mailto:aapmorais@ua.pt)

§ [Roman.Pasechnik@thep.lu.se](mailto:Roman.Pasechnik@thep.lu.se)

## INTRODUCTION

The Standard Model (SM) is currently the best theory at disposal to accurately describe three of the four fundamental interactions in nature at the subatomic level. It is based upon modern Quantum Field Theory (QFT) and its predictions have matched some of the most stringent tests [1–7]. Despite its success, there are clear phenomenological indications that the SM is not the ultimate picture, such as neutrinos being massive particles [8], the existence of Dark Matter (DM) [9] or the unexplained structure of the SM fermion families. Furthermore, both its gauge structure, mathematically described by the symmetry  $SU(3)_C \times SU(2)_L \times U(1)_Y$ , as well as its matter content, are purely phenomenologically driven and a consensual first principles explanation for their origin is still lacking. In fact, it is a remarkable theoretical challenge to explain and even eventually to derive the basic properties of the SM from a unified concept at high-energy scales. Typically, Grand Unified Theories (GUTs) feature unification of the SM gauge couplings into a single one by means of embedding the SM symmetries into a larger simple gauge group at a certain high energy-scale, commonly dubbed the GUT scale. In this way, the SM Higgs, matter and gauge fields, denoted by green, blue and pink labels, respectively, in Tab. I, can be a part of larger representations of the GUT symmetry group.

$T^4 \ltimes SO(3,1)$	$SU(3)_C \times SU(2)_L \times U(1)_Y$
(1)	(1, 2, 3)
(2)	$3 \times (1, 2, -3) + 3 \times (1, 1, 6) + 3 \times (\bar{3}, 1, -4) + 3 \times (\bar{3}, 1, 2) + 3 \times (3, 2, 1)$
(4)	$(8, 1, 0) + (1, 3, 0) + (1, 1, 0)$

TABLE I: The SM field content transformation properties under the gauge and Poincaré symmetries. (1), (2) and (4) denote scalars, spin-1/2 Weyl fermions and spin-1 vectors in four dimensions respectively.

Historically, the first and simplest way to achieve such a gauge unification is by utilising the  $SU(5)$  gauge symmetry at the GUT scale [10]. The three gauge interactions are a remnant of a more fundamental one where the SM vector bosons are different components of a single **24** dimensional representation as shown in Tab. II. However, the matter sector is only partially unified where the three fermionic generations belong to three distinct  $\bar{5} + 10$  spin-1/2 copies. The Higgs sector, on the other hand, is enlarged to a spinless  $\bar{5}$  irreducible representation (irrep), bringing along new coloured scalars. It is well known that the latter need to be rather heavy, typically with masses above  $10^{16}$  GeV in order to prevent the proton from rapidly decaying, while the doublet component is required to be at the TeV scale. The need for such a remarkable hierarchy is known as the *doublet-triplet splitting problem* [11] and is recognized as one of the theoretical challenges of minimal four-dimensional  $SU(5)$  GUTs.

Another possibility came with the  $SO(10)$  GUT [12] where, besides gauge field unification, one can also unify all the SM fermions of an entire matter family into a single 16-dimensional  $SO(10)$  representation as shown in Tab. III. Furthermore, the three matter **16**-plets contain a SM-singlet each offering three generations of right-handed neutrinos and the possibility

$T^4 \ltimes SO(3,1)$	$SU(5)$
(1)	( <b>5</b> )
(2)	$3 \times (\bar{\mathbf{5}}) + 3 \times (\mathbf{10})$
(4)	( <b>24</b> )

TABLE II: The SM field content embedded in  $SU(5)$  with transformation properties under the gauge and Poincaré symmetries.

$T^4 \ltimes SO(3,1)$	$SO(10)$
(1)	( <b>10</b> )
(2)	$3 \times (\mathbf{16})$
(4)	( <b>45</b> )

TABLE III: The SM field content embedded in  $SO(10)$  with its transformation properties under the gauge and Poincaré symmetries.

for explaining the observed active neutrino masses via a seesaw mechanism. In this context, the seesaw scale can be attributed to the  $SO(10)$  breaking scale such that the smallness of neutrino masses results from the large hierarchy between the GUT and the electroweak (EW) scales.

A particularly attractive option is the  $E_6$  GUT [13], where matter unification is realized in three copies of the fundamental **27** irrep. However, in its minimal form, the SM Higgs doublet is also part of a scalar **27**-plet suggesting a higher degree of unification if both the fermion and scalar counterparts are related by means of simple  $\mathcal{N} = 1$  supersymmetry (SUSY) transformations [14]. A SUSY  $E_6$  GUT is then the minimal theory featuring Higgs and matter unification in three distinct copies of **27** supermultiplets as summarized in Tab. IV.

$S^1 \ltimes [T^4 \ltimes SO(3,1)]$	$E_6$
$(2 \times \mathbf{1} + \mathbf{2})$	$3 \times (\mathbf{27})$
$(\mathbf{4} + \mathbf{2})$	( <b>78</b> )

TABLE IV: The SM field content embedded in SUSY  $E_6$  with the corresponding transformation properties under the gauge and super-Poincaré symmetries.  $S^1$  denotes simple  $\mathcal{N} = 1$  SUSY.

Note that the unification of matter fields both in  $SO(10)$  and  $E_6$  GUTs is realized independently for each generation without offering any fundamental reason to explain the family replication observed in nature. This can be accomplished at the level of a SUSY  $E_7$  GUT if the entire SM fermion and Higgs sectors are embedded in a single real **912** supermultiplet. The challenge that such a picture poses is on how to obtain chiral matter from a real

representation. While this is not realizable in four space-time dimensions, the presence of orbifolded extra dimensions (EDs) can leave massless chiral sectors in a low-energy SM-like effective field theory (EFT). While this can be achieved with one ED, SUSY representations become simpler in the case of two compact EDs. This enlarges the super-Poincaré symmetry to  $T^6 \ltimes \text{SO}(5, 1)$  with the minimal field content of Tab. V. Such a picture offers a possible

$S^1 \ltimes [T^6 \ltimes \text{SO}(5, 1)] \mid E_7$	
$(2 \times \mathbf{1} + \mathbf{4})$	<b>(912)</b>
$(\mathbf{6} + \mathbf{4})$	<b>(133)</b>

TABLE V: The SM field content embedded in SUSY  $E_7$  with the corresponding transformation properties under the gauge and super-Poincaré symmetries.  $S^1$  denotes simple  $\mathcal{N} = 1$  SUSY.

framework for both gauge unification and Higgs-matter-family unification where the three families can be naturally obtained.

The pattern of enlarging of the GUT symmetry can be seen through the Dynkin diagrams and follows the exceptional chain [15, 16],

$$\text{SU}(3)_C \times \text{SU}(2)_L \times \text{U}(1)_Y \subset \text{SU}(5) \subset \text{SO}(10) \subset E_6 \subset E_7 \subset E_8. \quad (0.1)$$

The largest group in this chain,  $E_8$ , has an unique property that its adjoint representation **248** coincides with its fundamental one [17]. This suggests that all the SM gauge and matter fields can be, in principle, unified into a single **248** representation provided that a maximal  $\mathcal{N} = 4$  SUSY is realised. Furthermore, it also provides an  $\text{SU}(3)$  family symmetry as a coset of  $E_8$  to  $E_6$  reduction [18–20].

There is a plethora of models that aim to build GUTs including family symmetries [18–31] and EDs [32–43]. These models require various independent groups and quite a large number of fields. The  $E_8$  group is a good bet for a complete unification of SM vectors, fermions and scalars, as well as both the gauge and Yukawa interactions, and has indeed been widely studied both in the context of string theory [44, 45] and within the framework of QFT [18, 46–58].

Similarly to  $E_7$ , the main challenge posed by  $E_8$  is that it is a real group – the same as the extended  $\mathcal{N} = 4$  SUSY theory – while the SM requires chiral representations. With orbifolded EDs, the compactification procedure could leave massless chiral sectors in a low-energy SM-like effective field theory (EFT). Furthermore, extended  $\mathcal{N} = 4$  SUSY in four dimensions can be obtained from a  $\mathcal{N} = 1$  SUSY ten-dimensional theory [59, 60]. The orbifolding mechanism provides a natural way to geometrically break a GUT symmetry group and to generate large masses for some or most of the unobserved states. However, a consistent way of getting the correct flavour structure and interactions in a SM-like low-energy EFT from the  $E_8$  GUT, that is compatible with all existing phenomenological constraints, has not yet been developed in the literature.

In this paper, we propose a particular realisation of a GUT based upon the  $E_8$  gauge symmetry and  $\mathcal{N} = 1$  SUSY in ten dimensions where the full SM matter, Higgs and gauge



$S^1 \ltimes [T^{10} \ltimes SO(9,1)]$	$E_8$
$(\mathbf{10} + \mathbf{8})$	$(\mathbf{248})$

TABLE VI: Full unification of the SM field content in a single adjoint **248** supermultiplet composed by a 10d real vector and a 10d Weyl/Majorana fermion.

field content is unified into a single  $E_8$  gauge superfield transforming as in Tab. VI. The  $T^6/(\mathbb{Z}_3 \times \mathbb{Z}_3)$  orbifold compactification breaks SUSY and the original gauge symmetry directly to that of the SM,  $E_8 \rightarrow SU(3)_C \times SU(2)_L \times U(1)_Y$ , leaving only the SM gauge and fermion fields massless. The operators responsible for the proton decay naturally appear to be strongly suppressed alleviating the need for a very strong hierarchy between the ED compactification scale and the EW one. While the Higgs doublets acquire a positive mass at one of the Wilson-line breaking scales, via the Renormalisation Group (RG) evolution, one of the Higgs doublet squared mass terms runs negative at a TeV scale, thus, triggering the EW symmetry breaking radiatively (REWSB).

The high-energy theory only has one arbitrary parameter, the  $E_8$  gauge coupling, while the details of the orbifold compactification procedure considered in this article provide two real and twelve complex additional arbitrary parameters coming from two radii, six complex Wilson-line effective vacuum expectation values (VEVs) and six complex Higgs VEVs. These parameters completely control the properties of the SM-like EFT emergent at low energies and all the related phenomenology at the EW scale and beyond, fully determining it.

The layout of the paper is as follows. In Sec. I the full definition of the  $E_8$  GUT is presented. In Sec. IA, a specific  $T^6/(\mathbb{Z}_3 \times \mathbb{Z}_3)$  orbifold is introduced and its compactification mechanism is studied in detail. In Sec. II, the low-energy EFT Lagrangian is presented, and the fermion and scalar mass spectra is derived. In Sec. III it is shown that the model predicts one of the possible DM candidates – the lightest Kaluza-Klein (KK) mode. In Sec. IV the processes that generate the highly-suppressed proton decay are analyzed. In Sec. V the running of the gauge couplings is presented as well as the relevant phenomenology it entails. Finally, in Sec. VI the main conclusions of this work are presented.

## I. THE TEN-DIMENSIONAL $E_8$ GUT

In this article, the  $\mathcal{N} = 1$  SUSY model of Tab. VI based on an  $E_8$  GUT in ten spacetime dimensions (10d) is introduced. The corresponding spacetime contains six compact EDs factorizable as  $\mathbb{R}^4 \times (T^2)^3$ , with  $T^2$  being a 2-torus, which are denoted by three complex coordinates  $z_i$  in what follows. The non-compact coordinates of the physical four-dimensional (4d) spacetime are then labeled as  $x^\mu \equiv x$ . This GUT is a pure super Yang-Mills (SYM) theory that contains a single 10d vector superfield  $\mathcal{V}_{\mathbf{248}}(x, z_i)$  in the adjoint (which is also the fundamental) representation of  $E_8$ . The 10d  $\mathcal{N} = 1$  SUSY then decomposes into  $\mathcal{N} = 4$  SUSY in 4d spacetime [59, 60] and needs to be broken through the orbifold boundary conditions to a simple  $\mathcal{N} = 1$  SUSY theory. In such a scenario, the single 10d vector superfield  $\mathcal{V}$

decomposes into a 4d vector superfield  $V$ , and a sector with three 4d chiral superfields  $\phi_i$ , one per complex ED, supplemented with an infinite tower of KK states for each of these superfields. A thorough description of the decomposition of the ED Poincaré representations is shown in Appendix A while further details about the procedure of a generic 10d orbifolding is reviewed in Appendix B. The Lagrangian and its decomposition are detailed in Appendix C.

Upon orbifolding, the super-Poincaré group on the first column of Tab. VI becomes incomplete and the full model's symmetry becomes

$$S^1 \ltimes [(T^4 \times T^6/\Gamma) \ltimes (\text{SO}(9,1)/F)] \ltimes E_8, \quad (1.1)$$

where  $S^1$  denotes  $\mathcal{N} = 1$  SUSY, the  $T$  denotes the translation group and  $\text{SO}(9,1)$  – the 10d Lorentz group. The discrete subgroup of ED translations  $\Gamma \simeq \mathbb{Z}^6 \subset T^6$  is called the lattice group<sup>1</sup> and compactifies the EDs, while  $F$  is a discrete subgroup of ED rotations  $F \subset \text{SO}(6)$ , which defines the orbifolding. In this article, the case  $F \simeq \mathbb{Z}_3^F \times \mathbb{Z}_3^C$  is explored for the first time (where the superscripts  $F$  and  $C$  stand for family and colour respectively).

Both the lattice group  $\Gamma$  and the orbifolding group  $F$  transformations are accompanied by a gauge transformation, so that both  $\Gamma, F \subset E_8$ . Therefore, the spacetime symmetry no longer commutes with the gauge one, i.e.

$$\exists \quad \alpha \in \Gamma, \beta \in F, \gamma \in E_8 \quad | \quad [\alpha, \gamma] \neq 0, \quad [\beta, \gamma] \neq 0, \quad (1.2)$$

such that the gauge sector becomes sensitive to geometrical effects leading to its breaking.

In this model the EDs are orbifolded as  $\mathbb{T}^6/(\mathbb{Z}_3^F \times \mathbb{Z}_3^C)$  with

$$\begin{aligned} \mathbb{Z}_3^F : (x, z_1, z_2, z_3) &\sim (x, \omega^2 z_1, \omega^2 z_2, \omega^2 z_3), \quad \mathcal{V} \rightarrow e^{2i\pi q_8^F/3} \mathcal{V}, \\ \mathbb{Z}_3^C : (x, z_1, z_2, z_3) &\sim (x, \omega^3 z_1, \omega z_2, \omega^2 z_3), \quad \mathcal{V} \rightarrow e^{2i\pi q_8^C/3} \mathcal{V}, \end{aligned} \quad (1.3)$$

where  $\omega = e^{2i\pi/3}$  denotes the complex cubic root of unity and  $q_8^{C,F}$  are the Abelian charges under the  $T^8$  generators of  $\text{SU}(3)_{C,F}$  symmetry groups from the decomposition [17]

$$E_8 \supset E_6 \times \text{SU}(3)_F \supset \text{SU}(3)_C \times \text{SU}(3)_L \times \text{SU}(3)_R \times \text{SU}(3)_F, \quad (1.4)$$

respectively. The lattice of the  $\mathbb{T}^6$  tori is defined by the coordinate transformations

$$z_i \sim z_i + \tau_i^r \quad \text{with} \quad \tau_i^1 = 2\pi R_i \quad \text{and} \quad \tau_i^2 = 2\pi e^{i\pi/3} R_i, \quad (1.5)$$

where the  $R_i$  are the radii of the different tori. Note that each torus is built from two circles of equal radii. Each lattice translation is accompanied by a gauge transformation  $U_{i=1,2,3}^r$  which is called a Wilson line

$$\mathcal{V}(x, z_i) = U_i^r \mathcal{V}(x, z_i + \tau_i^r). \quad (1.6)$$

A non-trivial  $U_i^r$  gauge transformation, i.e. a Wilson line, can be seen as an effective VEV in the chiral superfields [61]. For consistency with the orbifolding group, it must be aligned

---

<sup>1</sup> This is a direct product of six times the group of integers

with a representation that has a zero mode in its KK tower. One must note that it is not an usual VEV, as it does not come from the minimization of a potential. Instead, it comes from the ED profiles of the scalar fields and makes the same impact on the theory as an ordinary VEV.

In what follows, a general continuous Wilson line will be associated to  $U_1^r$ , whose gauge transformation is consistent with Eq. (1.3), while those in  $z_{2,3}$  must be trivial and no discrete Wilson lines are assumed (i.e.  $U_{i=2,3}^r = 0$ ). Choosing the three different  $R_i$  and the fifteen arbitrary dimensionless parameters associated to the Wilson line (nine of them are chosen to vanish and six of them are aligned with the three right-handed sneutrinos and three flavons) in  $U_1^r$ , one completely defines the parameter space of the considered GUT. As described in detail in the next section, the model is based on an orbifold and Wilson line breaking mechanism that reduces  $E_8$  directly down to  $SU(3)_C \times SU(2)_L \times U(1)_Y$ , where the EW symmetry can further be broken radiatively.

### A. Orbifolding the EDs with $\mathbb{T}^6/(\mathbb{Z}_3^F \times \mathbb{Z}_3^C)$

The model proposed in this article is built upon the orbifold defined by Eq. (1.3). The first  $\mathbb{Z}_3$ , denoted as  $\mathbb{Z}_3^F$  in Eq. (1.3), breaks  $E_8 \rightarrow E_6 \times SU(3)_F$  while the second one,  $\mathbb{Z}_3^C$ , breaks  $E_8 \rightarrow E_6 \times SU(3)_C$  [62, 63]. Note that the second  $E_6$  group is a flipped one, which is not the standard exceptional GUT symmetry as the color group does not belong to it. By acting together both  $\mathbb{Z}_3^F$  and  $\mathbb{Z}_3^C$ , they effectively break into the intersection  $E_8 \rightarrow (E_6 \times SU(3)_F) \cap (E_6 \times SU(3)_C) = SU(3)_C \times SU(3)_L \times SU(3)_R \times SU(3)_F$ , with labels resembling the symmetries in the low-energy SM-like EFT limit. Although this is the breaking associated to the rotational boundary conditions only, it is useful to use this intersection group as a basis for describing the **248** in terms of the orbifold charges, as presented in Tab. VII.

The lattice of  $\mathbb{T}^6$  is factorized into three tori. Each torus is built from two circles which must have equal radii. Different tori can have different radii defined in Eq. (1.5), where  $R_i$  denotes the three different radii. The ED lattice must be invariant under the orbifold action to be consistent. One can see that the 6d lattice is built from three copies of the 2d lattice generated by the basis  $(1, e^{i\pi/3})$  which is just a normalization of Eq. (1.5). The orbifold action is generated by multiples of  $\omega = e^{2i\pi/3}$  so it acts on the lattice as

$$e^{i2\pi/3}(1, e^{i\pi/3}) = (-e^{i\pi/3}, -1), \quad (1.7)$$

which are just modular transformations (i.e. the transformed basis is just an integer linear combination of the original basis). Therefore the orbifold is consistent.

One of the features of orbifolds is the existence of singular points, which imply boundary conditions responsible for the symmetry breaking. The singular points are the ones invariant under the orbifold, i.e. the solution of the equations

$$\mathcal{Z}^{C,F}(z_i) = z_i, \quad \mathcal{Z}^{C,F}(z_i) = z_i + \tau_i^r, \quad (1.8)$$

where  $\mathcal{Z}^{C,F}$  denotes the action of the orbifold group  $\mathbb{Z}_3^{C,F}$  on the coordinates. It defines the

fixed points, which in this case are

$$\left( x, \left\{ 0, \frac{1 + e^{i\pi/3}}{3}, \frac{2 + 2e^{i\pi/3}}{3} \right\}, \left\{ 0, \frac{1 + e^{i\pi/3}}{3}, \frac{2 + 2e^{i\pi/3}}{3} \right\}, \left\{ 0, \frac{1 + e^{i\pi/3}}{3}, \frac{2 + 2e^{i\pi/3}}{3} \right\} \right). \quad (1.9)$$

A visualization of such an orbifold is shown in Fig. 1, which, for illustration, is focused on a single complex ED  $z_i$ . In (a), the unfolded compactified ED is shown where, to form the torus in (b), one identifies the green dotted lines together and the red dotted lines together, as dictated by Eq. (1.5). Three fixed points from Eq. (1.9) are represented with a blue dot and the coordinates must be multiplied by the corresponding  $R_i$ . The same coloured lines and points correspond to each other throughout all the figures. The folding of a  $\mathbb{Z}_3$  orbifold, dictated by Eq. (1.3) is schematically represented in (c). In particular, such a procedure is as follows:

1. First, one separates the whole space into two equilateral triangles.
2. Each equilateral triangle is then divided into three equal isosceles triangles.
3. Then, the three of them are rotated and identified together resulting in the rightmost of the four pictures in Fig. 1 (c). Note that the dotted lines from (a) and (b) must be identified with the purple one.

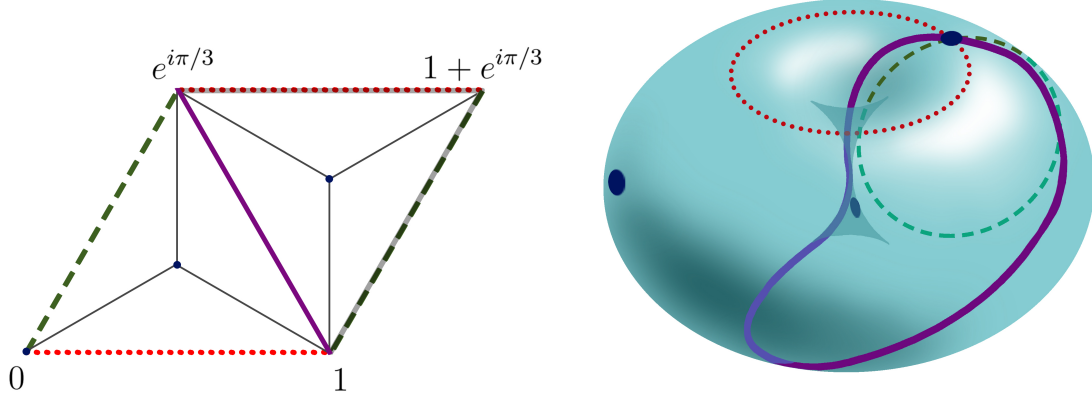
Even though the projective space can not be properly visualized, (d) is merely illustrative, and the  $\mathbb{T}^2/\mathbb{Z}_3$  would appear as it is shown. The three conical singularities correspond to the three fixed points, and the purple line also corresponds to the one in (a) and (b) after identification with the dotted ones is done.

As detailed in Appendix B, each field receives a different phase under the orbifold action depending on its charges defined in Eq. (1.3). The chiral superfields  $\phi_i$  receive an extra phase contribution coming from the one multiplying each  $z_i$ . Each field receives two charges, one for each  $\mathbb{Z}_3$  and the components of  $\mathcal{V}_{248}$  are split into components as shown in Tab. VII. The

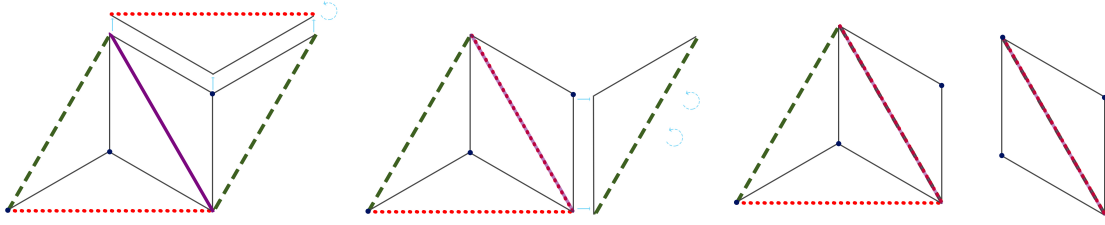
	$V$	$\phi_1$	$\phi_2$	$\phi_3$
$\mathcal{V}_{(8,1,1,1)}$	1, 1	$\omega^2, 1$	$\omega^2, \omega$	$\omega^2, \omega^2$
$\mathcal{V}_{(1,8,1,1)}$	1, 1	$\omega^2, 1$	$\omega^2, \omega$	$\omega^2, \omega^2$
$\mathcal{V}_{(1,1,8,1)}$	1, 1	$\omega^2, 1$	$\omega^2, \omega$	$\omega^2, \omega^2$
$\mathcal{V}_{(1,1,1,8)}$	1, 1	$\omega^2, 1$	$\omega^2, \omega$	$\omega^2, \omega^2$
$\mathcal{V}_{(\bar{3},3,3,1)}$	1, $\omega^2$	$\omega^2, \omega^2$	$\omega^2, 1$	$\omega^2, \omega$
$\mathcal{V}_{(3,\bar{3},\bar{3},1)}$	1, $\omega$	$\omega^2, \omega$	$\omega^2, \omega^2$	$\omega^2, 1$

	$V$	$\phi_1$	$\phi_2$	$\phi_3$
$\mathcal{V}_{(1,\bar{3},3,3)}$	$\omega, 1$	1, 1	1, $\omega$	1, $\omega^2$
$\mathcal{V}_{(3,3,1,3)}$	$\omega, \omega$	1, $\omega$	1, $\omega^2$	1, 1
$\mathcal{V}_{(\bar{3},1,\bar{3},3)}$	$\omega, \omega^2$	1, $\omega^2$	1, 1	1, $\omega$
$\mathcal{V}_{(1,3,\bar{3},\bar{3})}$	$\omega^2, 1$	$\omega, 1$	$\omega, \omega$	$\omega, \omega^2$
$\mathcal{V}_{(\bar{3},\bar{3},1,\bar{3})}$	$\omega^2, \omega^2$	$\omega, \omega^2$	$\omega, 1$	$\omega, \omega$
$\mathcal{V}_{(3,1,3,\bar{3})}$	$\omega^2, \omega$	$\omega, \omega$	$\omega, \omega^2$	$\omega, 1$

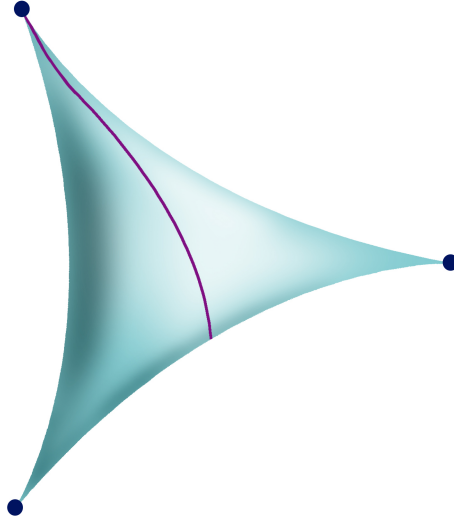
TABLE VII: Charges of each  $\mathcal{N} = 1$  superfield being  $\text{SU}(3)_C \times \text{SU}(3)_L \times \text{SU}(3)_R \times \text{SU}(3)_F$  multiplet under a  $\mathbb{Z}_3^F \times \mathbb{Z}_3^C$  orbifolding. Only the fields with both charges equal to unity have zero modes. The representations are color coded as **adjoint fields**, **Higgs and leptons**, **quarks**, **mirror Higgs and mirror fermions**, **mirror quarks**, and **family-neutral exotics**.



(a) The unfolded compactified ED space of a single coordinate  $z_i$ . (b)  $\mathbb{T}^2$  torus visualization. Colours are as in (a).



(c) Folding the orbifold.



(d) Illustrative visualization of the orbifold.

FIG. 1: Visualization of a single  $\mathbb{T}^2/\mathbb{Z}_3$  orbifold. The actual  $\mathbb{T}^6/(\mathbb{Z}_3^F \times \mathbb{Z}_3^C)$  orbifold employed in this work consists of the direct product of three copies of this orbifold.

zero massless modes containing the SM particle spectrum coming from the purely rotational boundary conditions (i.e. the ones with charge (1, 1)), for each chiral multiplet, are then

$$\begin{aligned}
V_\mu &: (\mathbf{8}, \mathbf{1}, \mathbf{1}, \mathbf{1}) + (\mathbf{1}, \mathbf{8}, \mathbf{1}, \mathbf{1}) + (\mathbf{1}, \mathbf{1}, \mathbf{8}, \mathbf{1}) + (\mathbf{1}, \mathbf{1}, \mathbf{1}, \mathbf{8}), \\
\phi_1 &: (\mathbf{1}, \bar{\mathbf{3}}, \mathbf{3}, \mathbf{3}), \\
\phi_2 &: (\bar{\mathbf{3}}, \mathbf{1}, \bar{\mathbf{3}}, \mathbf{3}), \\
\phi_3 &: (\mathbf{3}, \mathbf{3}, \mathbf{1}, \mathbf{3}).
\end{aligned} \tag{1.10}$$

So far, one has only considered the rotational boundary conditions while additional mass-splitting effects emerging from the Wilson-line effective VEVs must also be included. It is very important to note that the spectrum in Eq. (1.10) does not correspond to the massless field content of the theory at any point. It is shown here because it helps visualize the way in which the symmetry is being broken by the rotational boundary conditions. The *complete* breaking, which is happening simultaneously, does indeed involve the translation boundary conditions in the form of Wilson lines.

For ease of notation, in the remainder of this article, the representations in Eq. (1.10) are named as

$$V_\mu : \Delta_C + \Delta_L + \Delta_R + \Delta_F, \quad \phi_1 : \mathbf{L}, \quad \phi_2 : \mathbf{Q}_R, \quad \phi_3 : \mathbf{Q}_L. \tag{1.11}$$

Expressing the chiral superfields in terms of their gauge indices, where upper indices correspond to an antitriplet representation of SU(3) while down indices stand for a triplet one, one can further split them in terms of their components as

$$\begin{aligned}
\mathbf{L}^i_{jk} : \quad & \mathbf{L}^1_{1k} = H^0_{dk}, \quad \mathbf{L}^1_{2k} = H^-_{uk}, \quad \mathbf{L}^1_{3k} = \nu_k, \\
& \mathbf{L}^2_{1k} = H^+_{dk}, \quad \mathbf{L}^2_{2k} = H^0_{uk}, \quad \mathbf{L}^2_{3k} = e_k, \\
& \mathbf{L}^3_{1k} = \nu^c_k, \quad \mathbf{L}^3_{2k} = e^c_k, \quad \mathbf{L}^3_{3k} = \varphi_k, \\
\mathbf{Q}_R^i{}_j : \quad & \mathbf{Q}_R^1{}_j = d^c_j, \quad \mathbf{Q}_R^2{}_j = u^c_j, \quad \mathbf{Q}_R^3{}_j = D^c_j, \\
\mathbf{Q}_L^i{}_j : \quad & \mathbf{Q}_L^1{}_j = d_j, \quad \mathbf{Q}_L^2{}_j = u_j, \quad \mathbf{Q}_L^3{}_j = D_j,
\end{aligned} \tag{1.12}$$

where the color indices are not shown and the family ones are not expanded. To complete the notation, the complex conjugated chiral superfield representations are named  $\bar{\mathbf{L}}, \bar{\mathbf{Q}}_R, \bar{\mathbf{Q}}_L$ , while the remaining superfields transforming as  $(\bar{\mathbf{3}}, \mathbf{3}, \mathbf{3}, \mathbf{1})$  and  $(\mathbf{3}, \bar{\mathbf{3}}, \bar{\mathbf{3}}, \mathbf{1})$  are denoted as  $\mathbf{X}$  and  $\bar{\mathbf{X}}$ , respectively. The representations are color coded as **adjoint fields**, **Higgs**, **SM fermions**, **mirror Higgs**, **mirror fermions**, **right handed neutrinos**, **flavons**, and **family-neutral exotics**.

As stated before in Eq. (1.6), there are three Wilson lines  $U_i^r \equiv U_i$ , where both real degrees of freedom  $r = 1, 2$  form a complex one. They correspond to a gauge transformation which must comply with the consistency conditions coming from the Poincaré algebra

$$[U_i, U_j] = 0, \quad [U_i, U_i^F] = 0, \quad [U_i, U_i^C] = 0, \tag{1.13}$$

where  $U_i^{C,F}$  denote the gauge transformation that accompanies the orbifold action of  $\mathbb{Z}_3^{C,F}$  on a chiral superfield

$$\mathcal{Z}^{C,F}[\phi_i(x, z)] = U_i^{C,F} \phi_i(x, \mathcal{Z}^{C,F}[z]). \tag{1.14}$$

There are two distinct ways to solve the last two constraints in Eq. (1.13). The first one is by requiring

$$U_i^3 = 1, \quad (1.15)$$

which corresponds to the case of discrete Wilson lines, resulting in additional boundary conditions on the fixed points. For instance, before one considers the effect of such discrete Wilson lines, one has at the zero brane the  $U_i^{C,F}$  gauge transformation as a boundary condition in Eq. (1.8), while at the  $(1 + e^{i\pi/3})/3$  brane they read as  $U_i U_i^{C,F}$  and finally, at the  $2(1 + e^{i\pi/3})/3$  brane, one has  $U_i^2 U_i^{C,F}$ . Any other boundary condition would result in an incomplete SM field content as it would leave without zero modes a whole column, row or family from Eq. (1.12). This means that, in the considered GUT, a phenomenologically viable low-scale spectrum is not compatible with the presence of discrete Wilson lines.

The second possibility is to restrict the Wilson lines to representations where the orbifold action is trivial, i.e. zero modes. One can choose a continuous Wilson line which generates an effective VEV in the three  $\phi_{1,2,3}$  zero modes. However, due to the invariance under the translations defined in Eq. (1.5), from where the effective VEVs result, they have to commute with each other, complying with the first constraint of Eq. (1.13). The restrictions on the effective VEVs come from the  $E_8$  commutation relations in Eq. (D1) given in Appendix D, which in this case read as

$$\begin{aligned} [\langle \mathbf{L}_{jk}^i \rangle, \langle \mathbf{Q}_{Lab\ c} \rangle] &= \delta_b^i \epsilon_{kcd} \langle \overline{\mathbf{Q}}_{Ra\ j}^d \rangle, \\ [\langle \mathbf{L}_{jk}^i \rangle, \langle \mathbf{Q}_R^{a\ b\ c} \rangle] &= \delta_j^b \epsilon_{kcd} \langle \overline{\mathbf{Q}}_L^{ai\ d} \rangle, \\ [\langle \mathbf{Q}_{Lij\ k} \rangle, \langle \mathbf{Q}_R^{a\ b\ c} \rangle] &= \delta_i^a \epsilon_{kcd} \langle \overline{\mathbf{L}}_j^{bd} \rangle. \end{aligned} \quad (1.16)$$

There are three possible non-trivial commuting solutions. The first solution is for the effective VEV alignment of every triplet to be orthogonal to every antitriplet, for all C, L, R. Since there are three distinct effective VEVs, this either gives a VEV in every direction entirely breaking all gauge generators, or requires a specific alignment along which some of them vanish. The focus of the discussion in this article is based on this latter option. Another possibility is to consider a general VEV in all  $\phi_{1,2,3}$  components but requiring that every such VEV is aligned in their family structure. However, this would preserve an anomalous  $SU(2)_F \times U(1)_F$  family symmetry and is no longer considered. The chosen possibility in the present GUT formulation is then to have a general effective VEV in one chiral multiplet, that without any loss of generality is chosen to be  $\phi_1$ , and zero effective VEVs in the other ones  $\phi_{2,3}$ . Note that such a choice always preserves one  $SU(3)$  which is then identified with the SM colour group.

A general Wilson line has 27 complex components. Some of them can be rotated away by  $SU(3)_{L,R,F}$  transformations. There are 24 possible rotations, leaving 30 real parameters (or 15 complex ones). The effective VEVs can then be written as fifteen different  $yR_1$ , where  $y$  has a complex value that is specified inside the area defined in Fig. 1a and each is in a different alignment inside  $\langle \mathbf{L} \rangle$ . These effective VEVs, in general, will break the remaining symmetry. However, it will be assumed that nine of these parameters vanish, preserving a remnant  $SU(2)_L \times U(1)_Y$  symmetry. In turn, this leaves only six complex effective VEVs aligned with what we shall denote the right handed sneutrino  $\langle \tilde{\nu}^c \rangle$  and flavon  $\langle \varphi \rangle$  VEVs,



which are naturally at the scale  $\sim 1/R_1$ . The Higgs states are assumed to obtain a VEV radiatively, generating a much smaller scale and breaking the EW symmetry of the SM but preserving the  $U(1)_{\text{e.m.}}$  of electromagnetism, with the corresponding charge,

$$Q_{\text{EM}} = \frac{1}{6}[\sqrt{3}T_8^L + \sqrt{3}T_8^R - 3T_3^L - T_3^R]. \quad (1.17)$$

The chosen Wilson line configuration breaks the gauge quartification symmetry down to that of the SM, i.e.

$$SU(3)_C \times SU(3)_L \times SU(3)_R \times SU(3)_F \rightarrow SU(3)_C \times SU(2)_L \times U(1)_Y, \quad (1.18)$$

leaving in the low-energy SM-like EFT the following massless fields only:

$$\begin{aligned} V_\mu &: (\mathbf{8}, \mathbf{1}, 0) + (\mathbf{1}, \mathbf{3}, 0) + (\mathbf{1}, \mathbf{1}, 0), \\ \phi_1 &: 3 \times (\mathbf{1}, \mathbf{2}, -3) + 3 \times (\mathbf{1}, \mathbf{1}, 6) + 3 \times (\mathbf{1}, \mathbf{2}, 3) + 3 \times (\mathbf{1}, \mathbf{2}, -3) + 3 \times (\mathbf{1}, \mathbf{1}, 0) + 3 \times (\mathbf{1}, \mathbf{1}, 0), \\ \phi_2 &: 3 \times (\mathbf{\bar{3}}, \mathbf{1}, -4) + 3 \times (\mathbf{\bar{3}}, \mathbf{1}, 2) + 3 \times (\mathbf{\bar{3}}, \mathbf{1}, 2), \\ \phi_3 &: 3 \times (\mathbf{3}, \mathbf{2}, 1) + 3 \times (\mathbf{3}, \mathbf{1}, -2), \end{aligned} \quad (1.19)$$

which in what follows are respectively denoted as

$$\begin{aligned} V_\mu &: G_\mu + W_\mu + B_\mu, \\ \phi_1 &: L_i + e_i^c + h_{ui} + h_{di} + \varphi_i + \nu_i^c, \\ \phi_2 &: u_i^c + d_i^c + D_i^c, \\ \phi_3 &: Q_i + D_i, \end{aligned} \quad (1.20)$$

with  $i = 1, 2, 3$ . These are the massless superfields resulting from the compactification procedure, containing the SM fermions and gauge bosons, as well as three-right handed neutrinos  $\nu_i^c$ , six Higgs doublets  $h_{ui}, h_{di}$ , three flavons  $\varphi_i$ , three vector-like color triplet pairs  $D_i^c, D_i$ , and the associated superpartners. Such a field content will be further split as a result of the Wilson line effective VEVs, leaving solely the SM fermions, color coded in blue, and gauge bosons, color coded in magenta, as the only massless states in the theory at low energies (i.e. below the Wilson-line breaking scale).

## B. Gauge anomaly cancellation

The original theory is based on the  $E_8$  gauge group with matter contained in a single adjoint representation – the only 10d Weyl/Majorana fermion lies in this real representation – thus, at the fundamental level, the model is free from gauge anomalies. As mentioned above, the 10d superfield decomposes into an infinite tower of KK modes of 4d superfields and each **248** representation is broken into nine different sets, one for each of the possible orbifold charges in Tab. VII. One can then expand the chiral superfields as

$$\phi_i(x, z_i) = \sum_{s=0}^{\infty} \sum_{a,b=0,1,2} \phi_i^{sab}(x) f(z_j)_{sab}. \quad (1.21)$$



with  $s$  denoting the KK level (coming from a schematic Fourier-like decomposition of the 6d) while  $a, b = 0, 1, 2$  (coming from the splitting of each  $\mathbb{Z}_3^{C,F}$  orbifolding. Since there is a full **248** for each value of  $s$  the anomalies cancel in each set.

Below the compactification scale, the gauge group is simultaneously broken by the rotation and translation boundary conditions. They break  $E_8 \rightarrow SU(3)_C \times SU(2)_L \times U(1)_Y$  with the massless field content shown in Eq. (1.19) comprising the SM fields with additional SM singlets and vector-like fermions. Therefore, the massless sector of the theory is also anomaly free [64].

One must remark that the Wilson lines behave like effective VEVs but they are not related to spontaneous symmetry breaking. They come from boundary conditions on translations, just as the orbifolding comes from boundary conditions on rotations. As alluded to above, both rotation and translation boundary conditions simultaneously induce the breaking and thus, when studying the low-energy EFT, both of their mass contributions must be integrated out altogether. Therefore, even though the model is built in terms of the fields listed in Eq. (1.11), there is no point in the theory when this spectrum appears as entirely massless, and therefore no anomalies are present at any stage.

As this model is set in an orbifold, which is not a continuous spacetime, one must pay special attention to the discontinuous points. This orbifold has 27 fixed ED points listed in Eq. (1.9). At these ED points, which are 4d branes, the boundary conditions force some of the 4d fields to vanish (i.e. their ED profiles are zero at all the fixed points), so that they do not have the full  $E_8$  symmetry nor the full  $E_8$  representation. Their symmetry, which is defined in a 4d spacetime, can only be studied in a fixed specific gauge where the Wilson line behaves like an effective VEV as they are disconnected in EDs. In this gauge all fields are periodic in the compact dimensions as described in Eq. (B6). In any other gauge the fields are discontinuous multiple-valued functions, and their study requires techniques beyond the standard complex analysis. The gauge symmetry in these points is  $SU(3)_C \times SU(2)_L \times U(1)_Y$  with the massless field content specified in Eq. (1.19), with no extra gauge freedom. Therefore, there are no anomalies generated in the fixed points either [65]. The considered GUT has no localized fields, therefore there are no extra contributions to the anomaly rendering the model anomaly free at all steps without the need for any additional fields.

### C. Differences from string theory

The fact that this model is built in 10d with SUSY and has  $E_8$  as a gauge group may bring string theory (ST) to mind. However, some of the concepts discussed in this work would not be compatible with a ST but still comprise a phenomenologically viable QFT framework. This section describes the key differences between the current model and a ST based one.

In superstring theory the spacetime dimension is fixed, since only in 10d the conformal anomaly of the worldsheet is canceled. In the model presented in this article, 10d is chosen since  $\mathcal{N} = 1$  SUSY can be decomposed into  $\mathcal{N} = 4$  SUSY in 4d allowing a full (gauge-matter) unification of the SM. Even though this also happens in 7d, 8d and 9d theories [59], only 10d allows to obtain the complete SM matter sectors in the required gauge representations

and with the observed family structure. Note that it is also possible to consider more than ten dimensions at the cost of loosing minimality.

In ST, the existence of a graviton lies at the core of its motivation. For instance, in the heterotic string theory case, the gauge group  $E_8 \times E'_8$  plays a key role in the cancellation of anomalies in supergravity<sup>2</sup>. For the GUT proposed in this article, a single  $E_8$  is chosen since it unifies all the representations of the SM into a single one, while gravity lies beyond the scope of the current analysis.

As discussed in the previous section, the considered model is free from gauge anomalies which would not be the case in a ST based framework. First, the decomposition in Eq. (1.21) would be incomplete in ST due to the presence of winding modes around each of the circles of each of the torus. Thus, since they do not add up to a complete **248** irrep, this typically leads to emergence of gauge anomalies. ST also contains twisted states which are inherently localized at the fixed branes and equally lie in incomplete  $E_8$  representations, also contributing to the gauge anomaly problem. Furthermore, there can be strings localized in a brane or connecting two of them. These would only “feel” a fraction of the Wilson line, or none at all, while the ST must be kept anomaly free for all values of the continuous Wilson line [66]. In QFT with only bulk states the continuous Wilson lines do alleviate the gauge anomaly problem [65]. So, the gauge anomaly cancellation is a particularly important feature of this model as it is a QFT with no localized fields, which would not be possible in ST. Notice also that gravity lies at the core of any ST-based framework and the gravitational anomaly cancellation between the gravitino, dilatino and gauginos defines the gauge group. However, there is no known consistent QFT of gravity at present.

The model presented in this work has a Lorentz anomaly since there is a single 10d chiral – left by definition – fermion in the **248**  $E_8$  representation<sup>3</sup>. Since it is a global symmetry, that is not viewed as a problem as the 10d Lorentz symmetry is broken by the orbifold compactification anyway. However, it would be a problem if one includes gravity. In this case, gravity would be added by upgrading the global Poincaré symmetry to a local one, which is equivalent to full coordinate invariance, i.e. General Relativity. The simplest, but not unique, way to cancel the anomaly realised in ST is to add an extra  $E'_8$  **248** 10d right chiral supermultiplet or 248  $E_8$  singlets. If SUSY becomes local then there is also a spin-3/2 10d chiral gravitino. The minimal way to cancel the anomaly is to add 247 singlet 10d left chiral superfields, although it is a more symmetric approach to add a single 10d right chiral superfield  $E_8$  singlet, usually called dilaton, and an  $E_8$  **248** 10d left chiral supermultiplet [67]. As in ST an adjoint chiral multiplet can not be added by itself, one must add a second gauge symmetry  $E'_8$ .

Finally, it is worth mentioning that if one sticks to a QFT approach as realised in this work, gravity can in principle be an emergent phenomenon instead of treating it as a fundamental one as in the ST-based framework [68–70]. In this case, the 10d super-Poincaré symmetry stays global and its anomaly would not be a problem, while it is broken by the orbifold compactification anyway. If an emergent local symmetry arises after compactification one would end up with an effective 4d theory of gravity. As the field content in this model will neither generate any 4d super-Poincaré nor mixed anomalies, no extra field content would

<sup>2</sup>  $SO(32)$  also solves this problem but is not considered to be a preferred option.

<sup>3</sup> Note that 10d chirality is not the same as 4d chirality, as discussed in Appendix A.

be required in that case. However, none of the proposed QFT models of gravity are deemed to be fully consistent and each setup requires different constraints. The current work is thus free of gravity, although extra work would be needed to include it and will be done elsewhere.

## II. EFFECTIVE LAGRANGIAN

In order to study phenomenological implications of the considered GUT, the next step is to build the EFT Lagrangian from the fields given in Eq. (1.10) that are relevant below the compactification scale. They must respect the quartification symmetry  $SU(3)_C \times SU(3)_L \times SU(3)_R \times SU(3)_F$  that can only be broken through the effective, Wilson line, VEVs in  $\langle \mathbf{L} \rangle \sim \langle \varphi_i \rangle, \langle \nu_i^c \rangle$ . Furthermore, the higher-order operators are mediated by heavy KK modes. In Appendix C, the basic steps to obtain an effective Lagrangian from a general superpotential like the one that emerges in the considered GUT are described. The general superpotentials of the GUT under discussion are obtained in Appendix E. From Eq. (C6), the low-energy EFT Lagrangian is then defined in terms of the potentials  $\mathcal{K}, \mathcal{W}$  and  $\mathcal{H}$ .

At leading order, the gauge field strength superpotential  $\mathcal{H}$  takes the standard form (i.e.  $\mathcal{H}_A^B W^A W_B = W^A W_A$ ), the Kähler potential  $\mathcal{K}$  is also the standard one and, in addition, there is also a single superpotential term

$$\begin{aligned} \mathcal{W} &= y_1 \phi_1 \phi_2 \phi_3 = y_1 \epsilon^{ijk} \mathbf{L}_{mi}^l \mathbf{Q}_{Rj}^m \mathbf{Q}_{Llk} \\ &= y_1 \epsilon^{ijk} \left( h_{ui} u_j^c Q_k + h_{di} d_j^c Q_k \right. \\ &\quad \left. + [\varphi_i + \langle \varphi_i \rangle] D_j^c D_k + [\nu_i^c + \langle \nu_i^c \rangle] d_j^c D_k \right. \\ &\quad \left. + e_i^c u_j^c D_k + L_i Q_j D_k^c \right), \end{aligned} \quad (2.1)$$

where the second line gives the quark Yukawa terms, the third line provides masses to the vector-like triplets (through  $\langle \varphi \rangle$ ) and generates a  $d^c$ - $D^c$  mixing through  $\langle \nu^c \rangle$ , and finally the fourth line contains quark couplings to the triplets. The dimensionless coupling  $y_1$  absorbs the gauge coupling of the  $E_8$  theory evolved to the appropriate energy-scale and the corresponding Clebsch-Gordan coefficients (CGC).

It is interesting to note that, at leading order, there are quark Yukawa couplings but neither leptonic ones nor any  $\mu$  term is allowed in the theory. While the latter are forbidden by gauge invariance, the former result from a  $\sim \mathbf{L}^3$  term that vanishes due to antisymmetry of every  $SU(3)$  involved. These must be generated by integrating out heavy KK modes i.e. via higher-dimensional operators. There can be extra terms for the superpotential that emerge by integrating out the heavy modes at tree level, however, there is no tree-level diagram that could generate a  $\sim \mathbf{L}^3$  term. Loop diagrams generate these terms, but due to the SUSY nonrenormalization theorem they can only contribute to the Kähler potential.

Fermion masses are generated from SUSY breaking effects in the Kähler potential as can be seen in Appendix C. This takes place already at leading order via the  $\mathcal{D}$ -term

$$\langle \mathcal{D}_A \rangle = \sum_{ij} \langle \nu_i^c \rangle^\dagger t_A \langle \nu_j^c \rangle + \langle \varphi_i \rangle^\dagger t_A \langle \varphi_j \rangle + \langle \varphi_i \rangle^\dagger t_A \langle \nu_j^c \rangle + \langle \nu_i^c \rangle^\dagger t_A \langle \varphi_j \rangle \neq 0, \quad (2.2)$$

at the scale of the effective Wilson-line VEVs. At one-loop level, the leading-order term in the Kähler potential comes from the diagram shown in Fig. 2, which generates Majorana masses for right-handed neutrinos and flavons.

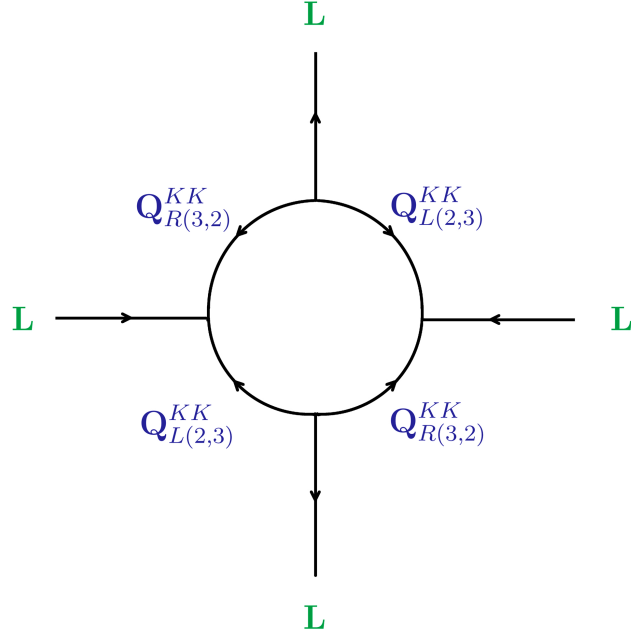


FIG. 2: A leading-order one-loop diagram for the Majorana-mass Kähler term. The mediators are KK modes from the  $(i)$ th chiral field. This generates an effective term  $\mathbf{L}^\dagger \mathbf{L} \mathbf{L}^\dagger$ . Higher powers are then found by adding extra pairs of external legs, accordingly.

The lepton Yukawa terms are zero at tree level since they involve the same triplet multiplied (cubed) in an antisymmetric way. In order to find nonvanishing terms one must contract three different triplets antisymmetrically. One can build an effectively different triplet by multiplying it with an adjoint effective VEV  $\Delta_{\mathbf{L},\mathbf{R},\mathbf{F}} \sim \mathbf{8}$  using  $\mathbf{3} \times \mathbf{8} \rightarrow \mathbf{3}$ . There are no adjoint scalars as zero modes in this model but those can be effectively provided by composite operators constructed from the triplet fields as follows

$$\mathbf{8}^i_j = \bar{\mathbf{3}}^i \mathbf{3}_j - \delta_j^i \bar{\mathbf{3}}^k \mathbf{3}_k / 3, \quad (2.3)$$

which then enter the diagram shown in Fig. 3. The leading-order term that generates the lepton Yukawa couplings is shown in Fig. 4. One can also build tree-level diagrams involving gauge superfields that would contribute to the superpotential as shown in Fig. 5.

### A. Effective low-energy Lagrangian

In order to obtain the SM-like EFT Lagrangian, one does not need to consider the full Lagrangian of the GUT since not every term of the latter is relevant at low energy scales. In

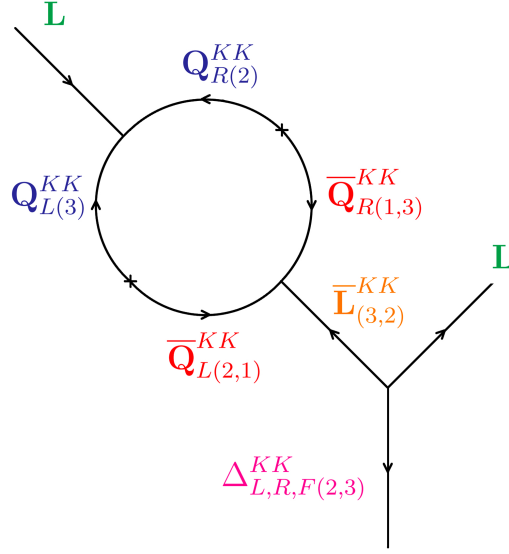


FIG. 3: The leading-order diagram for the effective adjoint VEV  $\Delta_{L,R,F} = \mathbf{L}^\dagger \mathbf{L}$ . There are two possible KK modes here that come from different chiral fields  $\phi_i$ .

fact, the part of the superpotential that is relevant at low energies is obtained by truncating the higher-order terms and yielding,

$$\mathcal{W}' = y_1 \epsilon^{ijk} \mathbf{L}_{mi}^l \mathbf{Q}_{Rj}^m \mathbf{Q}_{Llk} + \text{h.c.}, \quad (2.4)$$

where only the second and third generation quarks as well as the vector-like triplets obtain their masses through the superpotential. However, their mass matrix is completely anti-symmetric and can neither generate the observed flavour structure nor the fermion mass spectra that would fit the SM. The correct physical mass spectra and the flavour mixing structure of light fermions are then obtained after SUSY breaking effects take place. Upon compactification of the EDs the Wilson lines behave as effective VEVs in  $\mathbf{L}$ . In turn, one sees from Eq. (C13) in Appendix C that such effective VEVs cannot generate  $\mathcal{F}$ -term SUSY breaking, but rather, they do induce  $\mathcal{D}$ -term SUSY breaking already at the leading order. It then follows that, using Eq. (C11), fermion masses are obtained through the terms

$$-\frac{1}{2} \left\langle \frac{\partial^2 \mathcal{W}}{\partial \phi_i \partial \phi_j} \right\rangle_S \bar{\psi}_i \psi_{Lj} - i\sqrt{2} \left\langle \frac{\partial^2 \mathcal{K}}{\partial \phi_i^\dagger \partial \phi_j} \right\rangle_S S_i^\dagger t_A \bar{\psi}_j \lambda_{AL} + \frac{i}{2\sqrt{2}} \left\langle \frac{\partial \mathcal{H}_{AB}}{\partial \phi_i} \right\rangle_S \mathcal{D}_A \bar{\lambda}_B \psi_{Li}, \quad (2.5)$$

where the first one encodes the usual SUSY preserving fermion mass term coming from the superpotential, the second term is the usual SUSY preserving mass term for gauginos whereas the last one contains the new  $\mathcal{D}$ -term SUSY breaking effects. In the remainder of this section we use a notation expressed in terms of usual fields, rather than superfields, charged under the SM gauge symmetry. Following the standard notation adopted in the

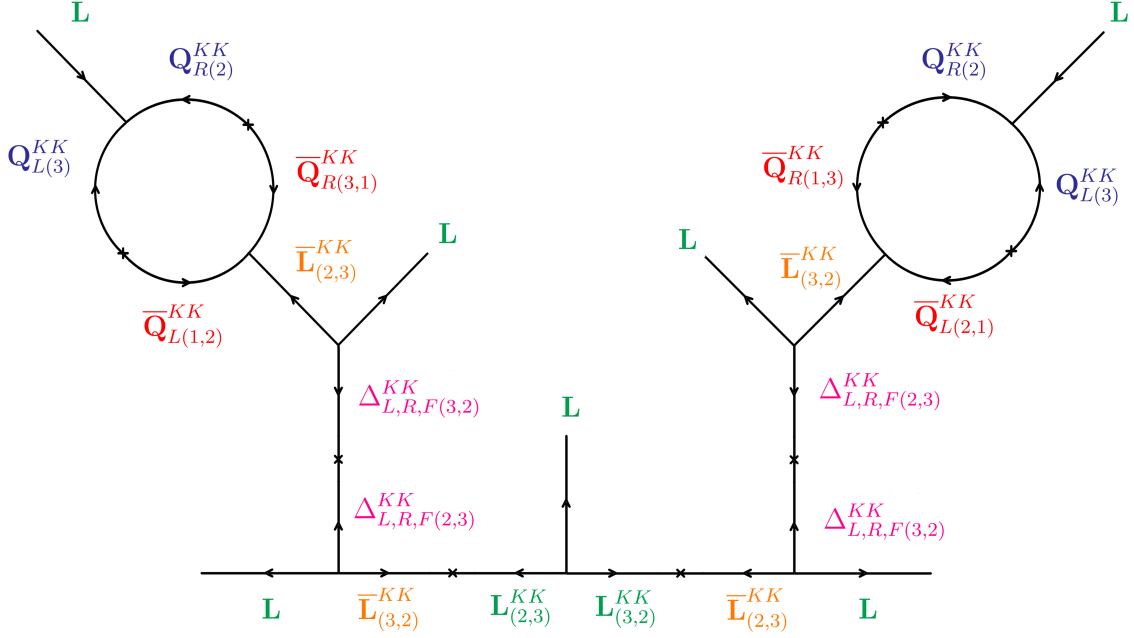


FIG. 4: The leading-order diagram for the effective lepton Yukawa couplings. As this is a loop diagram, it does not contribute to the superpotential, but to the Kähler potential. Note that this diagram must have different  $\Delta_{L,R,F}$  in each connection so that it does not vanish due to antisymmetry.

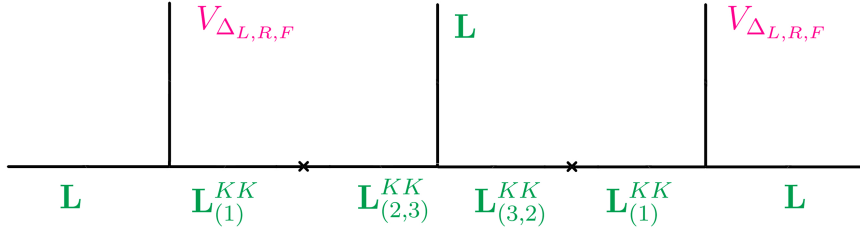


FIG. 5: The leading-order diagram for the effective lepton to gauge field couplings. As this is a tree-level diagram, it contributes to the superpotential through the  $\mathcal{H}$  function.

literature, the  $Q, L, u^c, d^c, \nu^c, D, D^c$  are defined to be fermions, with their scalar partners having an extra tilde  $\sim$  above their label. The  $H_{u,d}, \varphi$  are defined to be scalars and their fermion partners are denoted by an extra tilde  $\sim$  above their label.

### 1. Chiral fermions

The last term in Eq. (2.5) generates corrections to the fermion mass spectra through the one-loop diagrams shown in Fig. 6. The quark masses receive a correction proportional to  $\langle \mathcal{D} \rangle$  (left panel) while the leptons receive  $\langle \mathcal{D}^2 \rangle$  corrections proportional to two different effective adjoint VEVs (right panel) as contributions containing only one of such VEVs would vanish due to antisymmetry.

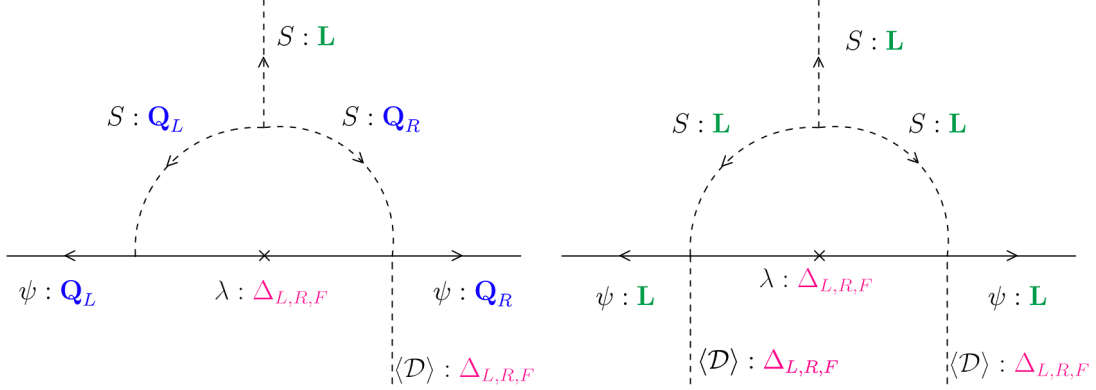


FIG. 6: The one-loop diagrams providing SUSY-breaking contributions to the light fermion masses i.e. built in terms of usual fields, not superfields. Here,  $\psi$  and  $S$  denote the fermion and scalar components of the corresponding superfields,  $\lambda$  is the gaugino and  $\langle \mathcal{D} \rangle$  is the adjoint VEV. In the left panel, the single adjoint VEV  $\langle \mathcal{D} \rangle$  in the quark diagram can also connect to the other vertex. In the right panel, the lepton diagram vanishes with a single  $\langle \mathcal{D} \rangle$  due to antisymmetry, so both adjoint VEVs are needed.

In order to simplify the corresponding expressions, one defines the shorthand notations

$$\begin{aligned} (\mathbf{w}^2)^i_j &\equiv \langle \tilde{\nu}^{c\dagger i} \tilde{\nu}_j^c \rangle + \langle \varphi^{\dagger i} \varphi_j \rangle, \\ \mathbf{w}^2 &\equiv (\mathbf{w}^2)^i_i. \end{aligned} \quad (2.6)$$

The mass terms for quarks and their vector-like counterparts then read as

$$\begin{aligned} \mathcal{L}_{mq} = & \epsilon^{ijk} \left\{ u_a^c Q_b \langle H_{ui} \rangle \left[ y_q \delta_j^a \delta_k^b + \frac{y_{Fq}}{\Lambda^2} ((\mathbf{w}^2)^a_j \delta_k^b - (\mathbf{w}^2)^b_k \delta_j^a) \right] \right. \\ & + d_a^c Q_b \langle H_{di} \rangle \left[ \left( y_q + \frac{y_{Rq} \langle \tilde{\nu}^{c\dagger s} \tilde{\nu}_s^c \rangle}{\Lambda^2} \right) \delta_j^a \delta_k^b + \frac{y_{Fq}}{\Lambda^2} ((\mathbf{w}^2)^a_j \delta_k^b - (\mathbf{w}^2)^b_k \delta_j^a) \right] \\ & + D_a^c D_b \left[ \langle \varphi_i \rangle \left( y_q + \frac{y_{Lq} \mathbf{w}^2}{\Lambda^2} + \frac{y_{Rq} \langle \varphi^{\dagger s} \varphi_s \rangle}{\Lambda^2} \right) \delta_j^a \delta_k^b + \langle \tilde{\nu}_i^c \rangle \frac{y_{Rq} \langle \tilde{\nu}^{c\dagger s} \varphi_s \rangle}{\Lambda^2} \delta_j^a \delta_k^b \right. \\ & + \frac{y_{Fq}}{\Lambda^2} ((\mathbf{w}^2)^a_j \delta_k^b - (\mathbf{w}^2)^b_k \delta_j^a) \left. \right] \\ & + d_a^c D_b \left[ \langle \tilde{\nu}_i^c \rangle \left( y_q + \frac{y_{Lq} \mathbf{w}^2}{\Lambda^2} + \frac{y_{Rq} \langle \tilde{\nu}^{c\dagger s} \tilde{\nu}_s^c \rangle}{\Lambda^2} \right) \delta_j^a \delta_k^b + \langle \varphi_i \rangle \frac{y_{Rq} \langle \varphi^{\dagger s} \tilde{\nu}_s^c \rangle}{\Lambda^2} \delta_j^a \delta_k^b \right. \\ & + \frac{y_{Fq}}{\Lambda^2} ((\mathbf{w}^2)^a_j \delta_k^b - (\mathbf{w}^2)^b_k \delta_j^a) \left. \right] + D_a^c Q_b \langle H_{di} \rangle \left[ \frac{y_{Rq} \langle \tilde{\nu}^{c\dagger s} \varphi_s \rangle}{\Lambda^2} \delta_j^a \delta_k^b \right] \left. \right\} + \text{h.c.} + \mathcal{O}(1/\Lambda^4), \end{aligned} \quad (2.7)$$

where the coupling constants  $y_{q,Rq,Lq,Fq}$  are redefined to absorb the inessential loop factors, gauge couplings and CGC. They are proportional to the previously introduced  $y_1$  coupling in the superpotential and may be different for each line as different fields run through the corresponding loops. The first line contains the up-type quark mass terms which are antisymmetric at the leading order and only contribute to two physical quark masses. The next-to-leading order corrections fill up the entire mass matrix generating a hierarchy between the lightest up quark and the heavier charm and top quarks. The second line contains the down-type quark masses which depend on up to three different Higgs VEVs and a new term that differs from the up quarks. This is enough to create a different mass structure and a viable Cabibbo–Kobayashi–Maskawa (CKM) mixing matrix similarly to the discussion in [20]. The third line contains vector-like  $SU(3)_C$  triplets masses generated at the compactification scale, which is desirable. The fourth line contains a large mixing between one of the extra vector-like states and the down-type quarks, meaning that the light down-type quark lies in a linear combination between them, further contributing to the CKM matrix. Finally, the fifth line contains an EW scale mixing between the vector-like and the down-type quarks.

The leading contributions to the masses of all leptons, both chiral and vector-like, are only obtained through two distinct insertions of the effective adjoint D-term VEVs  $\langle \mathcal{D} \rangle$ . This takes place at two loop level since there are no tree-level mass terms and the  $\mathbf{L}^3$  cubic term is radiatively induced. The lepton sector can then be expressed as

$$\begin{aligned}
\mathcal{L}_{ml} = & \frac{1}{\Lambda^4} \epsilon^{ijk} \left\{ \nu_a^c L_b \langle H_{ui} \rangle \mathbf{w}^2 \left[ y_{LRI} \langle \varphi^{\dagger s} \varphi_s \rangle \delta_j^a \delta_k^b + (y_{LFI} + y_{RFI}) ((\mathbf{w}^2)_j^a \delta_k^b - (\mathbf{w}^2)_k^b \delta_j^a) \right] \right. \\
& + e_a^c L_b \langle H_{di} \rangle \left[ y_{LRI} \mathbf{w}^2 \langle \varphi^{\dagger s} \varphi_s \rangle \delta_j^a \delta_k^b + (y_{LFI} \mathbf{w}^2 + y_{RFI} \langle \varphi^{\dagger s} \varphi_s \rangle) ((\mathbf{w}^2)_j^a \delta_k^b - (\mathbf{w}^2)_k^b \delta_j^a) \right] \\
& + \tilde{H}_{ua} L_b \left[ y_{RFI} (\langle \tilde{\nu}_i^c \rangle \langle \varphi^{\dagger s} \varphi_s \rangle + \langle \phi_i \rangle \langle \varphi^{\dagger s} \tilde{\nu}_s^c \rangle) ((\mathbf{w}^2)_j^a \delta_k^b - (\mathbf{w}^2)_k^b \delta_j^a) \right] \\
& + \tilde{H}_{da} \tilde{H}_{ub} \left[ y_{RFI} (\langle \tilde{\nu}_i^c \rangle \langle \tilde{\nu}^{c\dagger s} \varphi_s \rangle + \langle \phi_i \rangle \langle \tilde{\nu}^{c\dagger s} \tilde{\nu}_s^c \rangle) ((\mathbf{w}^2)_j^a \delta_k^b - (\mathbf{w}^2)_k^b \delta_j^a) \right] \\
& + \tilde{\varphi}_a L_b \langle H_{ui} \rangle \langle \varphi^{\dagger s} \tilde{\nu}_s^c \rangle \left[ y_{LRI} \mathbf{w}^2 \delta_j^a \delta_k^b + y_{RFI} ((\mathbf{w}^2)_j^a \delta_k^b - (\mathbf{w}^2)_k^b \delta_j^a) \right] \\
& + e_a^c \tilde{H}_{db} \langle H_{di} \rangle \langle \tilde{\nu}^{c\dagger s} \varphi_s \rangle \left[ y_{LRI} \mathbf{w}^2 \delta_j^a \delta_k^b + y_{RFI} ((\mathbf{w}^2)_j^a \delta_k^b - (\mathbf{w}^2)_k^b \delta_j^a) \right] \\
& + \nu_a^c \tilde{H}_{da} \langle H_{ui} \rangle \langle \tilde{\nu}^{c\dagger s} \varphi_s \rangle \left[ y_{LRI} \mathbf{w}^2 \delta_j^a \delta_k^b + y_{RFI} ((\mathbf{w}^2)_j^a \delta_k^b - (\mathbf{w}^2)_k^b \delta_j^a) \right] \\
& + \nu_a^c \tilde{H}_{ua} \langle H_{di} \rangle \left[ \langle \tilde{\nu}^{c\dagger s} \varphi_s \rangle y_{RFI} ((\mathbf{w}^2)_j^a \delta_k^b - (\mathbf{w}^2)_k^b \delta_j^a) \right] \\
& + \tilde{\varphi}_a \tilde{H}_{ub} \langle H_{di} \rangle \left[ (y_{LFI} \mathbf{w}^2 + y_{RFI} \langle \varphi^{\dagger s} \varphi_s \rangle) ((\mathbf{w}^2)_j^a \delta_k^b - (\mathbf{w}^2)_k^b \delta_j^a) \right] \\
& + \tilde{\varphi}_a \tilde{H}_{db} \langle H_{ui} \rangle \left[ (y_{LFI} \mathbf{w}^2 + y_{RFI} \langle \tilde{\nu}^{c\dagger s} \tilde{\nu}_s^c \rangle) ((\mathbf{w}^2)_j^a \delta_k^b - (\mathbf{w}^2)_k^b \delta_j^a) \right] \Big\} \\
& + \text{h.c.} + \mathcal{O}(1/\Lambda^6),
\end{aligned} \tag{2.8}$$

where the  $y_{LRI,LFI,RFI}$  are not independent and absorb CGCs, gauge couplings and loop factors, which are different for each line due to the distinct fields running through the corresponding loops. The first line contains the Dirac mass terms for neutrinos, the second



one provides the charged lepton mass terms whereas the third one includes R-parity violating Higgsino-lepton mixing, which can be rotated into the Higgsino (or vector-like lepton) masses. This means that the light SM-like charged leptons lie in a linear combination between them. The fourth line contains the Higgsino mass terms and the fifth one offers a mixing term between the neutrinos and the flavinos. Note that the latter will behave as three extra right-handed neutrinos. The remaining lines contain EW scale mixing between leptons and Higgsinos.

As described in Appendix B, the rotational boundary conditions preserve a  $U(1)_{\mathcal{R}}$  related to simple SUSY. The Wilson line effective VEVs break the remaining SUSY also breaking completely this symmetry. In usual supersymmetric models a discrete  $\mathbb{Z}_2^{\mathcal{R}} \subset U(1)_{\mathcal{R}}$ , denoted as R-parity, is typically preserved, which does not happen in the current model. The R-parity violating (RPV) terms  $\sim \tilde{H}_{ua} L_b$  can be rotated away by an unitary transformation which then generates two-loop terms like  $\sim y_{RPV}^{ijk} Q_i L_j d_k^c$ , whose strongest constraint reads as  $y_{RPV}^{111} < 0.001$  [71, 72]. As this is the only R-parity violating term, and it is proportional to the first-family neutrino Yukawa coupling, it is expected to be much below this constraint. In general, such terms appear to be strongly suppressed by two loops and a factor of  $1/\Lambda^4$  which is smaller than the existing experimental constraints.

It is important to note that the dominant contributions for the quark Yukawa couplings are of the order  $\mathcal{O}(1)$ , with subleading corrections scaling as  $\mathcal{O}(1/\Lambda^2)$ . However, the latter are dominant for one of the generations which is identified with the up and down quarks. On the other hand, all the lepton Yukawa terms arise at the same  $\mathcal{O}(1/\Lambda^4)$  order, which already suggests much larger mixing angles between leptons than those expected in the quark sector.

The representations that obtain effective VEVs also get large Majorana masses for the corresponding fermions, i.e.

$$\mathcal{L}_{mml} = \frac{y_{MI}}{\Lambda} (\nu_i^c \nu_j^c \langle \tilde{\nu}^{cti} \tilde{\nu}^{ctj} \rangle + \tilde{\varphi}_i \tilde{\varphi}_j \langle \tilde{\varphi}^{\dagger i} \tilde{\varphi}^{\dagger j} \rangle + \nu_i^c \tilde{\varphi}_j \langle \tilde{\nu}^{cti} \tilde{\varphi}^{\dagger j} \rangle), \quad (2.9)$$

where  $y_{MI}$  absorbs extra CGC, gauge couplings and loop factors. Note that both right-handed neutrinos and flavinos get large Majorana masses providing a seesaw mechanism with three very light neutrinos and six heavy ones. However, one of the latter does not receive a large Majorana mass as it corresponds to the goldstino. Therefore, this model offers five right-handed neutrinos with masses of the order  $\mathcal{O}(\Lambda_3)$  while the remaining one is an EW scale sterile neutrino.

## 2. Gauginos

While the SUSY-breaking gaugino masses are obtained from the third term in Eq. (2.5), those arising from the broken generators of the gauge group acquire their leading order masses from the second term, with the corresponding expressions detailed in Appendix E. The vector boson and gaugino masses for a given broken generator are proportional to  $\langle \varphi^{\dagger i} \varphi_i \rangle, \langle \tilde{\nu}^{cti} \tilde{\nu}_i^c \rangle, \langle \varphi^{\dagger i} \tilde{\nu}_i^c \rangle, \langle \varphi_i \rangle + \langle \tilde{\nu}_i^c \rangle$ , which have to be large (i.e. close to the compactification scale). This requires four of the six effective VEVs to be large (with, at least, one for each family index), while allowing two of them to be arbitrarily small. Likewise, their complex

phases are arbitrary. This leaves the gluino, winos and binos all massless with eigenvectors

$$\tilde{g}_a = \lambda_a^C, \quad \tilde{W}_{1,2,3} = \lambda_{1,2,3}^L, \quad \tilde{B} = \sqrt{3}\lambda_8^L - 3\lambda_3^R + \sqrt{3}\lambda_8^R. \quad (2.10)$$

The leading SUSY breaking contributions to the non-diagonal gaugino mass form  $M_A^\dagger M_B$  are of the order  $\sim \langle \mathcal{D}_A \mathcal{D}_B \rangle$  and have the same mass structure as the SUSY preserving one, so they may be ignored. This comes from the fact that the same effective VEV that breaks the quartification GUT symmetry is the one that breaks SUSY such that they are aligned.

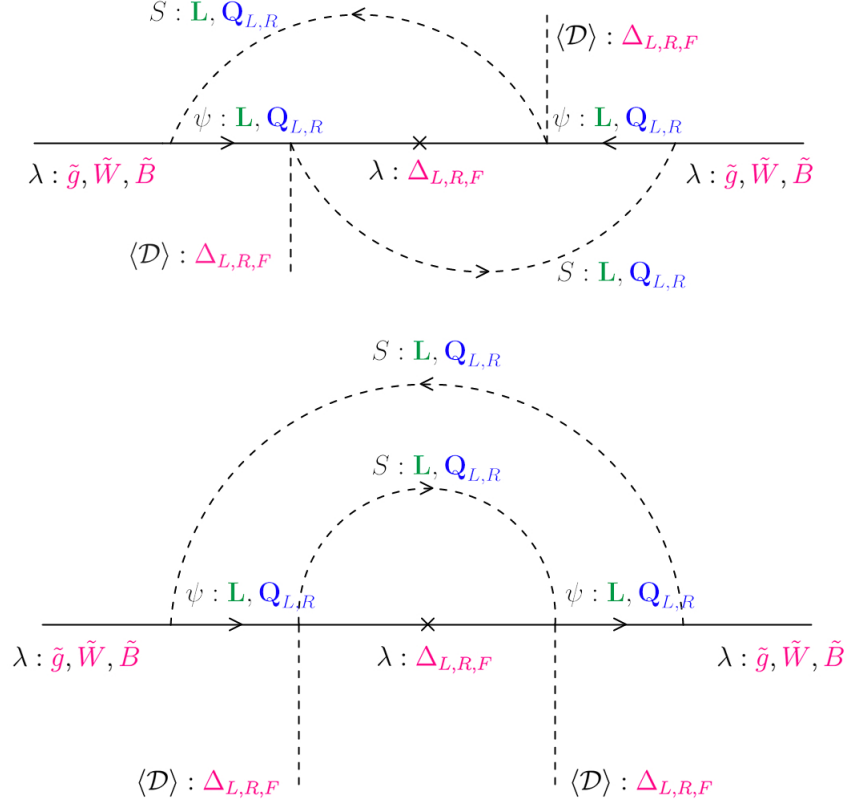


FIG. 7: The two loop diagrams for SUSY-breaking gaugino masses. The  $\langle \mathcal{D} \rangle$  does not have any SM charges so it must couple via loops.

The unbroken gauginos, on the other hand, cannot acquire a tree-level SUSY breaking mass. As  $\langle \mathcal{D} \rangle$  preserves the SM, it does not communicate SUSY breaking directly. Instead, such a communication has to take place through the two loop diagrams shown in Fig. 7, providing the mass terms for the remaining gauginos as

$$\mathcal{L}_{mg} = \frac{\mathbf{w}^5}{\Lambda^4} \left( y_{g\lambda} \tilde{g}\tilde{g} + y_{W\lambda} \tilde{W}\tilde{W} + y_{B\lambda} \tilde{B}\tilde{B} \right), \quad (2.11)$$

where, as usual, the effective couplings absorb the CGCs and loop factors, which are different for each gaugino as distinct fields run through the loops. This effectively defines the usual

soft gaugino mass as

$$m_{1/2} \sim g^4 l^2 \frac{\mathbf{w}^5}{\Lambda^4}, \quad (2.12)$$

where  $l^2$  is the two-loop suppression factor, and  $g$  is the corresponding gauge coupling.

### 3. Scalar masses

The scalar mass terms come from the scalar potential which is obtained by considering Eq. (C11) and substituting the truncated series from Eq. (C16) in

$$\mathcal{L}_S = - \frac{\partial^2 \mathcal{K}}{\partial \phi_j^\dagger \partial \phi_b} \Big|_S \frac{\partial \mathcal{W}}{\partial \phi_j} \Big|_S \frac{\partial \mathcal{W}}{\partial \phi_b^\dagger} \Big|_S - \frac{1}{2} \left[ \frac{\partial \mathcal{K}}{\partial \phi_i} \Big|_S t_A S_i + \frac{\partial \mathcal{K}}{\partial \phi_i^\dagger} \Big|_S t_A S_i^\dagger \right] \left[ \frac{\partial \mathcal{K}}{\partial \phi_j} \Big|_S t_A S_j + \frac{\partial \mathcal{K}}{\partial \phi_j^\dagger} \Big|_S t_A S_j^\dagger \right]. \quad (2.13)$$

The effective VEVs  $\langle \tilde{\nu}^c \rangle, \langle \varphi \rangle$  enter the potential a priori, as they come from the Wilson lines, i.e. the ED profiles of the fields, and are not determined by its minimization. The SUSY preserving mass terms, coming from the first term in Eq. (2.13), read as

$$\begin{aligned} \mathcal{L}_{mss} = & y_q (\delta_i^a \delta_j^b - \delta_j^a \delta_i^b) \left\{ \tilde{u}_a^c \tilde{u}^{c\dagger i} \langle H_{ub} H_u^{\dagger j} \rangle + (\tilde{Q}_a \langle H_{ub} \rangle) (\tilde{Q}^{\dagger i} \langle H_u^{\dagger j} \rangle) \right. \\ & + \tilde{d}_a^c \tilde{d}^{c\dagger i} (\langle H_{db} H_d^{\dagger j} \rangle + \langle \tilde{\nu}_b^c \tilde{\nu}^{c\dagger j} \rangle) + (\tilde{Q}_a \langle H_{db} \rangle) (\tilde{Q}^{\dagger i} \langle H_d^{\dagger j} \rangle) \\ & \left. + \tilde{D}_a^c \tilde{D}^{c\dagger i} \langle \varphi_b \varphi^{\dagger j} \rangle + \tilde{D}_a \tilde{D}^{\dagger i} (\langle \varphi_b \varphi^{\dagger j} \rangle + \langle \tilde{\nu}_b^c \tilde{\nu}^{c\dagger j} \rangle) \right\}, \end{aligned} \quad (2.14)$$

which means that only  $SU(3)_C$  charged scalars have SUSY preserving mass terms.

The second term in Eq. (2.13), on the other hand, contains the SUSY breaking scalar masses through the  $\langle \mathcal{D} \rangle$ -term contribution which, in variance to the gaugino sector, can couple to every scalar at leading order,

$$\begin{aligned} \mathcal{L}_{msd} = & \tilde{Q}_a \tilde{Q}^{\dagger i} \left[ y_{DF}(\mathbf{w}^2)_i^a \right] + \tilde{u}_a^c \tilde{u}^{c\dagger i} \left[ y_{DF}(\mathbf{w}^2)_i^a \right] + \tilde{d}_a^c \tilde{d}^{c\dagger i} \left[ y_{DF}(\mathbf{w}^2)_i^a + y_{DR} \langle \tilde{\nu}^{c\dagger j} \tilde{\nu}_j^c \rangle \right] \\ & + \tilde{D}_a \tilde{D}^{\dagger i} \left[ y_{DF}(\mathbf{w}^2)_i^a + y_{DL} \delta_i^a \mathbf{w}^2 \right] + \tilde{D}_a^c \tilde{D}^{c\dagger i} \left[ y_{DR} \delta_i^a \langle \varphi^{\dagger j} \varphi_j \rangle + y_{DF}(\mathbf{w}^2)_i^a \right] \\ & + \tilde{d}_a^c \tilde{D}^{c\dagger i} \left[ y_{DR} \langle \tilde{\nu}^{c\dagger j} \varphi_j \rangle \right] + \tilde{D}_a^c \tilde{d}^{c\dagger i} \left[ y_{DR} \langle \varphi^{\dagger j} \tilde{\nu}_j^c \rangle \right] \\ & + H_{da} H_d^{\dagger i} \left[ y_{DF}(\mathbf{w}^2)_i^a + y_{DR} \delta_i^a \langle \tilde{\nu}^{c\dagger j} \tilde{\nu}_j^c \rangle \right] + H_{ua} H_u^{\dagger i} \left[ y_{DF}(\mathbf{w}^2)_i^a \right] \\ & + \tilde{L}_a H_d^{\dagger i} \left[ y_{DR} \langle \tilde{\nu}^{c\dagger j} \varphi_j \rangle \right] + H_{da} \tilde{L}^{\dagger i} \left[ y_{DR} \langle \varphi^{\dagger j} \tilde{\nu}_j^c \rangle \right] \\ & + \tilde{L}_a \tilde{L}^{\dagger i} \left[ y_{DF}(\mathbf{w}^2)_i^a + y_{DR} \delta_i^a \langle \varphi^{\dagger j} \varphi_j \rangle \right] + \tilde{e}_a^c \tilde{e}^{c\dagger i} \left[ y_{DF}(\mathbf{w}^2)_i^a + y_{DL} \delta_i^a \mathbf{w}^2 \right] \\ & + \tilde{\nu}_a^c \tilde{\nu}^{c\dagger i} \left[ y_{DF}(\mathbf{w}^2)_i^a + y_{DL} \delta_i^a \mathbf{w}^2 + y_{DR} \delta_i^a \langle \tilde{\nu}^{c\dagger j} \tilde{\nu}_j^c \rangle \right] + \tilde{\nu}_a^c \varphi^{\dagger i} \left[ y_{DR} \langle \tilde{\nu}^{c\dagger j} \varphi_j \rangle \right] \\ & + \varphi_a \varphi^{\dagger i} \left[ y_{DF}(\mathbf{w}^2)_i^a + y_{DL} \delta_i^a \mathbf{w}^2 + y_{DR} \delta_i^a \langle \varphi^{\dagger j} \varphi_j \rangle \right] + \varphi_a \tilde{\nu}^{c\dagger i} \left[ y_{DR} \langle \varphi^{\dagger j} \tilde{\nu}_j^c \rangle \right], \end{aligned} \quad (2.15)$$

where the effective coupling constants absorb the gauge couplings and CGCs. Note that all scalar mass terms have  $\langle \mathcal{D} \rangle$ -term contributions at leading order, while next-to-leading

contributions like the  $\mu H_u H_d$  term appear only at  $\mathcal{O}(1/\Lambda^3)$ . These effectively define the soft scalar masses to be  $m_0^2 \sim \mathbf{w}^2$ .

### III. DARK MATTER CANDIDATE

In  $R$ -parity preserving SUSY theories, the Lightest Supersymmetric Particle (LSP) is stable and hence is considered to be a suitable DM candidate. Since the proposed GUT does not preserve  $R$ -parity, such a state is allowed to decay. However, as the  $R$ -parity violating interactions are highly suppressed with the LSP decay proportional to certain powers of Yukawa couplings, it can contribute to the DM phenomenology.

As described in Appendix C, the ED fields decompose into KK modes as

$$\phi_i(x, z) = \sum_{s=0}^{\infty} \sum_{a,b=0,1,2} \phi_i^{sab}(x) f(z)_{sab}, \quad (3.1)$$

where  $f(z_j)_{sab}$  are orthonormal functions obeying to

$$\int dz f(z)_{sab} (f(z)^{\dagger rcd}) = \delta_s^r \delta_a^c \delta_b^d, \quad (3.2)$$

with the zero mode  $f_{000}$  being a constant. One then concludes that

$$\int dz f(z)_{sab} = 0, \quad (3.3)$$

for a non-zero mode. Therefore, there can not be any term in the Lagrangian with a single KK mode and any number of zero modes for which the KK state could decay. This implies that the Lightest KK Particle (LKP) is stable and may be a DM candidate [73–77].

All KK modes receive masses proportional to  $1/R_{1,2,3}$ . The lightest KK mode in this model would be the first KK mode of the SM Higgs doublet, as it gets a radiatively driven negative mass squared to break the EW symmetry. This particle would be a stable LKP. The next-to-lightest ones would be the first KK modes of the gluons and photons which do not receive EW scale mass contributions. The next ones are all SM fermions and extra Higgs bosons. Note that the mass differences between these fields are proportional to the EW scale, but the KK masses must be at compactification scale, which is orders of magnitude larger. This calls for a strong almost degenerate mixing which provides a rich DM phenomenology and interesting opportunities for DM searches at colliders and in astrophysics measurements. The latter consideration goes beyond the scope of this paper and will be pursued elsewhere.

### IV. PROTON DECAY

Like in many of the existing GUTs, in the considered model, there will be high-energy processes that mix leptons with quarks, so there may be interactions that cause the proton to decay. It is straightforward to notice that in the trinification sector of the model, the

adjoint representations (for gauge and chiral superfields)  $\Delta_{\mathbf{C},\mathbf{L},\mathbf{R},\mathbf{F}}$  preserve baryon and lepton number, therefore they do not mediate proton decay. However, the SU(5) generators that trigger proton decay also lie inside  $E_8$ . These are the  $\mathbf{X}$  and  $\bar{\mathbf{X}}$ , that together with the trinification ones, complete the  $E_6$  generators. The terms involving these massive gauge fields are

$$\mathcal{K}_X \sim \mathbf{L}e^{-2\mathbf{X}_V}\mathbf{Q}_R^\dagger + \mathbf{L}e^{-2\bar{\mathbf{X}}_V}\mathbf{Q}_L^\dagger + \mathbf{Q}_L e^{-2\bar{\mathbf{X}}_V}\mathbf{Q}_R^\dagger + \text{h.c.}, \quad (4.1)$$

which could, in principle, mediate proton decay. However, these terms are not available for the physical quarks and leptons, i.e. the zero modes. Each of the terms must be invariant under the orbifold charges, thus there can not be a term with two zero modes and one KK mode, as discussed in Sec. III. Remarkably, the orbifold charges in Tab. VII protect the broken gauge field terms from generating proton decay [78].

One can also write the similar terms involving chiral superfields in the same representation

$$\mathcal{W}_X \sim \mathbf{L}\mathbf{X}\bar{\mathbf{Q}}_R + \mathbf{L}\bar{\mathbf{X}}\bar{\mathbf{Q}}_L + \bar{\mathbf{L}}\bar{\mathbf{X}}\mathbf{Q}_R + \bar{\mathbf{L}}\mathbf{X}\mathbf{Q}_L + \mathbf{Q}_L\bar{\mathbf{X}}\bar{\mathbf{Q}}_R + \mathbf{Q}_R\mathbf{X}\bar{\mathbf{Q}}_L + \text{h.c.}, \quad (4.2)$$

which do not generate proton decay themselves but can, through a loop, provide the following terms

$$\mathcal{K}_{pX} \sim \frac{\alpha^6 l^2}{M_X^2} \left( \mathbf{L}\mathbf{Q}_R^\dagger \mathbf{L}\mathbf{Q}_L^\dagger + \mathbf{L}\mathbf{Q}_R^\dagger \mathbf{Q}_L \mathbf{Q}_R^\dagger \right) + \text{h.c.}, \quad (4.3)$$

where  $l$  is a loop factor and  $g$  is the gauge coupling. The second term is a typical dimension-six SUSY proton decay term. By expanding its indices

$$\mathcal{K}_{pX} \sim \frac{g^6 l^2}{M_X^2} \mathbf{L}_{bi}^a \mathbf{Q}_{Lak} \mathbf{Q}_{Ref}^\dagger \mathbf{Q}_{Rhl}^\dagger \epsilon^{ijk} \epsilon_{kfl} \epsilon^{aeh} + \text{h.c.}, \quad (4.4)$$

it can be seen that it vanishes due to the antisymmetric product on the  $SU(3)_R$  indices (as well as the omitted color ones). Note, however, that by adding an effective adjoint VEV as in Fig. 8 leads to the terms

$$\begin{aligned} \mathcal{K}_{pX} &\sim \frac{g^8 l^2}{M_X^2 \Lambda^2} \mathbf{L}_{bi}^a \mathbf{Q}_{Lak} \mathbf{Q}_{Ref}^\dagger \langle \tilde{\Delta}_h^m \rangle \mathbf{Q}_{Rml}^\dagger (\delta_f^i \delta_l^k - \delta_l^i \delta_f^k) \epsilon^{beh} + \text{h.c.} \\ &\sim \frac{g^8 l^2}{M_X^2 \Lambda^2} L_i Q_k u_f^\dagger d_l^\dagger \langle \tilde{\nu}^{c\dagger s} \tilde{\nu}_s^c \rangle (\delta_f^i \delta_l^k - \delta_l^i \delta_f^k) + \text{h.c.}, \end{aligned} \quad (4.5)$$

that indeed mediate proton decay. The proton may then decay (through these terms) into  $K$  mesons by means of a flavour-changing process as well as into the mesons  $\pi, \eta, \omega, \rho$  while preserving flavour [79]. Note that in Eq. (4.5), the Kronecker- $\delta$  factors forbid flavour-index preserving proton decay terms. Since most of the first family of fermions lies in the flavour index 1, the main decay mode occurs in the flavour-changing channel. The corresponding decay rate is [24]

$$\Gamma_{p \rightarrow K+L} \sim \frac{g^{18} l^4}{\Lambda^4} \langle \tilde{\nu}^{c\dagger s} \tilde{\nu}_s^c \rangle^2 \frac{m_p^5}{M_X^4}, \quad (4.6)$$

where  $g$  is the universal gauge coupling at the  $E_8$  unification scale<sup>4</sup>,  $M_X$  is the GUT/com-pactification scale, and  $m_p$  is the proton mass.

<sup>4</sup> Note that the mediators  $\mathbf{X}, \bar{\mathbf{X}}$  get a mass at the highest breaking scale, as described in Appendix F, therefore the gauge coupling must correspond to the one at this scale, named  $g_8$  in Sec. V A.

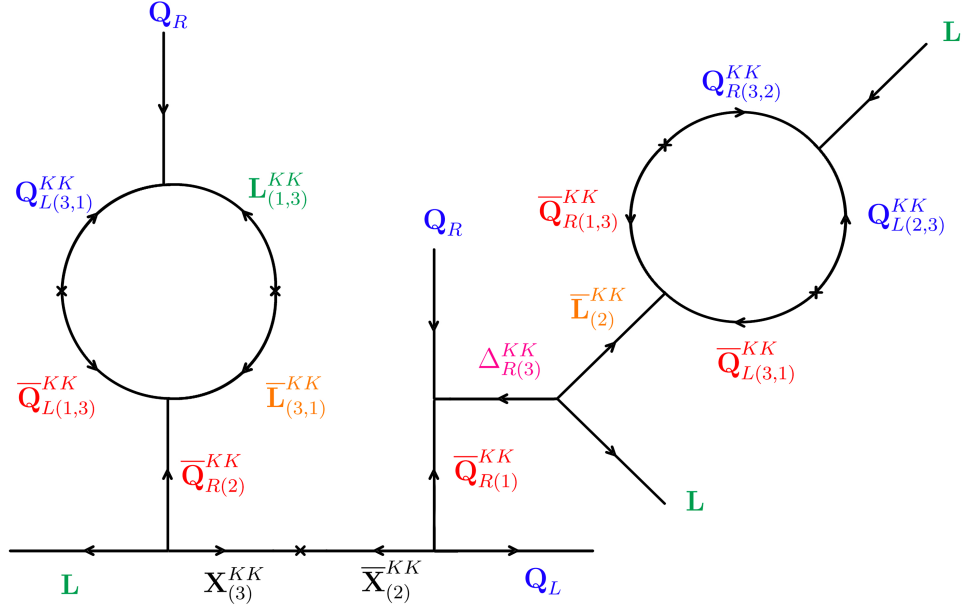


FIG. 8: Two-loop diagram for the leading-order proton decay processes.

The flavour-changing proton decays  $p \rightarrow \bar{\nu}_{e,\mu} + K^+$  or  $p \rightarrow (\bar{e}, \bar{\mu}) + K^0$  require terms with three quarks and an electron or muon, or a neutrino [80]. These processes are less constrained than the proton decay into pions [81]:

$$\tau_{p \rightarrow K+L} = 6.6 \times 10^{-3} \tau_{p \rightarrow \pi+L}, \quad (4.7)$$

with the most stringent bound on the proton lifetime [82]

$$\tau_{p \rightarrow \pi+L} < 1.7 \times 10^{34} \text{ yrs}. \quad (4.8)$$

The proton decay constraints set a limit on the GUT/compactification scale from Eq. (4.6) as

$$\Lambda = M_X > g^{9/2} l \frac{\langle \tilde{\nu}^{c\dagger s} \tilde{\nu}_s^c \rangle^{1/2}}{\Lambda} 7.7 \times 10^{15} \text{ GeV}, \quad (4.9)$$

where the loop suppression as well as the gauge coupling may bring it down by many orders of magnitude from typical values found in other known GUTs, as it is discussed below in Sec. V A.

The extra triplets inside  $\mathbf{Q}_L, \mathbf{Q}_R$  may also mediate proton decay. Their coupling to SM fermions is detailed in Eq. (2.1). For proton decay to happen, it needs to couple solely to quarks, i.e. there must be a term  $DQQ, D^c u^c d^c$ , which is absent in the theory. Therefore, they do not directly mediate proton decay [24].

From the Kähler potential in Eq. (E2) one can extract the possible  $QQQL$  terms mediated by KK modes

$$\begin{aligned} \mathcal{K}'_p = & \frac{y_5}{\Lambda^5} \epsilon_{ijk} \epsilon^{opq} \mathbf{Q}_{R\ o}^i (\tilde{\Delta}_R)^j_n \mathbf{Q}_{R\ p}^n (\tilde{\Delta}_F)^a_q \mathbf{Q}_{R\ a}^k \\ & + \frac{y_6}{\Lambda^5} \epsilon^{ijk} \epsilon^{opq} \mathbf{Q}_{Lio} (\tilde{\Delta}_L)^a_j \mathbf{Q}_{Lap} (\tilde{\Delta}_F)^b_q \mathbf{Q}_{Lkb} . \end{aligned} \quad (4.10)$$

It follows from the structure of  $\Delta = \mathbf{L}^\dagger \mathbf{L}$ , and since only one lepton is required, one of the  $\mathbf{L}$  must be taking its VEV, which can only be introduced by right-handed neutrinos or flavons. Therefore, no proton decay is generated through KK modes of the light fields.

Even though there are no proton decay terms in Eq. (4.10), one can obtain the terms

$$\begin{aligned} \mathcal{K}'_p \subset & \frac{y_5}{\Lambda^5} \epsilon^{opq} d_o^c \langle (\tilde{\Delta}_R)^j_2 \rangle u_p^c \langle (\tilde{\Delta}_F)^a_q \rangle D_a^c \\ & + \frac{y_6}{\Lambda^5} \epsilon^{opq} d_o \langle (\tilde{\Delta}_L)^2_j \rangle u_p \langle (\tilde{\Delta}_F)^b_q \rangle D_b , \end{aligned} \quad (4.11)$$

which vanish from Eq. (E9) due to  $\langle (\tilde{\Delta}_R)^j_2 \rangle = \langle (\tilde{\Delta}_L)^2_j \rangle = 0$ . This means that the triplets  $(D, D^c)$  do not mediate proton decay (up to  $\mathcal{O}(1/\Lambda^5)$ , which is more suppressed than the  $\mathbf{X}$  mediation).

Other decay processes, such as  $n-\bar{n}$  oscillations and the flavour-changing processes other than the dominant one considered above would be mediated by the same fields, but appear up to  $\mathcal{O}(1/\Lambda^{11})$ , whose experimental constraints can be easily satisfied [83].

## V. GAUGE COUPLING UNIFICATION

The different gauge couplings in the SM that characterize the interaction strengths of the strong and EW forces evolve with the energy scale at a rate that depends on the field content. In a consistent GUT they must merge into a unique coupling, which in the model presented in this work is described by the  $E_8$  symmetry and denoted as  $g_8$ .

The presence of extra spacetime dimensions, and thus KK modes in the mass spectrum, has an impact on the running of the gauge couplings. In particular, such KK modes become important above a certain cut-off scale  $\mu_{\text{KK}}$  where they start playing a dominant role on the RG flow. Typically, the usual logarithmic running is modified acquiring a power-law structure which depends on the number of extra compact dimensions as discussed in [84, 85]. In general terms, the one-loop beta functions of a certain parameter  $\mathcal{P}$  should be modified according to

$$\beta_{\mathcal{P}}^{(1)} \rightarrow \beta_{\mathcal{P}}^{(1)} + [S(\mu, \delta) - 1] \tilde{\beta}_{\mathcal{P}}^{(1)} , \quad (5.1)$$

where the usual logarithmic running is represented by  $\beta_{\mathcal{P}}^{(1)}$  while the contribution of the KK modes is encoded in  $\tilde{\beta}_{\mathcal{P}}^{(1)}$ . The power-law running is governed by the  $[S(\mu, \delta) - 1]$  term with [84–86]

$$S(\mu, \delta) = X_\delta \left( \frac{\mu}{\mu_{\text{KK}}} \right)^\delta \quad \text{for} \quad \mu \geq \mu_{\text{KK}} , \quad (5.2)$$

and where  $\delta$  represents the number of extra spacetime dimensions, and  $\mu_{\text{KK}}$  – the scale at which the KK modes enter the particle spectrum. The  $X_\delta$  factor is given by

$$X_\delta = \frac{2\pi^{\delta/2}}{\delta\Gamma(\delta/2)}, \quad (5.3)$$

with  $\Gamma(x)$  being the Euler gamma function.

A study of the evolution of the gauge couplings has been performed here, in order to show that one can consistently unify all known interactions. Therefore, we demonstrate explicitly that the framework presented in this article is a good candidate for a GUT. At one-loop level it is convenient to recast the gauge couplings in terms of the inverse structure constants whose evolution in 4d is simply given by

$$\alpha_A^{-1}(\mu) = \alpha_0^{-1} - \frac{b_A}{2\pi} \log \frac{\mu}{\mu_0}. \quad (5.4)$$

The label A identifies a given gauge group with the gauge coupling  $g_A$  such that  $\alpha_A = g_A^2/(4\pi)$ , while  $\alpha_0^{-1}$  denotes the value of the inverse structure constant at the initial energy-scale  $\mu_0$ . Once the mass threshold scale  $\mu_{\text{KK}}$  (where the KK modes become relevant) is reached the structure constants of a theory with  $\delta$  EDs evolve according to the power-law

$$\alpha_A^{-1}(\mu) = \alpha_0^{-1} - \frac{b_A}{2\pi} \log \frac{\mu}{\mu_0} + \frac{\tilde{b}_A}{2\pi} \log \frac{\mu}{\mu_{\text{KK}}} - \frac{\tilde{b}_A X_\delta}{2\pi\delta} \left[ \left( \frac{\mu}{\mu_{\text{KK}}} \right)^\delta - 1 \right]. \quad (5.5)$$

The value of the  $b_A$  and  $\tilde{b}_A$  coefficients will determine how fast a given gauge coupling evolves between any two scales. These coefficients depend on the field content decomposed into 4d Lorentz representations as well as their corresponding gauge representation. For non-Abelian gauge groups they are both given by

$$b_A, \tilde{b}_A = -\frac{11}{3}C_2(G) + \frac{4}{3}\kappa_F T(F) + \frac{1}{3}\kappa_S T(S), \quad (5.6)$$

where  $\kappa_F = \frac{1}{2}$  for Weyl fermions,  $\kappa_S = 1$  ( $\frac{1}{2}$ ) for complex (real) scalars,  $C_2(G)$  is a group Casimir in the adjoint representation while  $T(F)$  and  $T(S)$  are the Dynkin indices for fermions and scalars, respectively. Similarly, for the case of U(1) symmetries the beta-function coefficients read as

$$b'_A, \tilde{b}'_A = -\frac{11}{3} \sum_v \left( \frac{Q_v}{2} \right)^2 + \frac{4}{3}\kappa_F \sum_f \left( \frac{Q_f}{2} \right)^2 + d \frac{1}{3}\kappa_S \sum_s \left( \frac{Q_s}{2} \right)^2, \quad (5.7)$$

with  $Q_v$ ,  $Q_f$  and  $Q_s$  being the Abelian charges of the vector, fermion and scalar degrees of freedom of the theory.

In what follows, the seven distinct energy scales  $\Lambda_{0,\dots,6}$ , are denoted as:

- $\Lambda_0$  is defined by the smallest radius  $R_2$  or  $R_3$ , related to the 10d to 6d compactification procedure as well as the  $E_8 \rightarrow E_6 \times \text{SU}(3)_C$  breaking (as described in Appendix F).



- $\Lambda_1$  is defined as the scale where the effect of the  $E_8$  KK modes wears out.
- $\Lambda_2$  is defined by the largest radius  $R_1$ , related to the 6d to 4d compactification and to  $E_6 \rightarrow SU(3)_L \times SU(3)_R \times SU(3)_F$  breaking.
- $\Lambda_3$  defines the Wilson line scale which breaks SUSY as well as  $SU(3)_C \times SU(3)_L \times SU(3)_R \times SU(3)_F$  into the SM. All scalar and gaugino masses are generated at this scale.
- $\Lambda_4$  is defined as the scale where the effect of the lightest KK modes wears out.
- $\Lambda_5$  is defined as the scale where the lightest BSM states, such as vector-like matter, are integrated out.
- $\Lambda_6$  is identified with the EW scale.

The hierarchy between the radii of the EDs is arbitrary. The scale where the effect of the KK modes wears out must be about one order of magnitude below their corresponding compactification scale. It will be assumed that  $\Lambda_2 \approx \Lambda_3$ , i.e. the trinification and the  $E_6$  phases are compressed, such that the generic symmetry breaking scheme to consider is given by

$$\begin{aligned}
\{E_8\}_{10d} &\xrightarrow{\Lambda_0} \{E_6 \times SU(3)_C\}_{6d}^{KK} \xrightarrow{\Lambda_1} \{E_6 \times SU(3)_C\}_{6d}^0 \xrightarrow{\Lambda_2} \\
&\{U(1)_Y \times SU(2)_L \times SU(3)_C\}_{4d}^{KK-1} \xrightarrow{\Lambda_3} \{U(1)_Y \times SU(2)_L \times SU(3)_C\}_{4d}^{KK-2} \xrightarrow{\Lambda_4} \\
&\{U(1)_Y \times SU(2)_L \times SU(3)_C\}_{4d}^0 \xrightarrow{\Lambda_5} \{U(1)_Y \times SU(2)_L \times SU(3)_C\}_{4d-NHDM}^0,
\end{aligned} \tag{5.8}$$

with the superscript  $\{\dots\}^{KK,0}$  denoting an RG flow involving KK excitations or only zero modes. Note that there are two scales with different KK superscripts with the SM gauge symmetry, as some KK modes wear out faster due to the Wilson line. There are also two scales with 0 superscripts and SM gauge symmetry, as the first one includes Higgsinos and gauginos while the last one only considers the usual SM field content with an N Higgs doublet model (NHDM). The detailed effective field content at each energy scale is described in Appendix G.

### A. Origin of low-scale Unification

This section presents a study of the unification of gauge couplings in the model. The analysis follows a purely agnostic approach without assuming any prior unification scale. The aim is to derive it from the theoretical constraints and then confront it with the proton decay bound and other phenomenological limits. The values of all the coefficients used in this section are shown in Appendix G.

The SM gauge couplings are expressed as  $g_1 \equiv g_Y$ ,  $g_2 \equiv g_L$  and  $g_3 \equiv g_C$  at the EW scale in terms of the universal  $E_8$  gauge coupling  $g_8$  and the intermediate symmetry breaking scales

as

$$\begin{aligned}
\alpha_{i,3}^{-1}(m_Z) = & \alpha_8^{-1} - \frac{\tilde{b}_{6,3}^{\text{VI}}}{2\pi} \log\left(\frac{\Lambda_0}{\Lambda_1}\right) + \frac{\tilde{b}_{6,3}^{\text{VI}}\pi^2}{72} \left[10^{6\log\left(\frac{\Lambda_0}{\Lambda_1}\right)} - 1\right] - \frac{\tilde{b}_{6,3}^{\text{V}}}{2\pi} \log\left(\frac{\Lambda_1}{\Lambda_2}\right) \\
& + \frac{\tilde{b}_{6,3}^{\text{V}}}{4} \left[10^{2\log\left(\frac{\Lambda_1}{\Lambda_2}\right)} - 1\right] + \frac{b_{i,3}^{\text{IV}}}{2\pi} \log\left(\frac{\Lambda_2}{\Lambda_3}\right) - \frac{\tilde{b}_{i,3}^{\text{IV}}}{2\pi} \log\left(\frac{\Lambda_2}{\Lambda_3}\right) \\
& + \frac{\tilde{b}_{i,3}^{\text{IV}}}{4} \left[10^{2\log\left(\frac{\Lambda_2}{\Lambda_3}\right)} - 1\right] - \frac{\tilde{b}_{i,3}^{\text{III}}}{2\pi} \log\left(\frac{\Lambda_3}{\Lambda_4}\right) + \frac{\tilde{b}_{i,3}^{\text{III}}}{4} \left[10^{2\log\left(\frac{\Lambda_3}{\Lambda_4}\right)} - 1\right] \\
& + \frac{b_{i,3}^{\text{II}}}{2\pi} \log\left(\frac{\Lambda_4}{\Lambda_5}\right) + \frac{b_{i,3}^{\text{I}}}{2\pi} \log\left(\frac{\Lambda_5}{m_Z}\right),
\end{aligned} \tag{5.9}$$

with  $m_Z$  being the SM  $Z$ -boson mass that defines the EW scale and  $i = 1, 2$ . Note that, for convenience, the gauge couplings are recast in terms of the corresponding inverse structure constants. Taking into account the  $E_6 \times \text{SU}(3)_C$  phase, and in particular region VI, one can also write

$$\begin{aligned}
\alpha_3^{-1}(\Lambda_0) = & \alpha_3^{-1}(\Lambda_1) - \frac{5}{2\pi} \log\left(\frac{\Lambda_0}{\Lambda_1}\right) + \frac{5\pi^2}{72} \left[10^{6\log\left(\frac{\Lambda_0}{\Lambda_1}\right)} - 1\right], \\
\alpha_6^{-1}(\Lambda_0) = & \alpha_6^{-1}(\Lambda_1) - \frac{5}{2\pi} \log\left(\frac{\Lambda_0}{\Lambda_1}\right) + \frac{5\pi^2}{72} \left[10^{6\log\left(\frac{\Lambda_0}{\Lambda_1}\right)} - 1\right],
\end{aligned} \tag{5.10}$$

with  $\alpha_3^{-1}(\Lambda_0) = \alpha_6^{-1}(\Lambda_0) \equiv \alpha_8^{-1}$  which, as a result of Eq. (G12) implies that  $\alpha_3^{-1}(\Lambda_1) = \alpha_6^{-1}(\Lambda_1)$ . In other words, all gauge interactions of the theory, which also include family gauge group, must already unify at the  $\Lambda_1$  scale and run equally all the way up to the  $E_8$  scale. In fact, all components of the 10d **248** vector superfield contribute to the running both via KK towers in 6 and 10 dimensions, according to Tab. XIX.

Using Eqs. (5.9) and (5.10) one can numerically solve them with respect to the unification scales as well as the values of the unified couplings  $g_8(\Lambda_0)$  and  $g_6(\Lambda_1)$ . Recall that the scale hierarchies must obey  $\log_{10}\left(\frac{\Lambda_0}{\Lambda_1}\right) < \log_{10}\left(\frac{\Lambda_1}{\Lambda_4}\right) \sim \mathcal{O}(1)$ . Therefore, scenarios where such hierarchies are up to 20% off from  $\mathcal{O}(1)$ , are the only ones accepted as valid solutions. In the numerical scan we have fixed  $\Lambda_5 = 1$  TeV allowing  $\log_{10} \Lambda_4/\text{GeV}$  to randomly vary between 4 and 15. A numerical routine written in `Python` engineered to find the roots of non-linear systems was developed and processed at the `blafis`<sup>5</sup> and `ARGUS` computer clusters as part of the overall computing infrastructure at the University of Aveiro. The results obtained are shown in Fig. 9.

It is rather relevant to highlight that, from the top-left or the bottom-left panels in Fig. 9, consistent scenarios in the model that obey all theoretical constraints feature an unification scale approximately 10-orders of magnitude lighter than that of conventional GUT scenarios. It is also particularly significant to mention that no preferred GUT scale in the calculation was imposed. Therefore, all points obtained unveil the space of viable solutions that the model can offer without even ever reaching the boundary values set in the scan for the  $\Lambda_4$  scale ( $[10^4, 10^{15}]$  GeV). In essence, with a  $E_8$ -GUT scale ranging from 1000 TeV up

<sup>5</sup> Technical details can be found at the Gr@v's website [87].

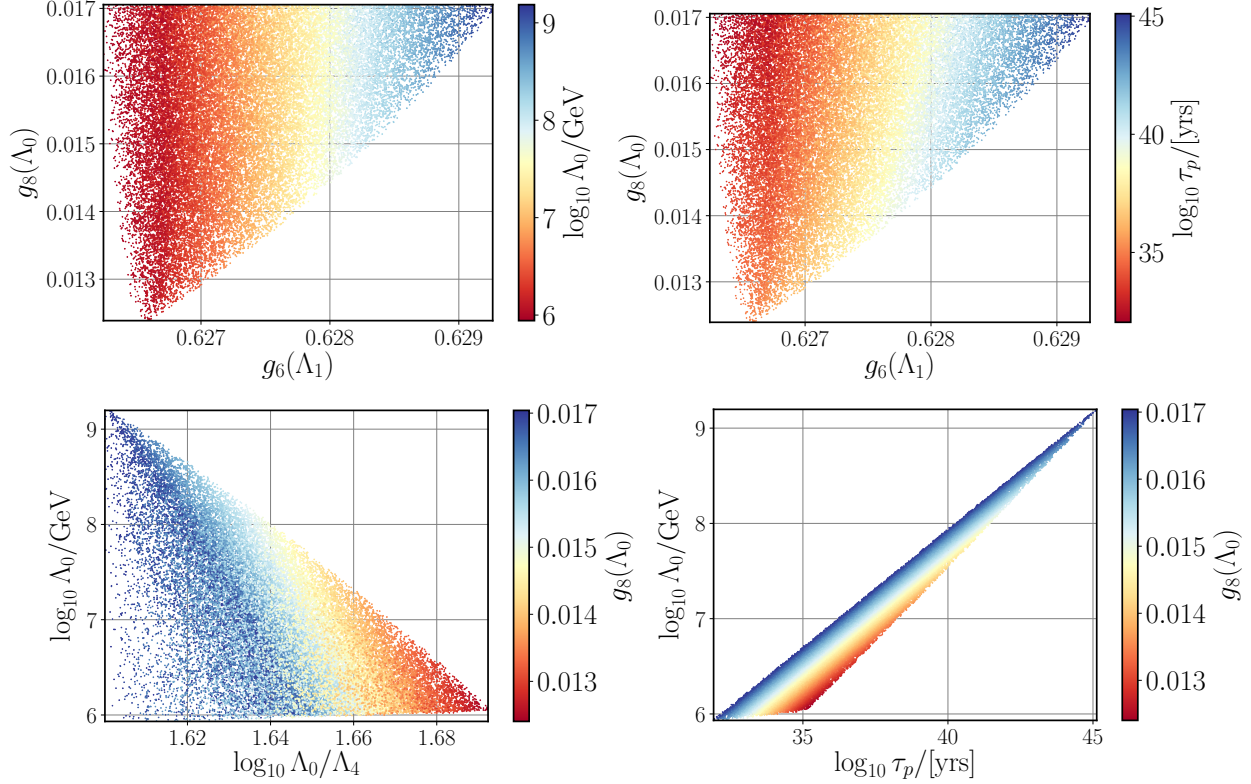


FIG. 9: Scenarios consistent with exact gauge coupling unification. We show in the y-axis of the top panels the value of the  $g_8$  gauge coupling at the  $E_8$  compactification scale whereas the x-axis represents both  $E_6$  and the  $SU(3)_C$  gauge coupling at the  $\Lambda_1$  scale. On the left panel the colour gradation represents the  $E_8$  unification scale while on the right panel it denotes the proton lifetime in years. On the bottom panel we show the relation between the proton lifetime, the  $E_8$  scale and the universal  $g_8$  coupling.

to 1000 PeV, the model can be classified as a *low-scale Grand Unified Theory* potentially accessible to the next generations of particle colliders. Furthermore, it has been verified that all such points pass one of the most stringent constraints known for GUT models, the proton lifetime. This can be seen in the upper-right and bottom-right panels of Fig. 9 where the prediction, using Eq. (4.6), is that the proton must decay to kaons with a lifetime ranging from  $\tau_{p \rightarrow K+L} \sim \mathcal{O}(10^{32})$  yrs to  $\tau_{p \rightarrow K+L} \sim \mathcal{O}(10^{45})$  yrs. Note that in this calculation, the loop factor appearing in Eq. (4.6) has been set to a value of the order  $\mathcal{O}(0.1)$ . Smaller values may further suppress the decay rate to kaons. Once again, no prior constraint regarding proton decay has been imposed in the analysis and it is rather tantalizing to note that the lowest unification scale value found, denoted as scenario (a) in Tab. VIII, corresponds to a proton lifetime of approximately two times the current experimental lower bound  $\tau_{p \rightarrow K+L} > 1.1 \times 10^{32}$  yrs. Last but not least, the model predicts rather constrained values for the  $g_8$  and  $g_6$  gauge couplings at their respective scales. For instance, it is found that  $g_6(\Lambda_1) \approx 0.63$ , whereas the universal gauge-Yukawa unification coupling is  $0.01 < g_8(\Lambda_0) < 0.02$ . In total, the effect of the KK modes last for about 1.6 – 1.7 orders of magnitude (due to the hierarchy

between the radii of the ED tori) with the smallest values of  $g_8$  being obtained for the maximal scale separation as shown in the bottom-left panel of Fig. 9.

The power-law behaviour of the RG equations (RGEs) is indeed responsible for the possibility of consistently achieving low-scale unification. Similar arguments were previously noted as e.g. in ([84, 85]). However, the model presented in this work is, to the best of the authors' knowledge, the first low-scale  $E_8$ -GUT realization that incorporates the SM gauge interactions and the family replication observed in nature, both within the same framework, and that is consistent with proton decay limits.

For a more concrete visualization Fig. 10 shows four selected benchmark scenarios of the evolution of the gauge couplings from the unification scale down to the EW one. The scales involved in the running, the values of the  $g_8$  and  $g_6$  gauge couplings and the proton lifetime are specified in Tab. VIII. All four panels clearly demonstrate that the model can consistently unify all fundamental interactions, including family, in  $E_8$  and that the unification scale can be realized well below the conventional GUT scale. It is clear that the effect of KK modes is crucial to realize such a low-scale Grand Unification picture resulting in a very weakly coupled theory at high-energy scale. An appealing consequence of scenarios (a) (b) and

Scenario	$\log_{10} \frac{\Lambda_0}{\text{GeV}}$	$\log_{10} \frac{\Lambda_1}{\text{GeV}}$	$\log_{10} \frac{\Lambda_2}{\text{GeV}}$	$\log_{10} \frac{\Lambda_3}{\text{GeV}}$	$\log_{10} \frac{\Lambda_4}{\text{GeV}}$	$\log_{10} \frac{\Lambda_5}{\text{GeV}}$	$g_8(\Lambda_0)$	$g_6(\Lambda_2)$	$\tau_p/[\text{yrs}]$
(a)	5.94	5.14	5.11	4.98	4.33	3.0	$1.63 \times 10^{-2}$	0.626	$1.82 \times 10^{32}$
(b)	6.06	5.22	5.09	5.02	4.37	3.0	$1.24 \times 10^{-2}$	0.627	$1.45 \times 10^{35}$
(c)	7.01	6.18	6.04	5.98	5.34	3.0	$1.38 \times 10^{-2}$	0.627	$1.18 \times 10^{38}$
(d)	9.19	8.39	8.25	8.18	7.58	3.0	$1.69 \times 10^{-2}$	0.629	$1.27 \times 10^{45}$

TABLE VIII: Threshold scales and values of the  $E_8$  and  $E_6$  gauge couplings at their respective breaking scales for the four plots in Fig. 10. The last column provides an estimate for the proton lifetime in its kaon decay channel.

(c) in Tab. VIII is that the next generation of particle colliders with center of mass energies of the order of  $\sqrt{s} = 100$  TeV may already be able to probe, to a certain extent, the low-energy unification picture proposed in this article. It is important to stress that there were no consistent high-scale unification scenarios found in our analysis. Therefore, this is a big departure from standard GUT theories which have a typical unification scale  $\sim 10^{16}$  GeV.

While the  $E_8$  breaking scale,  $\Lambda_0$ , meets the proton decay limits, other energy-scales involved in the running may also have their own experimental constraints. Particularly relevant is the  $\Lambda_3$  scale where the breaking of the  $SU(3)_L \times SU(3)_R$  left-right symmetry takes place. Current experimental limits bound  $W_R$  gauge bosons to be heavier than [88]

$$m_{W_R} > 3.7 \text{ TeV}, \quad (5.11)$$

while the strongest bound on extra  $Z'$  bosons is [81]

$$m_{Z'} > 4.5 \text{ TeV}. \quad (5.12)$$

Since all points generated in the numerical scan result in  $\Lambda_3 \gtrsim 100$  TeV, the model is also unconstrained by direct searches for heavy gauge bosons at the LHC. In fact, another

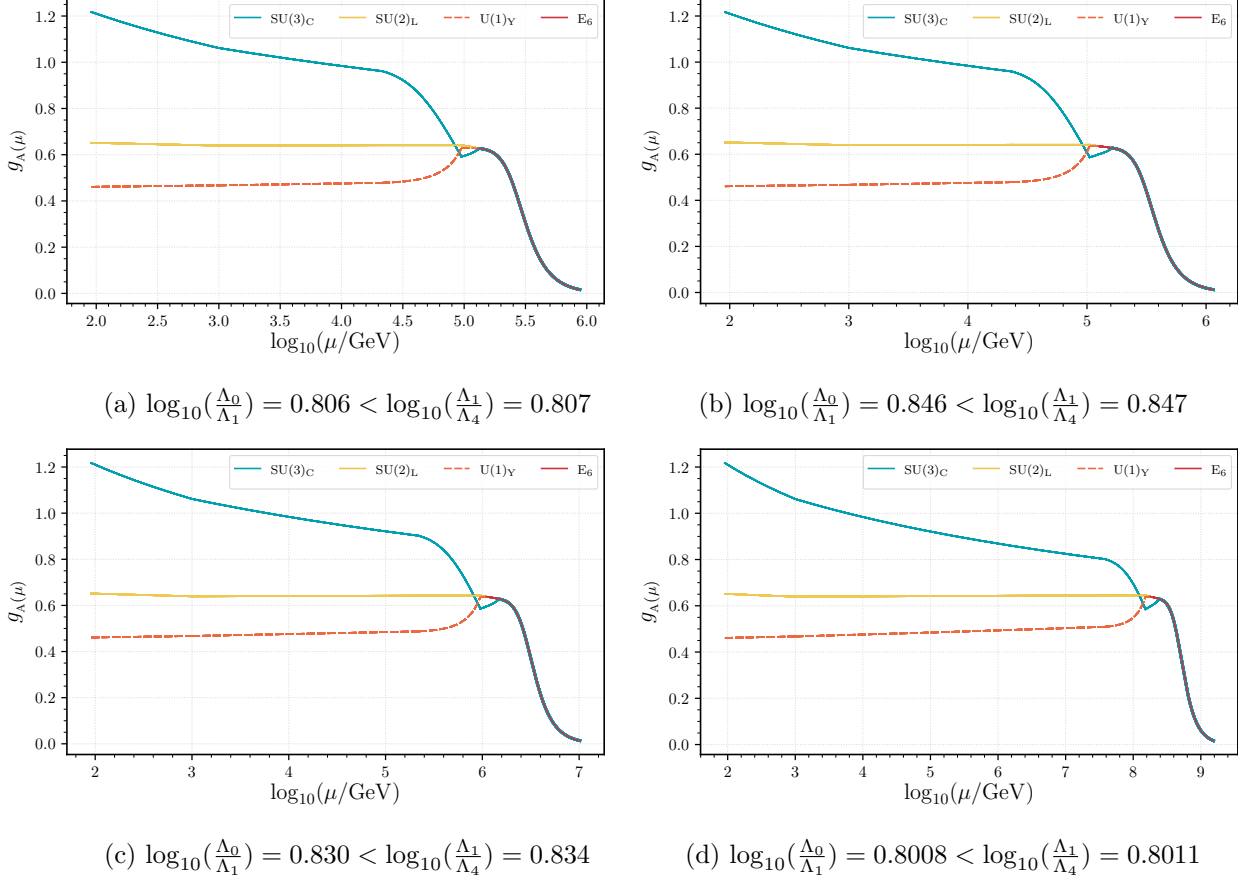


FIG. 10: RG evolution of the gauge couplings for four selected scenarios. Scale hierarchies agree with the consistency criterion defined above Eq. (5.8). The  $U(1)_Y$  line denotes the running of the GUT-normalized  $\sqrt{\frac{5}{3}}g_Y$  gauge coupling.

prediction emerging from the analysis is that such particles, in the context of this GUT, must only manifest themselves, at future colliders, between the scales of approximately 100 TeV and 100 PeV.

The  $\Lambda_3$  scale is also characterized by the breaking of SUSY. One can then define a SUSY breaking mass parameter  $m_0 = \Lambda_3$  that, up to threshold corrections (both at tree and loop level), sets an overall size for the scalar masses. The strongest bound comes from direct squark searches at the LHC that constrain  $m_0$  as [81]

$$m_0 > 1.6 \text{ TeV}, \quad (5.13)$$

which is well below  $\Lambda_3$ . In fact, it is expected that the mass of all scalars in the model are not far from  $\Lambda_3$  even after RG running effects are taken into account. However, the model can only be viable if a colour neutral EW doublet becomes light and can radiatively break the EW symmetry. A proof of concept analysis to such a crucial question will be presented in Sec. VC.

The masses of all KK modes in the model are integer multiples of the  $\Lambda_0$  and  $\Lambda_3$  scales. The strongest phenomenological constraints on the size of EDs result from Flavour Changing Neutral Currents (FCNC), essentially caused by KK gluons as well as EW  $S, T, U$  precision observables, which can be mostly affected by KK  $W_R$  bosons. Current searches pose a lower bound on the size of KK excitations that reads as [89, 90]

$$\frac{1}{R_{1,2,3}} > 6 \text{ TeV} , \quad (5.14)$$

also safely below the prediction of the model where the lighter KK modes should be as heavy as 100 TeV.

## B. Constraints from gaugino masses

Finally, gaugino masses are generated at two-loop level and thus are expected to be smaller than the  $\Lambda_3$  scale. Therefore, their role in the model should be carefully discussed. The strongest restriction may come from direct searches for gluino masses which, according to Fig. 90.2 (right-panel) of [81] must be bounded as

$$m_{\tilde{g}} > 2 \text{ TeV} . \quad (5.15)$$

Note that all scalars but the Higgs boson are expected to be of the order of the  $\Lambda_3$  scale. Exclusion limits for charginos and neutralinos should also be seen in a context where the only light scalar is the Higgs boson. Therefore, the most stringent constraints on their mass can be read off from Fig. 90.5 (right-panel) of [81]. For instance, with a neutralino mass up to approximately 250 GeV the limit on the chargino mass reads

$$m_{\tilde{\chi}^\pm} > 650 \text{ GeV} . \quad (5.16)$$

The latter becomes unconstrained when the neutralino mass is heavier than 300 GeV. Finally, neutralino masses are bounded from below as

$$m_{\tilde{\chi}^0} > 116 \text{ GeV} . \quad (5.17)$$

For a better indication of the excluded regions one can see the red contour in Fig. 90.5 (right-panel) of [81]. However, it is relevant to mention that these limits are merely indicative since current searches assume that neutralinos are stable particles, which does not apply in this case. In fact, the model proposed in this article does not possess R-parity and both the gaugino and Higgsino (or vector-like lepton) components of the charginos and neutralinos do decay into lighter states, including SM-like leptons.

For a reliable comparison of the gaugino masses predicted by the model under consideration with current experimental bounds, one needs to study the RG evolution of the gluino, wino and bino mass parameters from the  $\Lambda_3$  scale, where they are generated, down to  $\Lambda_5 = 1 \text{ TeV}$ . At this stage, and for a cleaner analysis, a simplified *proof-of-concept* estimation is performed with the following assumptions:



- Below the  $\Lambda_3$  scale, besides gauginos and Higgsinos, whose masses are radiatively generated, only two Higgs doublets are considered. This will avoid unnecessary complications for the level of accuracy being asked for. In essence, at this level, the EFT scenario resembles a type-II 2HDM with additional vector-like fermions (gauginos and Higgsinos).
- The running only includes contributions from the dominant, tree-level generated, interactions with both D-term and F-term origin. Those are the top and bottom quark ones,  $y_t$  and  $y_b$ , as well as four gaugino-Higgs-Higgsino Yukawa couplings denoted as  $y_{\tilde{w}1}$ ,  $y_{\tilde{w}2}$ ,  $y_{\tilde{b}1}$  and  $y_{\tilde{b}2}$ . The labels 1 and 2 identify the coupling to down-type and up-type Higgs doublets, respectively. For completeness, the relevant interactions to consider read as

$$\mathcal{L} \supset y_t u^c Q H_u + y_b d^c Q H_d + y_{\tilde{b}1} \tilde{b} \tilde{H}_d H_d + y_{\tilde{b}2} \tilde{b} \tilde{H}_u H_u + y_{\tilde{w}1} \tilde{w} \tilde{H}_d H_d + y_{\tilde{w}2} \tilde{w} \tilde{H}_u H_u, \quad (5.18)$$

where explicit contraction of gauge indices has been omitted.

- The gaugino-Higgs-Higgsino Yukawa couplings are tree-level matched to SUSY D-terms. Using the results in the Appendix C of [20] (see Tab. 17) to determine, to a first approximation, their values at the  $\Lambda_3$  scale gives

$$y_{\tilde{b}1} = y_{\tilde{b}2} = y_{\tilde{w}1} = \sqrt{2}g_1, \quad y_{\tilde{w}2} = \sqrt{2}g_2. \quad (5.19)$$

The simplified model was implemented in SARAH 4.14.3 [91] and the RGEs describing the evolution of the 4d theory were determined. With this information, contributions from KK modes are trivially included using the particle content in Tab. XVI. Notice that due to left and right-chiralities, internal loops of KK fermions must contribute with a factor of two in the coefficients of the beta functions [92]. The RGEs of the gaugino masses, including KK modes, read as

$$\begin{aligned} \kappa\beta_{M_{\tilde{g}}}^{(1)} &= \kappa\tilde{\beta}_{M_{\tilde{g}}}^{(1)} = -18M_{\tilde{g}}g_3^2, \\ \kappa\beta_{M_{\tilde{w}}}^{(1)} &= M_{\tilde{w}}(-12g_2^2 + y_{\tilde{w}1}^2 + y_{\tilde{w}2}^2), \quad \kappa\tilde{\beta}_{M_{\tilde{w}}}^{(1)} = -12M_{\tilde{w}}g_2^2\kappa, \\ \kappa\beta_{M_{\tilde{b}}}^{(1)} &= 2M_{\tilde{b}}(y_{\tilde{b}1}^2 + y_{\tilde{b}2}^2), \quad \kappa\tilde{\beta}_{M_{\tilde{b}}}^{(1)} = 0, \end{aligned} \quad (5.20)$$

with  $\kappa = 16\pi^2$ . The  $y_{\tilde{b}i}$  and  $y_{\tilde{w}i}$  beta functions can be found in Appendix H. The gauge coupling's contributions for  $M_{\tilde{g}}$  and  $M_{\tilde{w}}$  dominate the running for both the logarithmic and the power-law stages. Furthermore, the negative beta function coefficient for such terms implies that  $M_{\tilde{g}}$  and  $M_{\tilde{w}}$  must grow as the RG scale is lowered. On the contrary, the bino mass must slowly decrease as a result of a pure logarithmic and positive running. The main question to address here is how light can a gaugino be at the  $\Lambda_3$  scale such that its mass at the  $\Lambda_5$  scale can evade experimental constraints. For a clean analysis a generalized gaugino mass parameter  $m_{1/2}$  is defined, whose leading order contribution is given by Eq. (2.12). Using the expression for  $\mathbf{w}^2$  in Eq. (E9), and, based on the ED spacetime geometry, it must

be proportional to  $1/R_1$  which is here called  $\Lambda_3$  and its proportionality constant  $\xi$ . Assuming that each Wilson line effective VEV can lie in the range  $0.01\Lambda_3$  up to  $6\pi\Lambda_3$  one can write

$$\mathbf{w}^2 = \xi^2 \Lambda_3^2, \quad \text{with} \quad 1 \lesssim \xi^2 \lesssim 100. \quad (5.21)$$

Replacing this in Eq. (2.12),  $m_{1/2}$  can then be expressed as

$$m_{1/2} \approx \xi^5 l^2 g_3^4 \Lambda_3, \quad (5.22)$$

where  $l$  is a loop factor and  $g_3$  the  $SU(3)_C$  gauge coupling, which, at the  $\Lambda_3$  scale, is smaller than  $g_1$  and  $g_2$ , thus representing the most restrictive example for the estimate. Four representative possibilities of a sample of randomly generated values for the size of the product  $\xi^{5/2}l$  were selected, and, for each of the benchmark scenarios under consideration, the gaugino mass RGEs were numerically integrated in order to determine the  $\Lambda_5$  scale values of the gluino, wino and bino mass parameters. Fixing the bottom and top Yukawa couplings at the  $\Lambda_3$  scale to  $y_b \approx g_3 = 0.6$  and  $y_t = 0.85$ , reproduces EW scale values with the correct sizes. The results are shown in Tab. IX. Overall, it is observed that the model is consis-

$\xi^{5/2}l$	$m_{1/2}/\text{TeV}$				$M_{\tilde{g}}(\Lambda_5)/\text{TeV}$				$M_{\tilde{w}}(\Lambda_5)/\text{TeV}$				$M_{\tilde{b}}(\Lambda_5)/\text{TeV}$			
	(a)	(b)	(c)	(d)	(a)	(b)	(c)	(d)	(a)	(b)	(c)	(d)	(a)	(b)	(c)	(d)
0.094	0.109	0.120	1.09	173	0.953	1.08	9.83	1550	0.296	0.334	3.02	469	0.107	0.118	1.07	166
0.141	0.246	0.269	2.46	389	2.15	2.42	22.2	3490	0.667	0.748	6.82	1056	0.242	0.265	2.41	373
0.47	2.73	2.99	27.3	4320	23.9	26.9	246	38800	7.40	8.31	75.7	11700	2.69	2.95	26.7	4140
0.94	10.9	11.9	109	17300	95.3	107	983	155000	10.7	33.1	302	46900	5.99	11.7	107	16600

TABLE IX: Universal gaugino mass parameter  $m_{1/2}$  and low-scale values for physical gaugino masses in terms of the product of the loop parameter  $l$  and the Wilson line overall scale  $\omega$ , for each of the four benchmark scenarios under consideration. Red numbers indicate likely excluded scenarios whether orange, green, magenta and blue denote still boarder line allowed, allowed and accessible to either LHC or future 100 TeV colliders, possibly still at the reach of 100 TeV colliders and well beyond the reach of 100 TeV collision experiments.

tent with direct searches for gaugino masses apart from scenarios (a) and (b) if the product  $\xi^{5/2}l = 0.094$  or smaller. If this is the case then the  $E_8$  breaking scale would have to be larger than  $\log_{10}(\Lambda_0/\text{GeV}) > 6.06$ . On the other hand, for the case of  $\mathbf{w}^2 = \xi^2 \Lambda_3^2 = 0.141$ , those same benchmark scenarios become allowed and can be rather interesting already in the context of gaugino searches at the LHC run III. For the values of  $\xi^{5/2}l$  in Tab. IX scenario (d) seems to be essentially out of reach, even of a 100 TeV collider. Note that with the current estimate we are neither imposing a specific size for the loop factor  $l$  nor for the Wilson line overall scale  $\xi$  leaving such details for a dedicated work. However, it is possible to comment that, if one has, for example,  $l \sim 0.01$ , then, scenarios (a) and (b) on the first line of Tab. IX strongly disfavour  $\xi^2 \lesssim 6$ , i.e.  $\mathbf{w}^2 \lesssim 6\Lambda_3^2$ . For illustration purposes, the left panel of Fig. 11 presents scenario (a) with  $\xi^{5/2}l = 0.141$ , while on the right panel scenario (d) with  $\xi^{5/2}l \approx 0.01$  (not in Tab. IX) is showcased. This figure also highlights the importance of KK modes in the running, significantly contributing to enhance the gluino and wino masses. Such an effect is more pronounced for lower unification scale scenarios.



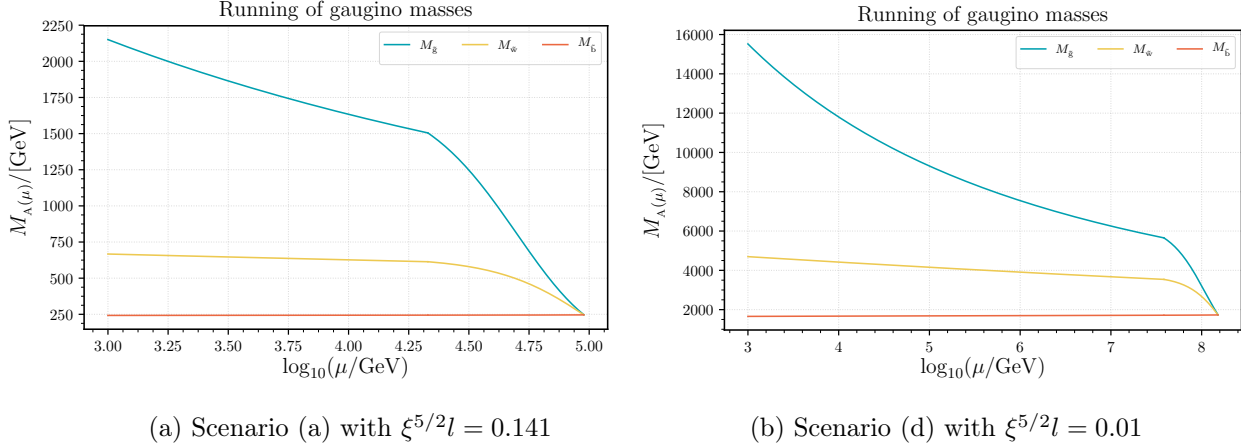


FIG. 11: RG running of the gaugino masses.

A dedicated analysis to the determination of  $l$  is beyond the scope of this article. However, it can significantly refine both the prediction for gaugino masses as well as possibly further constraining the GUT scale. Note that proton decay limits are also relaxed when loop factors become smaller than  $l \lesssim 0.1$ . This suggests that the stricter constraints, but at the same time the most interesting new-physics smoking gun signatures of the model, may come from gaugino-like particle searches at collider experiments.

### C. Radiative breaking of the EW symmetry – a proof-of-concept analysis

The masses of all scalars in the model, including those of all six Higgs doublet candidates, three of them up-type specific and three down-type specific, are tree-level generated at the  $\Lambda_3$  scale. They are induced by Wilson-line effective VEVs and their size is then of the order  $O(\Lambda_3)$ , well above the EW scale. The question then is whether the model is consistent with a valid Higgs sector and, in particular, with the EW scale. While the possibility of postulating Wilson-line VEVs along the  $SU(2)_L \times U(1)_Y$  breaking direction at the EW-scale is not forbidden, there is no fundamental reason for the latter to be realized well below  $\Lambda_3$ . On the other hand, a rather appealing scenario is that of *radiative EW symmetry breaking* (REWSB), where the EW scale,  $\Lambda_6$ , is quantum generated through the RG evolution of the Higgs mass parameter.

The goal in what follows is to show that the EW symmetry can be broken at the desired scale, i.e. 100 GeV to 1 TeV, for a scalar potential generated at a much larger energy-scale. To this end a simplified picture is sufficient while an exhaustive and lengthy analysis is beyond the scope of this article. Therefore, the same type-II 2HDM scenario with an extended fermion sector used above for the running of gaugino masses will be considered.

Let the scalar potential be:

$$V(H_u, H_d) = m_1^2 H_d^\dagger H_d + m_2^2 H_u^\dagger H_u + \lambda_1 (H_d^\dagger H_d)^2 + \lambda_2 (H_u^\dagger H_u)^2 + \lambda_3 (H_d^\dagger H_d)(H_u^\dagger H_u) \\ + \lambda_4 (H_d^\dagger H_u)(H_u^\dagger H_d) + \frac{1}{2} \lambda_5 [(H_u^\dagger H_d)^2 + \text{h.c.}] + m_{12}^2 (H_u^\dagger H_d + \text{h.c.}) . \quad (5.23)$$

Recall that Higgsino masses are radiatively generated at one-loop and therefore are lighter than the  $\Lambda_3$  scale. This means that Higgsino bilinear interactions must also be included in the RG evolution of the theory parameters. While the model contains three Higgsino families in this proof-of-concept analysis we only consider one generation such that the bilinear terms can be cast as

$$M_E \tilde{H}_u \tilde{H}_d + M_{EL} \tilde{H}_u L + \text{h.c.} . \quad (5.24)$$

Our target is to understand whether  $m_1^2$  or  $m_2^2$  can run to negative values such that, at the EW scale, the vacuum in the  $SU(2)_L \times U(1)_Y$  direction is destabilized. The beta-functions of the Higgs mass parameters read as

$$\begin{aligned} \kappa \beta_{m_1^2}^{(1)} &= -\frac{9}{10} g_1^2 m_1^2 - \frac{9}{2} g_2^2 m_1^2 + 12 \lambda_1 m_1^2 + 4 \lambda_3 m_2^2 + 2 \lambda_4 m_2^2 + 6 m_1^2 y_b^2 \\ &\quad + 2 (m_1^2 - 8 M_b^2) y_{b1}^2 + 3 (m_1^2 - 8 M_{\tilde{w}}^2) y_{\tilde{w}1}^2 - 4 M_E^2 y_{b1}^2 - 6 M_E^2 y_{\tilde{w}1}^2, \\ \kappa \tilde{\beta}_{m_1^2}^{(1)} &= -\frac{9}{10} g_1^2 m_1^2 - \frac{9}{2} g_2^2 m_1^2 + 12 \lambda_1 m_1^2 + 4 \lambda_3 m_2^2 + 2 \lambda_4 m_2^2 + 12 m_1^2 y_b^2 \\ &\quad + 4 (m_1^2 - 8 M_b^2) y_{b1}^2 + 6 (m_1^2 - 8 M_{\tilde{w}}^2) y_{\tilde{w}1}^2 - 8 M_E^2 y_{b1}^2 - 12 M_E^2 y_{\tilde{w}1}^2, \\ \kappa \beta_{m_2^2}^{(1)} &= -\frac{9}{10} g_1^2 m_2^2 - \frac{9}{2} g_2^2 m_2^2 + 12 \lambda_2 m_2^2 + 4 \lambda_3 m_1^2 + 2 \lambda_4 m_1^2 + 6 m_2^2 y_t^2 \\ &\quad + 2 (m_2^2 - 8 M_b^2) y_{b2}^2 + 3 (m_2^2 - 8 M_{\tilde{w}}^2) y_{\tilde{w}2}^2 - 4 (M_E^2 + M_{LE}^2) y_{b2}^2 \\ &\quad - 6 (M_E^2 + M_{LE}^2) y_{\tilde{w}2}^2, \\ \kappa \tilde{\beta}_{m_2^2}^{(1)} &= -\frac{9}{10} g_1^2 m_2^2 - \frac{9}{2} g_2^2 m_2^2 + 12 \lambda_2 m_2^2 + 4 \lambda_3 m_1^2 + 2 \lambda_4 m_1^2 + 12 m_2^2 y_t^2 \\ &\quad + 4 (m_2^2 - 8 M_b^2) y_{b2}^2 + 6 (m_2^2 - 8 M_{\tilde{w}}^2) y_{\tilde{w}2}^2 - 8 (M_E^2 + M_{LE}^2) y_{b2}^2 \\ &\quad - 12 (M_E^2 + M_{LE}^2) y_{\tilde{w}2}^2, \end{aligned} \quad (5.25)$$

where  $\kappa = 16\pi^2$ . The quartic couplings and Higgsino mass parameters beta-functions can be found in Appendix H. As the RG scale evolves towards lower values, the  $y_t$  and  $y_b$  parameters, whose sign is positive, become larger and start dominating the running. This means that both  $m_1^2$  and  $m_2^2$  run towards smaller values.

The Higgs sector quartic couplings are of D-term origin. As a first approximation, using the results in the appendix of [20], the  $SU(2)_L$  gauge coupling can be matched as follows

$$-\lambda_1 \approx -\lambda_2 \approx -\lambda_3 \approx \lambda_4 \approx \lambda_5 \approx \frac{1}{4} g_2^2, \quad (5.26)$$

whereas Higgsino and gaugino masses are assumed to be of the same order. In Fig. 12 one example point is shown for each of the four scenarios under consideration in Tab. VIII where REWSB is successfully achieved. The EW-scale values of the  $m_1$  and  $m_2$  mass parameters are

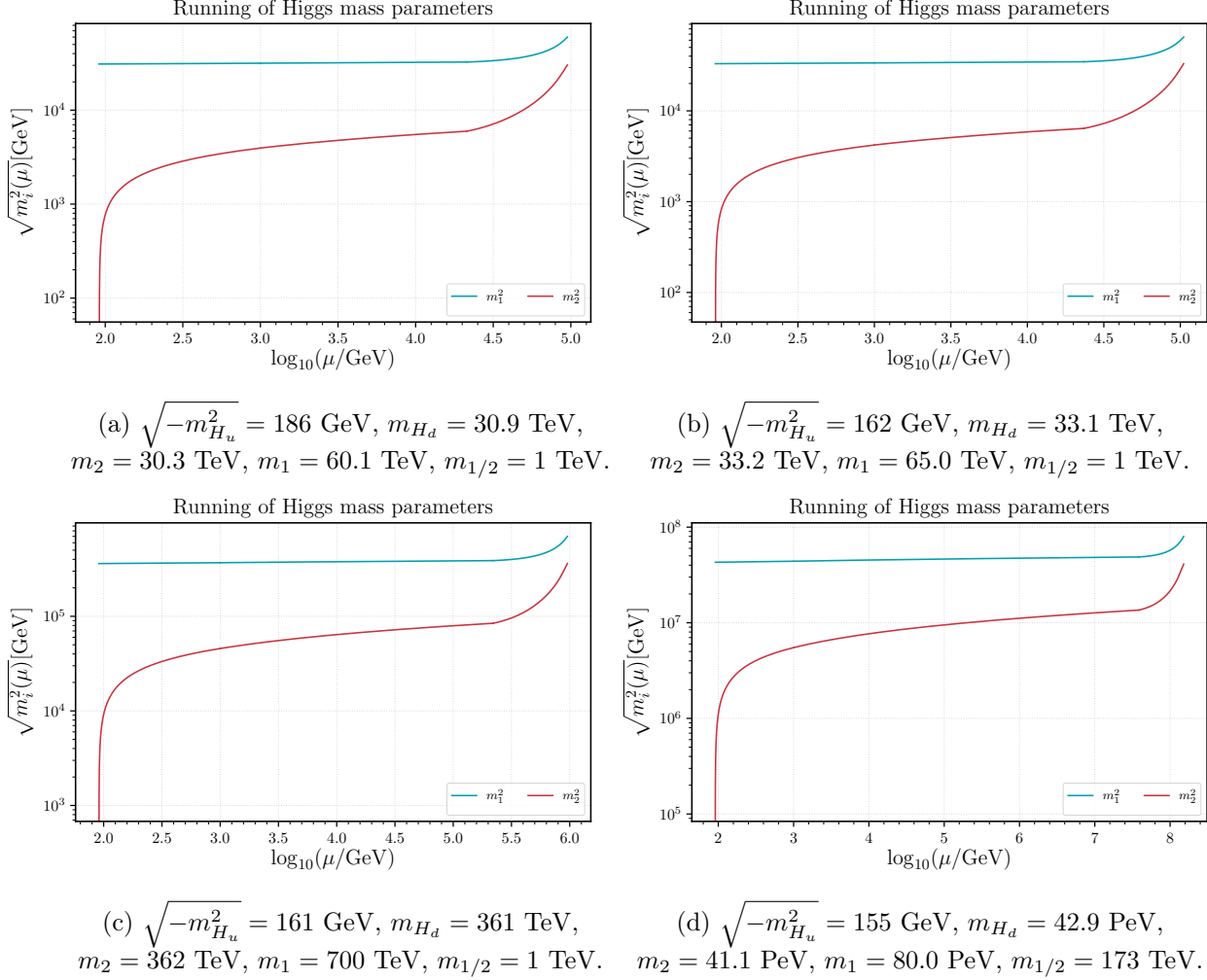


FIG. 12: RG running of the Higgs mass parameters. The values of  $m_1$  and  $m_2$  at the  $Z$ -boson mass scale are denoted as  $m_{H_d}$  and  $m_{H_u}$ , respectively.

denoted as  $m_{H_d}$  and  $m_{H_u}$ , respectively. In the four example points shown, it is the squared mass of the up-type Higgs doublet that runs to negative values, thus driving the breakdown of the EW symmetry. It is also seen that  $m_{H_u}$  can acquire a magnitude compatible with that of the EW scale, i.e.  $m_{H_u} \sim \mathcal{O}(100 \text{ GeV})$ , if the ratio  $m_1/m_2 \approx 2$  at the  $\Lambda_3$  scale. On the other hand, the magnitude of the  $m_{H_d}$  parameter only differs from that of  $m_1$  approximately by a factor of two. This is indeed a reliable possibility consistent with Eq. (2.15) (fourth line) where it can be seen that  $m_1 > m_2$ . Furthermore, there is enough freedom to choose the necessary mass splitting between  $m_1$  and  $m_2$  in order to consistently drive REWSB. A similar behaviour in the full, six-doublet case is expected, with the lightest, up-specific doublet developing a negative squared mass value and inducing REWSB. Indeed, the running of the Higgs mass parameter is dominantly controlled by the top-quark Yukawa coupling term as the EW scale is approached,  $\kappa\beta_{m_2^2}^{(1)} \approx 6m_2^2 y_t^2$ , which means that the lighter  $m_2^2$  is the faster

it will run negative. Even more tantalizing is the fact that the up-type Higgs doublets mass sub-matrix in Eq. (2.15) is rank-2. This means that, at leading order, independently of the scales involved, there is always a massless eigenstate. In turn, one expects that in the mass basis, there will always be a lighter scalar with squared mass radiatively generated and of order  $m_{H_u}^2 + l^2 \Lambda_3^2$ , with a loop factor  $l$ .

This picture suggests that only one light physical Higgs boson exists in the particle spectrum, well decoupled from the remaining heavy scalars. The model is then expected to be consistent with the alignment limit, where Higgs boson couplings to fermions and gauge bosons are essentially SM-like. The low-scale scenario revealed in this example, with only one light doublet, appears to be an emergent feature of the model that we expect to see replicated in the full six-doublet case.

### *Flavour Changing Neutral Currents*

The existence of more than one neutral Higgs states may mediate FCNCs which are highly constrained as they have not been detected experimentally. Having one up-type and one down-type Higgs specific doublets does not generate FCNCs. In this model, the lightest neutral Higgs scalar lies mainly inside  $H_{u1}$  (although it is a linear combination of all of them). The second lightest would come mainly from  $H_{d1}$ . As they come mainly from an up-type and down-type pair, they would generate negligible FCNCs.

The third lightest neutral Higgs is the main source of FCNCs. While the specific FCNCs depend on the couplings, with the lightest one having a mass of 125 GeV, the one that generates FCNCs must have a mass larger than 150 TeV to avoid all constraints, regardless of its couplings [93]. It can be seen in Fig. 12 that this condition can be met somewhere between the case (b) and (c). Therefore, there is a viable range of energies where the FCNCs generated by the model are negligible and naturally avoid experimental bounds.

### **D. An estimate for the quark mass spectra**

Similarly to what has been previously discussed in [19], the top and charm masses in this model are degenerate at tree-level. Therefore, a realistic mass spectrum must be induced beyond leading order. In what follows a proof of concept is shown, in order to demonstrate that the model contains the necessary freedom to consistently generate a realistic mass spectrum for the up-type quarks. Notice that the up-type quark sector deserves a special attention as it requires the larger corrections in the model while possessing less structure in comparison both to the down-type quark and the lepton sectors (see Eqs. (2.7) and (2.8)).

One of the key features of the model is a rich flavour structure that, besides three flavon and sneutrino VEVs, includes three generations of both up-specific and down-specific Higgs doublets. The up, charm and top quark masses depend on the up-specific Higgs doublet VEVs  $\langle H_{ui} \rangle$ , which at leading order, can be cast as as

$$m_{t,c} = y_q \sqrt{\langle H_{u1} \rangle^2 + \langle H_{u2} \rangle^2 + \langle H_{u3} \rangle^2}, \quad m_u = 0. \quad (5.27)$$

It is clear that a realistic mass spectrum requires corrections beyond zeroth order which, for the case of chiral up-type quarks, result from the left diagram in Fig. 6 and the first line in Eq. (2.7). Therefore, if one includes one-loop contribution, the corrected Lagrangian can be recast as

$$\mathcal{L}_{mq} = \epsilon^{ijk} u_a^c Q_b \langle H_{ui} \rangle \left[ y_q \delta_j^a \delta_k^b + \sum_{\Delta} \frac{N_{\Delta} f(m_{\Delta}, m_{aj}, m_{bk})}{\Lambda^2} ((\mathbf{w}^2)_j^a \delta_k^b - (\mathbf{w}^2)_k^b \delta_j^a) \right], \quad (5.28)$$

where the loop function is given by

$$f(m_{\Delta}, m_{aj}, m_{bk}) = \frac{1}{16\pi^2} \frac{8}{3} g^2 \frac{A_{S_i S_j S_k} m_{\Delta}}{m_{\Delta}^2 - m_{aj}^2} \left( \frac{m_{aj}^2 \log \frac{m_{bk}^2}{m_{aj}^2}}{m_{aj}^2 - m_{bk}^2} - \frac{m_{\Delta}^2 \log \frac{m_{bk}^2}{m_{\Delta}^2}}{m_{\Delta}^2 - m_{bk}^2} \right). \quad (5.29)$$

The  $y_{F_q}$  couplings in Eq. (2.7) are represented here by  $\sum_{\Delta} N_{\Delta} f(m_{\Delta}, m_{aj}, m_{bk})$  up to CGCs. While  $A_{S_i S_j S_k}$  denotes the scalar triple coupling  $S : \mathbf{L} \mathbf{Q}_L \mathbf{Q}_R$ ,  $m_{\Delta}$  is a SUSY preserving heavy gaugino mass and  $N_{\Delta}$  is a factor accounting for the multiplicity of index contractions in each of the two lower vertices in Fig. 6. Take for example  $\Delta = \lambda_L^8 \lambda_R^8$  where, using Eq. (E12),

$$m_{\Delta}^2 \equiv (M_L^{\dagger} M_R)_8 = g^2 \left( \frac{4}{3} \langle \tilde{\nu}^{c\dagger i} \tilde{\nu}_i^c \rangle - \frac{2}{3} \langle \varphi^{\dagger i} \varphi_i \rangle \right). \quad (5.30)$$

If the  $\langle \mathcal{D} \rangle$ -term insertion is on the left vertex there are three possible  $SU(2)_L$  index contractions whereas if  $\langle \mathcal{D} \rangle$  is inserted on the right vertex, as in the figure, there are three  $SU(2)_R$  independent contractions. This means that for such a gaugino propagator with mass  $m_{\Delta}^2$  we have  $N_{\Delta} = 6$ . The  $m_{bk}$  and  $m_{aj}$  parameters represent the linear mass of the scalar propagators  $\mathbf{Q}_L$  and  $\mathbf{Q}_R$  respectively. The latter are taken from the scalar potential in Eq. (2.15) and can be expressed in terms of the Wilson-line VEVs as

$$m_{ai}^2 = g^2 (\langle \tilde{\nu}^{c\dagger a} \tilde{\nu}_i^c \rangle + \langle \varphi^{\dagger a} \varphi_i \rangle). \quad (5.31)$$

Last but not least, the trilinear couplings  $A_{S_i S_j S_k}$  are of SUSY breaking origin and radiatively generated at one-loop. While a complete calculation of the trilinear sector is beyond the scope of this article, one sees by inspection of the second term in Eq. (2.13) and Eq. (E7) that the leading order contributions to the A-terms scale as

$$A_{S_i S_j S_k} \sim g^5 l \frac{\langle \mathcal{D} \rangle^2}{\Lambda_3^3}. \quad (5.32)$$

Noting that the size of the Wilson-line VEVs is limited from above to be smaller than  $6\pi$ , we can recast the D-term contribution as  $\mathcal{D} \sim c^2 \Lambda_3^2$ , with  $c < 6\pi$ , such that

$$A_{S_i S_j S_k} \sim g^5 l c^4 \Lambda_3. \quad (5.33)$$

While  $c$  is a non-trivial combination of Wilson-line VEVs, in what follows  $l \sim 0.01$  is considered. One also takes a conservative approach where  $\max(c) \approx 5$  such that  $A_{S_i S_j S_k} \lesssim 0.5 \Lambda_3$  in the numerical estimate.

In what follows it is convenient to redefine the Wilson-line effective VEVs in terms of the SUSY breaking scale  $\Lambda_3$  as

$$\langle \tilde{\nu}_i^c \rangle \equiv a_i \Lambda_3, \quad \langle \varphi_i \rangle \equiv b_i \Lambda_3, \quad (5.34)$$

with  $0.01 < a_i, b_i < 6\pi$  and where the upper limit is constrained by the orbifold geometry. For simplicity, solely  $\lambda_{L,R,F}^3$  and  $\lambda_{L,R,F}^8$  gauginos are considered as internal propagators in the left diagram of Fig. 6. A complete analysis is beyond the scope of this article. Finally, the three up specific Higgs doublet VEVs are cast as

$$\langle H_{ui} \rangle = \kappa_{ui} v_{EW}, \quad v_{EW} \approx 246 \text{ GeV}, \quad (5.35)$$

where, from the discussion in Sec. VC,  $|\kappa_{u1}| \gg |\kappa_{u2,3}|$  and  $|\kappa_{u1}|^2 + |\kappa_{u2}|^2 + |\kappa_{u3}|^2 < 1$  such that the EW breaking VEV is mostly aligned with the doublet that radiatively develops a negative squared mass. With this information, a parameter scan is set, varying the relative size of the Wilson line parameters  $a_i$  and  $b_i$ , where four representative scenarios were selected and shown in Tab. X. Since a complete determination of the SUSY breaking trilinear couplings is left for a dedicated study, in this example, and for illustrative purposes, they are fixed as

$$A_{\mathbf{L}_1 \mathbf{Q}_L \mathbf{Q}_R}^u = 0.0865, \quad A_{\mathbf{L}_2 \mathbf{Q}_L \mathbf{Q}_R}^u = 0.0646, \quad A_{\mathbf{L}_3 \mathbf{Q}_L \mathbf{Q}_R}^u = 0.0649. \quad (5.36)$$

Furthermore, the Higgs sector is chosen to be

$$\kappa_{u1} = 0.9, \quad \kappa_{u2} = -0.0115, \quad \kappa_{u3} = -0.0150, \quad (5.37)$$

such that the EW breaking VEV is mostly aligned with the first up-type Higgs doublet in agreement with the RG analysis above. This allows one to define the up-type quark masses at the  $\Lambda_3$  scale as

$$m_{u,c,t}(\Lambda_3) \approx \frac{v_{EW}}{\sqrt{2}} \sqrt{\kappa_{u1}^2 + \kappa_{u2}^2 + \kappa_{u3}^2} y_{u,c,t}(\Lambda_3). \quad (5.38)$$

It is interesting to note that with the appropriate choice of Wilson lines and a Higgs sector

Scenario	$a_1$	$a_2$	$a_3$	$b_1$	$b_2$	$b_3$	$m_t(\Lambda_3)/\text{GeV}$	$m_c(\Lambda_3)/\text{GeV}$	$m_u(\Lambda_3)/\text{MeV}$
(1)	0.102	6.572	2.525	0.061	5.023	0.973	174.02	1.627	0.791
(2)	0.052	3.153	0.916	0.102	6.872	2.275	173.70	1.670	1.661
(3)	0.111	5.023	0.993	0.0301	6.172	2.275	173.55	1.188	1.089
(4)	0.141	6.995	2.380	0.0101	3.953	0.994	174.39	1.922	2.553

TABLE X: Four example scenarios with consistent top, charm and up Yukawa couplings for  $g = 0.6$ .

mostly aligned with one of the up-specific doublets, the top, charm and up quark masses can be reproduced tantalisingly near their experimentally measured values. This proof-of-concept estimation is rather relevant as the tree-level relation in Eq. (5.27) puts one of the most stringent constraints on the model. Indeed, our estimation is suggesting that

a consistent up-type quark mass spectrum requires that the Wilson lines must obey the following hierarchies

$$\langle \tilde{\nu}_2^c \rangle \sim \langle \varphi_2 \rangle \gtrsim \langle \tilde{\nu}_3^c \rangle \sim \langle \varphi_3 \rangle > \langle \tilde{\nu}_1^c \rangle \sim \langle \varphi_1 \rangle, \quad (5.39)$$

with a maximum splitting among them, not larger than approximately two orders of magnitude. A complete analysis must also rely on RG effects where the largest, and perhaps the only really sizeable contribution, is on the running of the top-quark Yukawa coupling. Such effects are beyond the scope of this article and will be studied elsewhere.

An important question that is worth pursuing is whether the down-type quark sector is compatible with the up-type one. As a proof of concept estimation a potentially valid scenario may be accepted where the down, the strange and the bottom quark masses lie within one order of magnitude of their measured values. Due to unaccounted RG and threshold effects in this estimation, a configuration of the Higgs VEVs is assumed where  $\sum_{i=1}^3 \sqrt{\kappa_{ui}^2 + \kappa_{di}^2} \sim 1$  but not necessarily exact and up to a 5% uncertainty. Here the down-specific Higgs VEVs are defined as  $\langle H_{di} \rangle = \kappa_{di} v_{\text{EW}}$ .

Using the second to the fifth lines in Eq. (2.7), one can see that the  $D_a^c$  and the  $d_a^c$  right-handed quarks mix, which implies that all six left-handed and all six right-handed quarks must be included in the numerical estimation. For simplicity only the tree-level contribution are considered for the  $D^c D$  and  $d^c D$  mass terms (third and fourth lines in Eq. (2.7), respectively). The loop function is the same as in Eq. (5.29) where the  $m_{aj}$  and  $m_{bk}$  mass parameters are now taken from the third to the seventh terms in Eq. (2.15), which correspond to the scalar superpartners of the down-type quarks. Putting all together, and using the same Wilson lines as in Tab. X, the mass spectrum shown in Tab. XI is obtained at the  $\Lambda_3$  scale for

$$A_{\mathbf{L}_1 \mathbf{Q}_L \mathbf{Q}_R}^d = 0.015, \quad A_{\mathbf{L}_2 \mathbf{Q}_L \mathbf{Q}_R}^d = A_{\mathbf{L}_3 \mathbf{Q}_L \mathbf{Q}_R}^u = 0.011. \quad (5.40)$$

The down-type quark masses are also tantalizingly close to their measured values. In

Scenario	$\kappa_{d1}$	$\kappa_{d2}$	$\kappa_{d3}$	$m_b(\Lambda_3)/\text{GeV}$	$m_s(\Lambda_3)/\text{MeV}$	$m_d(\Lambda_3)/\text{MeV}$
(1)	-0.01	-0.3	0.01	6.642	204.2	0.176
(2)	-0.01	-0.31	-0.01	9.421	25.24	3.473
(3)	-0.01	-0.3	-0.01	7.618	97.57	1.618
(4)	0.01	-0.31	-0.31	5.809	93.52	1.180

TABLE XI: The down-type quark masses corresponding the the Wilson lines found in Tab. X.

particular, scenarios (3) and (4) reproduce the best results while in scenario (1) the strange mass is approximately a factor of two larger while the down quark is approximately an order of magnitude lighter. All in all, the results in Tabs. X and XI are rather promising showing that the rich Higgs and flavour structures of the model may very well allow a realistic mass spectrum, at least in the quark sector.

One can also discuss new physics implications emerging from the estimations in Tabs. X and XI. First, the three down type chiral quarks are accompanied by three vector-like triplet



counterparts. Setting the SUSY breaking scale  $\Lambda_3 = 100$  TeV the masses of the vector-like quarks (VLQs) as predicted by the four scenarios are shown in Tab. XII. With this estimate

Scenario	$m_B(\Lambda_3)/\text{PeV}$	$m_S(\Lambda_3)/\text{PeV}$	$m_D(\Lambda_3)/\text{PeV}$
(1)	27.31	27.21	2.274
(2)	25.77	25.77	0.358
(3)	26.15	26.08	2.011
(4)	27.36	27.34	0.963

TABLE XII: Vector-like quark masses corresponding the the Wilson lines found in Tab. X. The  $B$ ,  $S$  and  $D$  labels denote the vector-like bottom, strange and down quarks whose naming is solely based on their mass hierarchy in analogy with their chiral counterparts.

one can see that the scale of the VLQ masses is well beyond the reach of current collider experiments and no smoking gun signatures in such a sector are expected.

Last but not least, notice that upon expansion of the superpotential in Eq. (2.1), one obtains the following Yukawa interactions

$$\mathcal{L}_{LQ} \supset g\varepsilon^{ijk} \left( e_i^c u_j^c \tilde{D}_k + L_i Q_j \tilde{D}_k^c + \tilde{h}_{di} Q_k \tilde{d}_j^c + L_i \tilde{Q}_j D_k^c \right) + \mathcal{O} \left( \frac{1}{\Lambda^2} \right), \quad (5.41)$$

such that both  $\tilde{D}$  and a mixture of  $\tilde{D}^c - \tilde{d}^c$  behave as scalar singlet leptoquarks (LQs), whereas, due to the quark mixing  $D^c - d^c$ ,  $\tilde{Q}_j$  interacts as a scalar doublet LQ. Recall that the  $\tilde{h}_{di}$  Higgsinos, by virtue of their unification with leptons, can also be denoted as vector-like leptons as it was done in [20] and [94]. Using the same Wilson lines as in Tab. X the physical LQ masses for each of the four scenarios so far considered is presented in Tab. XIII. The doublet leptoquark mass for each of the rows is expressed as  $m_{\mathcal{U}_1} \sim \mathcal{O}(l\Lambda_3)$  because the

Scenario	$m_{\mathcal{D}_1}$	$m_{\mathcal{D}_2}$	$m_{\mathcal{D}_3}$	$m_{\mathcal{D}_1^c}$	$m_{\mathcal{D}_2^c}$	$m_{\mathcal{D}_3^c}$	$m_{\mathcal{D}_4^c}$	$m_{\mathcal{D}_5^c}$	$m_{\mathcal{D}_6^c}$	$m_{\mathcal{U}_1}$	$m_{\mathcal{U}_2}$	$m_{\mathcal{U}_3}$
(1)	523	524	738	43.5	61.6	521	523	523	737	$\mathcal{O}(l\Lambda_3)$	43.5	521
(2)	477	477	675	6.64	9.40	477	477	477	675	$\mathcal{O}(l\Lambda_3)$	6.64	477
(3)	501	502	707	38.5	54.5	499	501	501	706	$\mathcal{O}(l\Lambda_3)$	38.5	499
(4)	507	507	717	17.8	25.2	506	507	507	716	$\mathcal{O}(l\Lambda_3)$	17.8	506

TABLE XIII: Leading scalar leptoquark masses for the four example scenarios discussed in Tab. X. All masses are expressed in TeV. The mass eigenstates are cast with  $\mathcal{D}$  and  $\mathcal{U}$ .

tree-level mass form coming from the first term in Eq. (2.15) has rank two, thus containing a massless eigenvalue. While  $m_{\mathcal{U}_1}$  does contain EWSB scale effects, see Eq. (2.14), the dominant contributions are of radiative origin whose details are encoded, once again, in the loop factor  $l$ . One notes that, out of nine scalar singlet LQs and three doublets as predicted



by the model, two of the former and two of the latter can become rather light, and possibly at the reach of the LHC or future colliders, namely in scenario (2). Furthermore, the presence of such LQs can become relevant in light of the recently reported muon  $(g-2)_\mu$  [95] and B-physics anomalies, as discussed, for example, in [96–100]. It is important to remark that the model has no freedom to allow for a particular choice of LQ masses or any other BSM state. Instead, such a freedom can only be used to fit the chiral sector which will completely fix the domain of validity for the new physics predictions the model may be able offer. Further dedicated studies are needed for a comprehensive understanding which shall be discussed elsewhere.

### E. Smallness of neutrino masses

There are effectively six right handed neutrinos, three from the standard right handed fields  $\nu_i^c$  and three from the flavinos  $\tilde{\varphi}_i$ , which all but one obtain a Majorana mass at the  $\Lambda_3$  scale. The remaining one becomes a goldstino and behaves like a sterile neutrino. A Dirac mass term is also present at the EW scale but, like all lepton masses, they are suppressed by two loops. As there is a large mass difference between them, there is a standard seesaw mechanism in place, generating small left handed neutrino Majorana masses at the scale

$$m_{LL} \sim l^4 \frac{\langle H_u \rangle^2}{\Lambda_3} \frac{\mathbf{w}^4}{\Lambda^4}. \quad (5.42)$$

With the assumptions previously made,  $\mathbf{w}^2 \sim \Lambda^2$ , and depending on the loop factor being  $l \sim 0.1 - 0.01$ , the Majorana masses are required to be  $\Lambda_3 \sim 10^9 \text{ GeV} - 10^5 \text{ GeV}$  to achieve an  $m_{LL} \sim \mathcal{O}(\text{eV})$ . As seen in previous sections, this is exactly the expected range of  $\Lambda_3$  for the model, therefore the small neutrino masses can straightforwardly be explained. The knowledge of the exact neutrino mass scale would then help to define the GUT scale for this model.

## VI. CONCLUSION

A model with a single 10d gauge  $E_8$  superfield, effectively unifying all matter and gauge sectors of the SM, has been presented. The EDs are orbifolded as  $\mathbb{T}^6/(\mathbb{Z}_3^F \times \mathbb{Z}_3^C)$  whose extra dimensional rotational and translational boundary conditions break  $E_8 \rightarrow \text{SU}(3)_C \times \text{SU}(2)_L \times \text{U}(1)_Y$  after compactification. Furthermore, SUSY is broken in the process generating specific soft masses while gauge anomalies are absent at all levels without the need for extra fields.

The model contains a single arbitrary complex parameter, the gauge coupling, while the orbifold further introduces thirteen additional arbitrary complex parameters. These parameters completely define the model's freedom and it is shown that they are sufficient to generate a variety of phenomenologically viable low-scale scenarios of New Physics generally reproducing the basic properties of the SM. The model contains a viable flavour structure for all SM-like fermion masses. Furthermore, the mixing angles in the quark sector are naturally hierarchical while those in the lepton sector are expected to be consistent with a democratic

form. There are six right handed neutrinos which obtain a large Majorana mass so that a simple see-saw mechanism is in place.

Exact unification of the gauge couplings is achieved consistently. In particular, proton decay is strongly suppressed which enables a low unification scale (which is also the compactification scale) constrained to the range  $10^6 \lesssim M_{\text{GUT}} \lesssim 10^9$  GeV. While above the upper bound the gauge couplings can no longer meet without running into Landau poles, the lower one is set by proton lifetime. Therefore, the model necessarily contains unification at much lower scales than standard GUTs. Furthermore, the considered  $E_8$  GUT offers the required ingredients to consistently allow for radiative breaking of the EW symmetry as well as containing a single, light, SM-like Higgs boson candidate.

The most appealing New Physics candidates emergent from the discussed theory are vector-like fermions (gauginos and Higgsinos) as well as singlet and doublet leptoquark-like particles, which can manifest themselves not too far from the TeV scale or at the reach of near-future experiments. Most notably, even with a rather limited freedom but a remarkable predictive power, the model will allow for concrete New Physics predictions once the full SM-like sector is comprehensively derived from the details of the extra-dimensional space-time geometry.

## ACKNOWLEDGMENTS

The authors thank Mónica F. Ramírez for her support in generating the orbifold diagrams. This work has been supported in part by the MICINN (Spain) projects FIS2011-23000, FPA2011-27853-01, FIS2014-52837-P, FPA2014-53375-C2-1-P, Consolider-Ingenio MULTIDARK CSD2009-00064, SNI-CONACYT (México), by the Swedish Research Council grant, contract number 2016-05996, by the European Research Council (ERC) under the European Union's Horizon 2020 research and innovation programme (grant agreement No 668679), and by the FCT (Portugal) projects PTDC/FIS-PAR/31000/2017, CERN/FIS-PAR/0027/2019 and CERN/FIS-PAR/0002/2019. This work is also supported by the Center for Research and Development in Mathematics and Applications (CIDMA) through the Portuguese Foundation for Science and Technology (FCT), references UIDB/04106/2020 and, UIDP/04106/2020, and by national funds (OE), through FCT, I.P., in the scope of the framework contract foreseen in the numbers 4, 5 and 6 of the article 23, of the Decree-Law 57/2016, of August 29, changed by Law 57/2017, of July 19.

## Appendix A: ED field representations

Compactifying the EDs implies reduction of the Poincaré symmetry. The full global symmetry of the model is  $\mathcal{N} = 1$  super-Poincaré in 10d which has generators

$$\begin{aligned} [P^S, P^T] &= 0, & [M^{ST}, P^U] &= i(P^S \eta^{TU} - P^T \eta^{SU}), \\ [M^{ST}, M^{UV}] &= i(M^{SV} \eta^{TU} + M^{TU} \eta^{SV} - M^{SU} \eta^{TV} - M^{TV} \eta^{SU}), \\ \{Q_\alpha, \bar{Q}_{\dot{\beta}}\} &= 2\sigma_{\alpha\dot{\beta}}^S P_S, & [Q_\alpha, M^{ST}] &= (\sigma^{ST})^\beta_\alpha Q_\beta, \\ \{Q_\alpha, Q_\beta\} &= \{\bar{Q}_{\dot{\alpha}}, \bar{Q}_{\dot{\beta}}\} = 0, & [P_S, Q_\alpha] &= [P_S, \bar{Q}_{\dot{\beta}}] = 0, \end{aligned} \tag{A1}$$

where  $S = 0, 1, \dots, 3, 5, \dots, 10$  and  $\alpha, \dot{\beta} = 1, \dots, 8$ .

Specially relevant is the reduction of the Lorentz symmetry as every field lies in an irreducible representation of the Lorentz group before and after compactification. In  $N$  dimensions, the Lorentz group is  $\text{SO}(1, N-1)$ . After compactifying  $m$  spatial dimensions, it is reduced into  $\text{SO}(1, N-m-1)$ . The scalar fields are singlets of  $\text{SO}(1, N-1)$  and remain singlets of  $\text{SO}(1, N-m-1)$  after compactification. The vector fields have an  $(\mathbf{N})$  representation under  $\text{SO}(1, N-1)$ , as it is a vector with  $N$  components. It decomposes into an  $(\mathbf{N-m})$  vector and  $m \times (\mathbf{1})$  scalars under  $\text{SO}(1, N-m-1)$  after compactification. It is important to remark that all the studied vector fields are massless gauge vector fields, which have two degrees of freedom less than a general vector due to their gauge freedom and masslessness.

### 1. Fermions in EDs

Assuming a Minkowski metric with signature  $\eta^{MN} = \text{diag}(1, -1, \dots, -1)$ , the kinetic term for fermions reads

$$\mathcal{L}_\Psi = i\bar{\Psi}\Gamma^M\partial_M\Psi, \tag{A2}$$

where the Dirac matrices satisfy

$$\{\Gamma^M, \Gamma^N\} = 2\eta^{MN}. \tag{A3}$$

Starting from  $n$  even-dimensional Dirac matrices, one can define the  $n+1$  matrix multiplying every matrix

$$\Gamma^{n+1} = \Gamma^0 \cdot \Gamma^1 \dots \Gamma^n. \tag{A4}$$

Starting from  $n+1$  odd-dimensional Dirac matrices, the product  $\Gamma^0 \cdot \Gamma^1 \dots \Gamma^{n+1} = -1$ , is trivial, so it can not be used to build the  $n+2$  dimensional Dirac matrices. To do that one can define them in terms of the  $n$  dimensional Dirac matrices

$$\Gamma_{(n+2)d}^M = \begin{pmatrix} 0 & \Gamma_{nd}^M \\ \Gamma_{nd}^M & 0 \end{pmatrix}, \quad \Gamma_{(n+2)d}^{n+1} = \begin{pmatrix} 0 & \Gamma_{nd}^{n+1} \\ \Gamma_{nd}^{n+1} & 0 \end{pmatrix}, \quad \Gamma_{(n+2)d}^{n+2} = \begin{pmatrix} 0 & \mathbb{1}_{nd} \\ -\mathbb{1}_{nd} & 0 \end{pmatrix}, \tag{A5}$$

which are  $2^{n/2} \times 2^{n/2}$  matrices for even dimension  $d$  and  $2^{(n-1)/2} \times 2^{(n-1)/2}$ . Naturally, the fermion would have  $n/2$  components for even dimension or  $(n-1)/2$  components for odd dimension. However, this can be a reducible representation.

In even  $n$  dimensions, the  $n/2$  component fermion can be separated by eigenvalues of the matrix  $\Gamma_{nd}^{n+1}$  which defines the chirality. In odd  $n$  dimensions there is no chirality. A fermion satisfying  $\Psi = \pm \Gamma_{nd}^{n+1} \Psi$  is called a Weyl or a chiral fermion which exists for every even dimension. Note that chirality is different by a different matrix in every even dimension. One can also impose a real condition  $\Psi = \Psi^c$ , called Majorana condition, which can be satisfied non-trivially when  $n = 1, 2, 3, 4, 8, 9, 10$  (up to 10d). Only in  $n = 2, 10$  can both conditions be fulfilled simultaneously [101]. Note that for  $\mathcal{N} = 1$  SYM in  $n$  dimensions, one has a  $n$  dimensional vector and some representation of a  $n$  dimensional fermion. For SUSY to be consistent they must have the same degrees of freedom. This happens exactly in  $n = 4, 6, 10$ . In other spacetime dimensions, one has to also add scalar fields to match the degrees of freedom.

*a.  $\mathcal{N} = 1$  SUSY in six dimensions*

The  $\mathcal{N} = 1$  SYM theory in 6d is built from a gauge field  $A_M$  and a chiral fermion  $\Lambda$  in the adjoint representation with the Lagrangian

$$\mathcal{L}_{6d} = -\frac{1}{4}F_{MN}F^{MN} - i\bar{\Lambda}\Gamma^M D_M \Lambda, \quad (\text{A6})$$

where the Dirac matrices are  $8 \times 8$  components, the Dirac fermion has eight complex components, but the chiral fermion  $\Lambda = \frac{1}{2}(1 - \Gamma_7)\Lambda$  has four complex components<sup>6</sup>. The equations of motion of the 6d chiral fermion reduce the degrees of freedom to four. The 6d vector has six real components, whose gauge freedom and masslessness reduce them to four degrees of freedom. Together they form a 6d gauge vector supermultiplet.

By decomposing the 6d vector  $A_M$  into a 4d one  $A_\mu$  and two scalar components that form a complex scalar  $A = A_5 + iA_6$ , then writing the chiral fermion as  $\Lambda = (\chi, 0)^T$ , and decomposing the 6d chiral superfield into two 4d Majorana fermions  $\chi = (\lambda_1 - i\lambda_2)$ , the Lagrangian can be expanded as

$$\begin{aligned} \mathcal{L}_{6d} = & -\frac{1}{4}F_{\mu\nu}F^{\mu\nu} + (D_\mu A)^\dagger D^\mu A - i\bar{\lambda}\gamma^\mu D_\mu \lambda - i\bar{\psi}\gamma^\mu D_\mu \psi \\ & - \sqrt{2}[\lambda, \psi] - \sqrt{2}[\bar{\lambda}, \bar{\psi}] + \frac{1}{2}[A^\dagger, A]^2, \end{aligned} \quad (\text{A7})$$

this becomes a 4d  $\mathcal{N} = 2$  gauge supermultiplet built from a 4d  $\mathcal{N} = 1$  vector gauge supermultiplet and an adjoint chiral supermultiplet.

To build a matter 6d supermultiplet one would have to have a chiral fermion  $\Psi = \frac{1}{2}(1 + \Gamma_7)\Psi$  whose four degrees of freedom are matched by two complex scalars with the Lagrangian

$$\mathcal{L}_{6dm} = (D^\mu A)^\dagger D_\mu A + (D^\mu B)^\dagger D_\mu B + \frac{i}{4}\bar{\Psi}\gamma^\mu D_\mu \Psi, \quad (\text{A8})$$

---

<sup>6</sup> Note that the 6d chirality is not the same as 4d chirality. A 6d chiral fermion decomposes into a left and a right 4d chiral fermion pair

where, by decomposing the 6d chiral fermion  $\Psi$  into a 4d chiral left right fermion pair, one obtains an  $\mathcal{N} = 2$  hypermultiplet built from vector-like 4d chiral supermultiplet pair.

Note that there is no renormalizable 6d superpotential, just as there are no renormalizable  $\mathcal{N} = 2$  matter interactions. Therefore, an  $\mathcal{N} = 1$  SUSY 6d theory can be decomposed into an  $\mathcal{N} = 2$  SUSY 4d theory [101].

## 2. $\mathcal{N} = 1$ SUSY in ten dimensions

The  $\mathcal{N} = 1$  SYM theory in 10d is built from a gauge field  $A_M$  and a fermion  $\Lambda$  in the adjoint representation with the Lagrangian

$$\mathcal{L}_{10d} = -\frac{1}{4}F_{MN}F^{MN} - i\bar{\Lambda}\Gamma^M D_M \Lambda, \quad (\text{A9})$$

where the Dirac matrices have  $32 \times 32$  components, the Dirac fermion has 32 complex components. In 10d, a Weyl condition  $\Lambda = \frac{1}{2}(1 - \Gamma_{11})\Lambda$  can be imposed which reduces the fermion to sixteen components. In 10d (as well as in 2d) one can simultaneously impose the Majorana condition  $\Lambda = C\bar{\Lambda}^T$ , where  $C$  is the charge conjugation matrix, and further reduce the fermion into eight complex components. The equations of motion reduce the degrees of freedom down to eight. The vector has ten real components which are reduced by gauge freedom and masslessness to eight. Therefore, the fermion/scalar degrees of freedom are matched.

The 10d Weyl/Majorana fermion can be decomposed into four 4d Weyl (or Majorana as they are massless) fermions  $\lambda_{\bar{a}}$ , with  $\bar{a} = 1, 2, 3, 4$ , where they transform as a **4** of  $SU(4)$ , which is isomorphic to  $SO(6)$ , the ED rotation symmetry. The 10d vector can be decomposed into a 4d vector and six scalars  $X_{\tilde{i}} = A_{4+\tilde{i}}$ , where  $\tilde{i} = 1, \dots, 6$ , and they transform as a **6** of  $SO(6)$ . They have the following Lagrangian

$$\begin{aligned} \mathcal{L}_{10d} = & -\frac{1}{4}F_{\mu\nu}F^{\mu\nu} + (D_\mu X_{\tilde{i}})^\dagger D^\mu X_{\tilde{i}} - i\bar{\lambda}^{\bar{a}}\gamma^\mu D_\mu \lambda_{\bar{a}} \\ & + f_{\tilde{i}}^{\bar{a}\bar{b}}\lambda_{\bar{a}}[X_{\tilde{i}}, \lambda_{\bar{b}}] + f_{\bar{a}\bar{b}\tilde{i}}\bar{\lambda}^{\bar{a}}[X_{\tilde{i}}, \bar{\lambda}^{\bar{b}}] + \frac{1}{2}[X_{\tilde{i}}, X_{\tilde{j}}]^2, \end{aligned} \quad (\text{A10})$$

which is the Lagrangian of  $\mathcal{N} = 4$  SUSY in 4d [101].

## Appendix B: Orbifolding and compactification

As seen in the previous appendix, the ED fermionic representations always decompose into 4d Dirac fermions. To generate the chirality one assumes an incomplete ED Poincaré group. The full ED Poincaré symmetry  $O(6) \ltimes T^6$  can be orbifolded as

$$(O(6)/F) \ltimes (T^6/\Gamma), \quad (\text{B1})$$

with  $F$  and  $\Gamma$  being the discrete orbifold and lattice groups, associated to spacetime rotations and translations respectively. The subgroup  $SO(6)$  of the ED rotation symmetry  $O(6)$

becomes the  $SU(4)_{\mathcal{R}}$  symmetry of the extended SUSY. One can define the orbifold upon modding it out by any discrete subgroup of  $O(6) \simeq SO(6) \times \mathbb{Z}_2 \simeq SU(4) \times \mathbb{Z}_2$ . In particular, if one wants to preserve  $\mathcal{N} = 1$  SUSY, i.e. leaving one  $U(1)_{\mathcal{R}} \subset SU(4)_{\mathcal{R}}$  unbroken, then the orbifold must be expressed in terms of a discrete subgroup of  $SU(3)_{\mathcal{R}}$  [102, 103]. While such a discrete subgroup can be, in general, non-Abelian, the involved commutation relations overly constrain the orbifold boundary conditions diminishing the possibility for obtaining a realistic model below the compactification scale [104]. The most general Abelian discrete subgroup of  $SU(3)$  is  $\mathbb{Z}_N \times \mathbb{Z}_M$  [105] which enables to employ the latter as a discrete orbifold group in the considered approach, i.e.  $F \simeq \mathbb{Z}_N \times \mathbb{Z}_M$ .

It is worth noticing that a general  $F = \mathbb{Z}_N$  orbifolding procedure is defined by identifying the ED coordinates

$$(x, z_1, z_2, z_3) \sim (x, e^{2i\pi n_1/N} z_1, e^{2i\pi n_2/N} z_2, e^{2i\pi n_3/N} z_3), \quad (\text{B2})$$

with arbitrary integers  $n_i$ , satisfying  $n_1 + n_2 + n_3 = 0 \bmod 2N$ , so that  $\mathcal{N} = 1$  SUSY is preserved [106]. The boundary conditions may also involve non-trivial gauge transformations. In fact, the considered orbifold discrete group  $F$  does not commute with the generators of the  $E_8$  gauge group. A discrete  $\mathbb{Z}_N \subset E_8$  transformation can be defined, in general, as a specific  $\mathbb{Z}_N \subset U(1)_a \subset E_8$  subgroup where  $U(1)_a$  can be any  $U(1)$  subgroup of  $E_8$ . The  $\mathbb{Z}_N$  implies a gauge transformation on a field  $f$  denoted by a phase  $e^{2i\pi q_a^f/N}$ , where  $q_a^f$  is the  $U(1)_a$  charge the corresponding field  $f$ .

The boundary conditions act differently on vector  $V$  and chiral  $\phi$  components of the unique 10d gauge superfield  $\mathcal{V}(x, z_1, z_2, z_3)$  as follows [62, 63]

$$\begin{aligned} V(x, z_1, z_2, z_3) &= e^{2i\pi q_a^f/N} V(x, e^{2i\pi n_1/N} z_1, e^{2i\pi n_2/N} z_2, e^{2i\pi n_3/N} z_3), \\ \phi^i(x, z_1, z_2, z_3) &= e^{2i\pi n_i/N} e^{2i\pi q_a^f/N} \phi^i(x, e^{2i\pi n_1/N} z_1, e^{2i\pi n_2/N} z_2, e^{2i\pi n_3/N} z_3), \end{aligned} \quad (\text{B3})$$

so that each supermultiplet receives a phase associated to its charge and extended SUSY decomposition. Here, the  $V$  fields transform according to adjoint representation of the unbroken gauge group, i.e. the fields with identity boundary conditions. The representation of the light chiral superfield  $\phi_i$  is the fundamental one of the unbroken group and contains the fields with charge  $q_a^f = -n_i \bmod N$ . One then chooses a specific set of  $n_i$  integers in order to single out the massless fields in consistency with the SM gauge and matter field content.

To do an orbifolding  $\mathbb{Z}_N \times \mathbb{Z}_M$  one applies two independent  $\mathbb{Z}_N$  and  $\mathbb{Z}_M$  orbifoldings just as described, each one associated to different  $U(1)$  subgroups of  $E_8$ . Geometrically, the translation group is also modded out (compactified) to define the three tori as follows

$$z_i \sim z_i + \tau_i^r, \quad (\text{B4})$$

where  $\tau_i^r$  is the period in compact EDs, with  $r = 1, 2$  and  $i = 1, 2, 3$ . The lattice group which compactifies the EDs is defined as  $\Gamma = \{\tau_i^r\} \simeq \mathbb{Z}^6$ . In this case, the 10d gauge superfield  $\mathcal{V}(x, z_i)$  must also comply with periodicity boundary conditions up to a gauge transformation  $U$  that is arbitrarily chosen for each  $\tau_i^r$ , i.e.

$$\mathcal{V}(x, z_i) = U_i^r \mathcal{V}(x, z_i + \tau_i^r). \quad (\text{B5})$$

Therefore, similarly to the orbifold group  $F$ , as a transformation of the discrete lattice group  $\Gamma$  also implies an  $E_8$  gauge transformation, it will not commute with all of the  $E_8$  gauge group generators.

One can choose three arbitrary transformations  $U_{i=1,2,3}^r$  separately – one for each complex translation generator. A non-trivial  $U_i^r$  gauge transformation is called a Wilson line and is explicitly defined as follows

$$\mathcal{V}(x, z_i) = e^{i\alpha_i^{ar} z_i T_a} \tilde{\mathcal{V}}(x, z_i) \quad \text{with} \quad \tilde{\mathcal{V}}(x, z_i) = \tilde{\mathcal{V}}(x, z_i + \tau_i^r), \quad (\text{B6})$$

where  $T_a$  are the generators of the algebra associated to  $E_8$  and the  $\alpha_i^{ar}$  are the corresponding coefficients that define the specific gauge transformation. The  $\tilde{\mathcal{V}}$  are periodic functions of the EDs. The Wilson lines can be reabsorbed through an inverse gauge transformation  $\mathcal{V} \rightarrow U^{-1}\mathcal{V}$  generating an effective VEV in the ED components of the gauge vector in  $\mathcal{V}$ , which correspond to the 4d scalars in  $\phi_i$ . After the phase is reabsorbed, the components of  $\mathcal{V}(x, z_i)$  become

$$\begin{aligned} V(x, z_i) &= \tilde{V}(x, z_i), \\ \phi_i(x, z_i) &= \tilde{\phi}_i(x, z_i) + \sum_r \alpha_i^{ar} \tau_i^r T_a. \end{aligned} \quad (\text{B7})$$

Therefore, the Wilson line can be seen as an effective VEV in the chiral superfields with the corresponding representation [61]. One must note that it is not a usual VEV found in the QFT approach, as it does not come from the minimization of a given potential. Instead, it comes from the ED profiles of the scalar fields and it triggers a splitting in the mass spectrum just as an actual VEV does.

To maintain the super-Poincaré structure in the resulting 4d theory, the mutual action of the discrete groups realises as  $F\Gamma = \Gamma$ , i.e. the action of the orbifold rotations  $F$  must be equivalent to a lattice transformation  $\Gamma$ . As both, the discrete orbifold group  $F$  and the lattice group  $\Gamma$ , are assumed to be non-commuting with the  $E_8$  gauge group, a trivial action of  $F$  over  $\Gamma$  restricts the possible alignment of the Wilson lines. In this case it implies that the continuous Wilson lines must “live” in the representations where the orbifold rotations are trivial. This means that the effective VEV must lie in the chiral supermultiplets with zero modes. For consistency with the translation group Abelian structure they must all commute with each other.

Note that one can identify specific Wilson lines that do not induce an effective VEV. These are called discrete Wilson lines. An orbifold  $\mathbb{Z}_N$  is based on modding out a space rotation operator  $R$  that complies with  $R^N = I$ . It will also follow  $(R^q)^{N/q} = I$  when  $q$  and  $N/q$  are integers. If an orbifold rotation  $R$  is accompanied by a gauge transformation  $P$ , it will satisfy  $(P^q)^{N/q} = I$ , then a discrete Wilson line (defined by a gauge transformation  $U$ ) would comply with  $(UP^q)^{N/q} = I$ . It is therefore possible to treat them as extra rotation boundary conditions imposed on the non-origin branes. In the model presented in this paper no discrete Wilson lines are assumed.

As this paper is restricted to Abelian orbifolds, the accompanying gauge transformations must be Abelian. The orbifolded accompanying gauge transformations must also be Abelian, therefore they are generated by the Cartan subalgebra. The discrete Wilson lines must also

commute with the orbifold rotations, therefore they must also be generated by the Cartan subalgebra. None of these orbifold transformations can reduce the rank. Continuous Wilson lines need not commute, therefore they are not generated by the Cartan subalgebra (or they are generated by a rotated basis). Continuous Wilson lines can reduce the rank [107] and they are the ones used in this model.

### Appendix C: Full Lagrangian decomposition

The original Lagrangian in 10d reads

$$S = -\frac{1}{2}tr \int d^4x d^3z d^3\bar{z} d^2\theta [\mathfrak{W}_A^\alpha \mathfrak{W}_{A\alpha}] + \text{h.c.}, \quad (\text{C1})$$

where  $\mathfrak{W}_A^\alpha = \mathfrak{W}_A^\alpha(\mathcal{V})$  ( $A$  runs through the gauge indices) is the standard 10d gauge superfield strength

$$\mathfrak{W}^\alpha = \frac{i}{4}(\mathfrak{D}_\beta^T \epsilon^{\beta\gamma} \mathfrak{D}_\gamma) \mathfrak{D}_\alpha V(x, z_i, \theta), \quad \text{where} \quad \mathfrak{D}_\alpha = -\frac{\partial}{\partial \theta} - (\Gamma^M \theta)_\alpha \frac{\partial}{\partial x^M}, \quad (\text{C2})$$

where  $M$  runs through 10 dimensions,  $\alpha$  is the spinor index and  $\theta$  is a 10d Majorana/Weyl fermion. After compactification, the Lagrangian becomes [108]

$$S = tr \int d^4x d^3z d^3\bar{z} d^4\theta \left[ \phi^{i\dagger} e^{-2V} \phi_i + i \phi^{i\dagger} (\partial_i e^{2V}) - i (\bar{\partial}^i e^{-2V}) \phi_i + \frac{1}{2} e^{2V} \bar{\partial}^i \partial_i e^{-2V} \right] \\ - tr \int d^4x d^3z d^3\bar{z} d^2\theta \left[ \frac{1}{2} W_A^\alpha W_{A\alpha} - \frac{i}{6} \epsilon^{ijk} \phi_i [\phi_j, \phi_k] + \frac{1}{2} \epsilon^{ijk} \phi_i \partial_j \phi_k \right] + \text{h.c.}, \quad (\text{C3})$$

where each  $\phi_i, V$  are 4d chiral and gauge superfield, respectively but are functions on the 10d. Now,  $\theta$  is the standard 4d Majorana fermion coordinate. They are decomposed into an Fourier-like series of  $\text{SO}(6)$  modes

$$\phi_i(x, z_i) = \sum_{s=0}^{\infty} \sum_{a,b=0,1,2} \phi_i^{sab}(x) f(z_j)_{sab}, \quad (\text{C4})$$

with a similar decomposition for the  $V$ . The  $f$  are which are also eigenstates of the  $\mathbb{Z}_3 \times \mathbb{Z}_3$

$$\partial_i f(z_j)_{sab} = M_{isab} f(z_j), \quad (\text{C5})$$

where  $M_i \sim 1/R_i$ , in terms of the radii  $R_i$  defining each torus. These radii are arbitrary and independent. One can assume an arbitrary hierarchy between them.

Each of the original four superfields  $\phi_i, V$ , each within a given **248**, is split into an infinite series where each **248** split into nine different states. The relevant zero modes corresponding to  $f_{000}$  has a zero eigenvalue mass and are the only ones surviving at low energies. Integrating out the massive superfields one would obtain the effective action in the general form

$$S = \int d^4x d^4\theta \left[ \frac{1}{2} \mathcal{K}(\phi, \phi^\dagger e^{-2V}) \right] + \int d^4x d^2\theta \left[ 2\mathcal{W}(\phi) - \frac{1}{2} \mathcal{H}(\phi) W^\alpha W_\alpha \right] + \text{h.c.} \quad (\text{C6})$$



Using the coordinate

$$\hat{x}_\mu = x_\mu + \frac{1}{2}\bar{\theta}\gamma_5\gamma_\mu\theta, \quad (\text{C7})$$

one can expand the left chiral superfields as

$$\phi(\tilde{x}) = S(\tilde{x}) - \sqrt{2}\bar{\theta}\psi_L(\hat{x}) + \bar{\theta}\theta_L\mathcal{F}(\hat{x}), \quad (\text{C8})$$

where  $S$  is a scalar field,  $\psi_L$  is a left handed Weyl fermion and  $\mathcal{F}$  is an auxiliary scalar field. We use  $\eta^{\mu\nu} = \text{diag}(-1, 1, 1, 1)$ . The subindex  $L$  for fermions means  $\psi_L = P_L\psi = (1 - \gamma_5)\psi/2$ . The gauge superfield and superfield strength (in the Wess-Zumino gauge and suppressing gauge indices)

$$\begin{aligned} e^{-2V(x)} = & 1 - i(\bar{\theta}\gamma_5\gamma^\mu\theta)t_A A_{A\mu} + 2i(\bar{\theta}\gamma_5\theta)\bar{\theta}t_A\lambda_A(x) + \frac{1}{2}(\bar{\theta}\gamma_5\theta)^2 t_A\mathcal{D}_A \\ & - \frac{1}{2}(\bar{\theta}\gamma_5\gamma^\mu\theta)(\bar{\theta}\gamma_5\gamma^\nu\theta)t_A A_{A\mu}(x)t_B A_{B\nu}(x), \\ W_A(\hat{x}) = & \lambda_{AL}(\hat{x}) + \frac{1}{2}\gamma^\mu\gamma^\nu\theta_L F_{A\mu\nu} + \bar{\theta}\theta_L\gamma^\mu D_\mu\lambda_{AR} - i\theta_L\mathcal{D}_A(\hat{x}), \end{aligned} \quad (\text{C9})$$

where the spinor index  $\alpha$  has been suppressed and  $A$  denote the adjoint gauge indices. The  $t$  are the gauge algebra generators,  $A_\mu$  is the gauge vector,  $D_\mu = \partial_\mu + ig t \cdot A_\mu$  is the covariant derivative,  $F_{\mu\nu} = D_\mu A_\nu - D_\nu A_\mu$  is the gauge field strength tensor,  $\lambda$  is the gaugino Majorana fermion and  $\mathcal{D}$  is the scalar gauge auxiliary field. For convenience, one can define the evaluated function

$$\mathcal{K}|_S = \mathcal{K}|_{\phi_i \rightarrow S_i, V \rightarrow 0}, \quad (\text{C10})$$

of superfields into only the scalar components.

With this superfield decomposition, one can write the general action  $S = \int d^4x \mathcal{L}$  from

Eq. (C6) as [109]

$$\begin{aligned}
\mathcal{L} = & -\frac{1}{2} \frac{\partial^2 \mathcal{K}}{\partial \phi_i^\dagger \partial \phi_j} \Big|_S [(D_\mu S_i)^\dagger D^\mu S_j + \bar{\psi}_i \gamma^\mu D_\mu \psi_{Lj}] \\
& -\frac{1}{8} \mathcal{H}_{AB} |_S \left[ F_{A\mu\nu} F_B^{\mu\nu} - \frac{i}{2} \epsilon_{\alpha\beta\gamma\delta} F_A^{\alpha\beta} F_B^{\gamma\delta} + 4 \bar{\lambda}_A \gamma^\mu D_\mu \lambda_{BR} \right] \\
& -\frac{1}{2} \frac{\partial^2 \mathcal{W}}{\partial \phi_i \partial \phi_j} \Big|_S \bar{\psi}_i \psi_{Lj} - i\sqrt{2} \frac{\partial^2 \mathcal{K}}{\partial \phi_i^\dagger \partial \phi_j} \Big|_S S_i^\dagger t_A \bar{\psi}_j \lambda_{AL} \\
& +\frac{1}{2} \frac{\partial^2 \mathcal{K}}{\partial \phi_i^\dagger \partial \phi_j} \Big|_S \mathcal{F}_i^\dagger \mathcal{F}_j + \frac{\partial \mathcal{W}}{\partial \phi_i} \Big|_S \mathcal{F}_i - \frac{1}{2} \frac{\partial^3 \mathcal{K}}{\partial \phi_k \partial \phi_i^\dagger \partial \phi_j^\dagger} \Big|_S \bar{\psi}_i \psi_{Lj} \mathcal{F}_k - \frac{1}{4} \frac{\partial \mathcal{H}_{AB}}{\partial \phi_i} \Big|_S \bar{\lambda}_A \lambda_{BL} \mathcal{F}_i \\
& +\frac{1}{4} \mathcal{H}_{AB} |_S \mathcal{D}_A \mathcal{D}_B - \frac{\partial \mathcal{K}}{\partial \phi_i} \Big|_S t_A S_i \mathcal{D}_A + \frac{i}{2\sqrt{2}} \frac{\partial \mathcal{H}_{AB}}{\partial \phi_i} \Big|_S \bar{\lambda}_B \psi_{Li} \mathcal{D}_A \\
& +\frac{1}{2} \frac{\partial^3 \mathcal{K}}{\partial \phi_i \partial \phi_j \partial \phi_k^\dagger} \Big|_S \bar{\psi}_j \gamma^\mu \psi_{Rk} D_\mu \phi_i - \frac{1}{4\sqrt{2}} \frac{\partial \mathcal{H}_{AB}}{\partial \phi_i} \Big|_S \bar{\lambda}_B \gamma^\mu \gamma^\nu \psi_{Li} F_{A\mu\nu} \\
& +\frac{1}{8} \frac{\partial^4 \mathcal{K}}{\partial \phi_i \partial \phi_j \partial \phi_k^\dagger \partial \phi_l^\dagger} \Big|_S (\bar{\psi}_i \psi_{Lj})(\bar{\psi}_l \psi_{Rk}) + \frac{1}{8} \frac{\partial^2 \mathcal{H}_{AB}}{\partial \phi_i \partial \phi_j} \Big|_S (\bar{\lambda}_A \lambda_{BL})(\bar{\psi}_i \psi_{Lj}) \\
& + \text{h.c.} ,
\end{aligned} \tag{C11}$$

where the first and second line have the kinetic terms, the third line has terms with two fermions, which would generate fermion masses. The fourth line has the terms involving  $\mathcal{F}$ , the fifth line contains terms involving  $\mathcal{D}$ . These latter two lines would generate the scalar potential and further fermion masses after SUSY breaking. The sixth line has derivative couplings and the seventh one has four-fermion couplings.

The auxiliary fields solve the equations

$$\begin{aligned}
\frac{\partial^2 \mathcal{K}}{\partial \phi_j^\dagger \partial \phi_i} \Big|_S \mathcal{F}_i &= -\frac{\partial \mathcal{W}}{\partial \phi_j^\dagger} \Big|_S + \frac{1}{2} \frac{\partial^3 \mathcal{K}}{\partial \phi_k \partial \phi_i \partial \phi_j^\dagger} \Big|_S \bar{\psi}_k \psi_{Li} + \frac{1}{4} \frac{\partial \mathcal{H}}{\partial \phi_j^\dagger} \Big|_S \bar{\lambda}_A \lambda_{LA}, \\
\mathcal{H}_{AB} |_S \mathcal{D}_B &= \frac{\partial \mathcal{K}}{\partial \phi_i} \Big|_S t_A S_i + \frac{\partial \mathcal{K}}{\partial \phi_i^\dagger} \Big|_S t_A S_i^\dagger - \frac{i}{2\sqrt{2}} \frac{\partial \mathcal{H}_{AB}}{\partial \phi_i} \Big|_S \bar{\lambda}_B \psi_L + \frac{i}{2\sqrt{2}} \frac{\partial \mathcal{H}_{AB}}{\partial \phi_i^\dagger} \Big|_S \bar{\psi}_i \lambda_{LB}.
\end{aligned} \tag{C12}$$

Their VEVs, which would break SUSY, are then defined by

$$\left\langle \frac{\partial^2 \mathcal{K}}{\partial \phi_j^\dagger \partial \phi_i} \Big|_S \right\rangle \langle \mathcal{F}_i \rangle = -\left\langle \frac{\partial \mathcal{W}}{\partial \phi_j^\dagger} \Big|_S \right\rangle, \quad \langle \mathcal{H}_{AB} |_S \rangle \langle \mathcal{D}_B \rangle = \left\langle \frac{\partial \mathcal{K}}{\partial \phi_i} \Big|_S \right\rangle t_A \langle S_i \rangle + \left\langle \frac{\partial \mathcal{K}}{\partial \phi_i^\dagger} \Big|_S \right\rangle t_A \langle S_i^\dagger \rangle. \tag{C13}$$

Knowing that

$$\begin{aligned} \left. \frac{\partial^2 \mathcal{K}}{\partial \phi_j^\dagger \partial \phi_i} \right|_S &= \delta^{ij} - \tilde{\kappa}^{ij}(S, S^\dagger) = \delta^{ij} + \mathcal{O}(1/\Lambda^2), \\ \mathcal{H}_{AB}|_S &= \delta_{AB} - \tilde{\eta}_{AB}(S, S^\dagger) = \delta_{AB} + \mathcal{O}(1/\Lambda^3), \end{aligned} \quad (\text{C14})$$

one can use the geometric series expansion

$$\frac{1}{\delta - \tilde{\kappa}} = \sum_{n=0}^{\infty} \tilde{\kappa}^n, \quad \frac{1}{\delta - \tilde{\eta}} = \sum_{n=0}^{\infty} \tilde{\eta}^n, \quad (\text{C15})$$

so that we have the polynomial solution

$$\begin{aligned} \mathcal{F}_k &= \sum_n (\tilde{\kappa}^n)_{kj} \left[ - \left. \frac{\partial \mathcal{W}}{\partial \phi_j^\dagger} \right|_S + \frac{1}{2} \left. \frac{\partial^3 \mathcal{K}}{\partial \phi_s \partial \phi_i \partial \phi_j^\dagger} \right|_S \bar{\psi}_s \psi_{Li} + \frac{1}{4} \left. \frac{\partial \mathcal{H}_{AB}}{\partial \phi_j^\dagger} \right|_S \bar{\lambda}_A \lambda_{LB} \right], \\ \mathcal{D}_B &= \sum_n (\tilde{\eta}^n)_{AB} \left[ \left. \frac{\partial \mathcal{K}}{\partial \phi_i} \right|_S t_A S_i + \left. \frac{\partial \mathcal{K}}{\partial \phi_i^\dagger} \right|_S t_A S_i^\dagger - \frac{i}{2\sqrt{2}} \left. \frac{\partial \mathcal{H}_{AC}}{\partial \phi_i} \right|_S \bar{\lambda}_C \psi_L + \frac{i}{2\sqrt{2}} \left. \frac{\partial \mathcal{H}_{AC}}{\partial \phi_i^\dagger} \right|_S \bar{\psi}_i \lambda_{LC} \right], \end{aligned} \quad (\text{C16})$$

which can be plugged in Eq. (C11) to obtain the full Lagrangian.

## Appendix D: E<sub>8</sub> generators

The group E<sub>8</sub> can be fully described by the commutation algebra of its generators. The full list of 248 generators can be named just as the previously named field representations  $\Delta_C^a, \Delta_L^a, \Delta_R^a, \Delta_F^a, \mathbf{X}_{bc}^a, \bar{\mathbf{X}}_a^{bc}, \mathbf{L}_{bc}^a, \mathbf{Q}_{Lab\,c}, \mathbf{Q}_{R\,c}^a, \bar{\mathbf{L}}_a^{bc}, \bar{\mathbf{Q}}_L^{ab\,c}, \bar{\mathbf{Q}}_{Ra\,b}^c$ , noting that in this section, they are not fields but E<sub>8</sub> generators. They have the following index convention

- All indices run  $a = 1, 2, 3$  regardless of the corresponding SU(3).
- Upper index denotes antitriplet and lower index denotes triplet.
- The adjoint SU(3) generators  $\Delta$  have an antitriplet-triplet index of the corresponding group.
- All the other generators have three of the four SU(3) indices always in the order  $C, L, R, F$  and a blank space where a singlet is placed.

With these, the commutation relations can be written in Koca's convention [110]

$$\begin{aligned}
[\Delta_{A\ j}^i, \Delta_{B\ a}^b] &= (\delta_j^b \Delta_{A\ a}^i - \delta_a^i \Delta_{A\ j}^b) \delta_{AB}, \quad \text{for } A, B = C, L, R, F, \\
[\Delta_{C\ j}^i, \mathbf{X}_{bc}^a] &= \delta_j^a \mathbf{X}_{bc}^i - \frac{1}{3} \delta_j^i \mathbf{X}_{bc}^a, & [\Delta_{F\ j}^i, \mathbf{X}_{bc}^a] &= 0, \\
[\Delta_{L\ j}^i, \mathbf{X}_{bc}^a] &= -\delta_b^i \mathbf{X}_{jc}^a + \frac{1}{3} \delta_j^i \mathbf{X}_{bc}^a, & [\Delta_{R\ j}^i, \mathbf{X}_{bc}^a] &= -\delta_c^i \mathbf{X}_{bj}^a + \frac{1}{3} \delta_j^i \mathbf{X}_{bc}^a, \\
[\mathbf{X}_{bc}^a, \mathbf{X}_{jk}^i] &= -\epsilon_{dbj} \epsilon_{eck} \epsilon^{fai} \overline{\mathbf{X}}_f^{de}, & [\mathbf{X}_{bc}^a, \overline{\mathbf{X}}_i^{jk}] &= -\delta_i^a \delta_c^k \Delta_{L\ b}^j - \delta_i^a \delta_b^j \Delta_{R\ c}^k + \delta_b^j \delta_c^k \Delta_{C\ i}^a, \\
[\Delta_{C\ j}^i, \mathbf{L}_{bc}^a] &= 0, & [\Delta_{F\ j}^i, \mathbf{L}_{bc}^a] &= -\delta_c^i \mathbf{L}_{bj}^a + \frac{1}{3} \delta_j^i \mathbf{L}_{bc}^a, \\
[\Delta_{L\ j}^i, \mathbf{L}_{bc}^a] &= \delta_j^a \mathbf{L}_{bc}^i - \frac{1}{3} \delta_j^i \mathbf{L}_{bc}^a, & [\Delta_{R\ j}^i, \mathbf{L}_{bc}^a] &= -\delta_b^i \mathbf{L}_{jc}^a + \frac{1}{3} \delta_j^i \mathbf{L}_{bc}^a, \\
[\mathbf{L}_{bc}^a, \mathbf{L}_{jk}^i] &= -\epsilon_{dbj} \epsilon_{eck} \epsilon^{fai} \overline{\mathbf{L}}_f^{de}, & [\mathbf{L}_{bc}^a, \overline{\mathbf{L}}_i^{jk}] &= -\delta_i^a \delta_c^k \Delta_{R\ b}^j - \delta_i^a \delta_b^j \Delta_{F\ c}^k + \delta_b^j \delta_c^k \Delta_{L\ i}^a, \\
[\Delta_{C\ j}^i, \mathbf{Q}_{Lab\ c}] &= -\delta_a^i \mathbf{Q}_{Ljb\ c} + \frac{1}{3} \delta_j^i \mathbf{Q}_{Lab\ c}, & [\Delta_{F\ j}^i, \mathbf{Q}_{Lab\ c}] &= -\delta_c^i \mathbf{Q}_{Lab\ j} + \frac{1}{3} \delta_j^i \mathbf{Q}_{Lab\ c}, \\
[\Delta_{L\ j}^i, \mathbf{Q}_{Lab\ c}] &= -\delta_b^i \mathbf{Q}_{Laj\ c} + \frac{1}{3} \delta_j^i \mathbf{Q}_{Lab\ c}, & [\Delta_{R\ j}^i, \mathbf{Q}_{Lab\ c}] &= 0, \\
[\mathbf{Q}_{Lab\ c}, \mathbf{Q}_{Lij\ k}] &= \epsilon_{dbj} \epsilon_{eck} \epsilon^{fai} \overline{\mathbf{Q}}_L^{def}, & [\mathbf{Q}_{Lab\ c}, \overline{\mathbf{Q}}_L^{ijk}] &= -\delta_a^i \delta_c^k \Delta_{L\ b}^j - \delta_a^i \delta_b^j \Delta_{F\ c}^k - \delta_b^j \delta_c^k \Delta_{C\ i}^a, \\
[\Delta_{C\ j}^i, \mathbf{Q}_R^{ab\ c}] &= \delta_j^a \mathbf{Q}_R^{ib\ c} - \frac{1}{3} \delta_j^i \mathbf{Q}_R^{ab\ c}, & [\Delta_{F\ j}^i, \mathbf{Q}_R^{ab\ c}] &= -\delta_c^i \mathbf{Q}_R^{aj\ c} + \frac{1}{3} \delta_j^i \mathbf{Q}_R^{ab\ c}, \\
[\Delta_{L\ j}^i, \mathbf{Q}_R^{ab\ c}] &= 0, & [\Delta_{R\ j}^i, \mathbf{Q}_R^{ab\ c}] &= \delta_j^b \mathbf{Q}_R^{ai\ c} - \frac{1}{3} \delta_j^i \mathbf{Q}_R^{ab\ c}, \\
[\mathbf{Q}_R^{ab\ c}, \mathbf{Q}_R^{ij\ k}] &= \epsilon_{dbj} \epsilon_{eck} \epsilon^{fai} \overline{\mathbf{Q}}_{Rd\ e}^f, & [\mathbf{Q}_R^{ab\ c}, \overline{\mathbf{Q}}_{Ri\ j}^k] &= \delta_i^a \delta_c^k \Delta_{L\ j}^b - \delta_i^a \delta_j^b \Delta_{F\ c}^k + \delta_j^b \delta_c^k \Delta_{C\ i}^a, \\
[\mathbf{L}_{jk}^i, \mathbf{Q}_{Lab\ c}] &= \delta_b^i \epsilon_{kcd} \overline{\mathbf{Q}}_{Ra\ j}^d, & [\mathbf{L}_{jk}^i, \mathbf{Q}_R^{ab\ c}] &= \delta_j^b \epsilon_{kcd} \overline{\mathbf{Q}}_L^{ai\ d}, \\
[\mathbf{L}_{jk}^i, \mathbf{X}_{bc}^a] &= \delta_b^i \epsilon_{jcd} \mathbf{Q}_R^{ad\ c}, & [\mathbf{L}_{jk}^i, \overline{\mathbf{Q}}_L^{abc}] &= -\delta_k^c \epsilon^{ibd} \mathbf{X}_{dj}^a, \\
[\mathbf{L}_{jk}^i, \overline{\mathbf{Q}}_{Ra\ b}^c] &= \delta_k^c \epsilon_{jbd} \overline{\mathbf{X}}_a^{id}, & [\mathbf{L}_{jk}^i, \overline{\mathbf{X}}_a^{bc}] &= -\delta_j^c \epsilon^{ibd} \mathbf{Q}_{Lad\ k}, \\
[\mathbf{Q}_{Lij\ k}, \mathbf{Q}_R^{ab\ c}] &= \delta_i^a \epsilon_{kcd} \overline{\mathbf{L}}_j^{bd}, & [\mathbf{Q}_{Lij\ k}, \mathbf{X}_{bc}^a] &= \delta_i^a \epsilon_{jbd} \mathbf{L}_{ck}^d, \\
[\mathbf{Q}_{Lij\ k}, \overline{\mathbf{Q}}_{Ra\ b}^c] &= \delta_k^c \epsilon_{iad} \mathbf{X}_{jb}^d, & [\mathbf{Q}_{Lij\ k}, \overline{\mathbf{X}}_a^{bc}] &= \delta_j^b \epsilon_{iad} \mathbf{Q}_R^{dc\ k}, \\
[\mathbf{Q}_R^{ij\ k}, \mathbf{X}_{bc}^a] &= -\delta_c^j \epsilon^{iad} \mathbf{Q}_{Ldb\ k}, & [\mathbf{Q}_R^{ij\ k}, \overline{\mathbf{X}}_a^{bc}] &= -\delta_a^i \epsilon^{jcd} \mathbf{L}_{dk}^b,
\end{aligned} \tag{D1}$$

which, together with their complex conjugate relations, determine completely the corresponding Lie algebra.

## Appendix E: Detailed Lagrangian of the model

The superpotential was described in Eq. (2.1). Due to the non renormalization theorem, it does not receive any loop contributions. The SUSY breaking contributions from Eq. (2.2) do affect the Kähler and  $\mathcal{H}$  potential.

One can define the tensor<sup>7</sup>

$$\begin{aligned}\mathbf{K}_{p \ m \ n}^{i \ q \ r} = & (\mathbf{L}^\dagger)_{a \ }^{bc} (e^{-2V})_{p \ b \ c}^a{}^q{}^r \mathbf{L}_{mn}^i \\ & + \delta_m^q (\mathbf{Q}_L^\dagger)^{ab} (e^{-2V})_{a \ }^i{}^r{}^b \mathbf{Q}_{Lpn}/3 \\ & + \delta_p^i (\mathbf{Q}_R^\dagger)_b{}^a (e^{-2V})^b{}^r{}^a{}_m \mathbf{Q}_{Rn}^q/3,\end{aligned}\tag{E1}$$

so that the full Kähler potential is

$$\begin{aligned}\mathcal{K} = & \mathbf{K}_{i \ m \ n}^{i \ m \ n} + \frac{y_2}{\Lambda^2} \mathbf{K}_{p \ m \ n}^{i \ q \ r} \mathbf{K}_{i \ q \ r}^p{}^m{}^n + \frac{y_3}{\Lambda^4} \mathbf{K}_{p \ m \ n}^{i \ q \ r} \mathbf{K}_{l \ j \ k}^p{}^m{}^n \mathbf{K}_{i \ q \ r}^l{}^j{}^k \\ & + \frac{y_4}{\Lambda^5} \epsilon_{ijk} \epsilon^{lmn} \epsilon^{opq} \mathbf{L}_{lo}^i \mathbf{K}_{a \ m \ p}^j{}^b{}^c \mathbf{L}_{bc}^a \mathbf{K}_{d \ n \ q}^k{}^e{}^f \mathbf{L}_{ef}^d \\ & + \frac{y_5}{\Lambda^5} \epsilon_{ijk} \epsilon^{opq} \mathbf{Q}_{Ro}^i \mathbf{K}_{s \ n \ p}^s{}^j{}^m \mathbf{Q}_{Rm}^n \mathbf{K}_{t \ b \ q}^t{}^k{}^a \mathbf{Q}_{Ra}^b \\ & + \frac{y_6}{\Lambda^5} \epsilon^{ijk} \epsilon^{opq} \mathbf{Q}_{Lio}^i \mathbf{K}_{j \ s \ p}^a{}^s{}^b \mathbf{Q}_{Lab} \mathbf{K}_{k \ t \ q}^c{}^t{}^d \mathbf{Q}_{Lcd} \\ & + \epsilon^{ijk} \mathbf{L}_{ma}^l \mathbf{Q}_{Rb}^n \mathbf{Q}_{Lpc} \left[ \frac{y_7}{\Lambda^3} \mathbf{K}_{l \ n \ k}^p{}^m{}^a \delta_i^b \delta_j^c + \frac{y_8}{\Lambda^3} \mathbf{K}_{l \ n \ k}^p{}^m{}^b \delta_i^c \delta_j^a + \frac{y_9}{\Lambda^3} \mathbf{K}_{l \ n \ k}^p{}^m{}^c \delta_i^a \delta_j^b \right. \\ & + \frac{y_{10}}{\Lambda^5} \mathbf{K}_{d \ e \ j}^p{}^m{}^b \mathbf{K}_{l \ n \ k}^d{}^e{}^c \delta_i^a + \frac{y_{11}}{\Lambda^5} \mathbf{K}_{d \ e \ j}^p{}^m{}^a \mathbf{K}_{l \ n \ k}^d{}^e{}^b \delta_i^c + \frac{y_{12}}{\Lambda^5} \mathbf{K}_{d \ e \ j}^p{}^m{}^c \mathbf{K}_{l \ n \ k}^d{}^e{}^a \delta_i^b \left. \right] \\ & + \text{h.c.} + \mathcal{O}(1/\Lambda^6),\end{aligned}\tag{E2}$$

where the  $y$ 's are dimensionless constants completely determined by the CGC and loop factors. The scale  $\Lambda$  is the KK mass scale. The full superpotential reads

$$\mathcal{W} = y_1 \epsilon^{ijk} \mathbf{L}_{mi}^l \mathbf{Q}_{Rj}^m \mathbf{Q}_{Llk} + \text{h.c.} + \mathcal{O}(1/\Lambda^3).\tag{E3}$$

Finally, the gauge field strength superpotential can be expanded in the indices

$$\mathcal{H} W^\alpha W_\alpha = \mathcal{H}_{l \ m \ n \ o \ p \ q}^{a \ b \ c \ d \ e \ f} (W^\alpha)_{a \ b \ c}^l{}^m{}^n (W_\alpha)_{d \ e \ f}^o{}^p{}^q,\tag{E4}$$

with

$$\begin{aligned}\mathcal{H}_{l \ m \ n \ o \ p \ q}^{a \ b \ c \ d \ e \ f} = & \delta_o^a \delta_p^b \delta_q^c \delta_l^d \delta_m^e \delta_n^f \\ & + \frac{y_{13}}{\Lambda^3} \epsilon_{ilo} \epsilon^{rbe} \epsilon^{gcf} \mathbf{L}_{rg}^i \mathbf{L}_{mn}^a \mathbf{L}_{pq}^d \\ & + \frac{y_{14}}{\Lambda^3} \epsilon_{imp} \epsilon^{rcf} \mathbf{Q}_{Rr}^i \mathbf{Q}_{Rn}^b \mathbf{Q}_{Rq}^e \delta_o^a \delta_l^d \\ & + \frac{y_{15}}{\Lambda^3} \epsilon^{iad} \epsilon^{jcf} \mathbf{Q}_{Lij} \mathbf{Q}_{Lln} \mathbf{Q}_{Loq} \delta_p^b \delta_m^e \\ & + \epsilon^{icf} \left[ \frac{y_{16}}{\Lambda^3} \mathbf{L}_{mi}^a \mathbf{Q}_{Rp}^b \mathbf{Q}_{Loq} \delta_l^d \delta_n^e + \frac{y_{17}}{\Lambda^3} \mathbf{L}_{mn}^a \mathbf{Q}_{Rq}^b \mathbf{Q}_{Loi} \delta_l^d \delta_p^e + \frac{y_{18}}{\Lambda^3} \mathbf{L}_{mn}^a \mathbf{Q}_{Ri}^e \mathbf{Q}_{Loq} \delta_l^d \delta_p^b \right] \\ & + \text{h.c.} + \mathcal{O}(1/\Lambda^6).\end{aligned}\tag{E5}$$

---

<sup>7</sup> The index conventions are:

- Color indices are not shown explicitly.
- Last index is always the family index.
- Where there are three sets of indices, the first one is left and the second one is right, the final one is family.
- Upper index denotes antitriplet and lower index denotes triplet.

The Kähler potential in Eq. (E2) can be simplified. The first term contains the scalar and fermion kinetic terms. In any other term, the function  $\mathbf{K}$  can be approximated to only the  $\mathbf{L}$  part, which involves Wilson line effective VEVs. The  $y_2$  term would generate Majorana masses for right handed neutrinos and flavons. The  $y_3$  term would only generate subleading corrections and may be ignored. The second line contains lepton and Higgs interactions. The third and fourth line may contain proton decay terms of the form  $QQQL$ ; they are studied in Sec. IV. The last lines would bring corrections to the quark masses. Defining

$$(\tilde{\Delta}_L)^i{}_j = \mathbf{L}^i{}_{mn}(\mathbf{L}^\dagger)_j{}^{mn}, \quad (\tilde{\Delta}_R)^i{}_j = (\mathbf{L}^\dagger)_m{}^{in} \mathbf{L}^m{}_{jn}, \quad (\tilde{\Delta}_F)^i{}_j = (\mathbf{L}^\dagger)_m{}^{ni} \mathbf{L}^m{}_{nj}, \quad (\text{E6})$$

one can define the truncated Kähler potential

$$\begin{aligned} \mathcal{K}' = & (\mathbf{L}^\dagger)_a{}^{bc} (e^{-2V})_p{}^q{}_b{}^r{}_c \mathbf{L}^p{}_{qr} + (\mathbf{Q}_L^\dagger)^{ab} (e^{-2V})_a{}^r{}_b{}^i \mathbf{Q}_{Lir} + (\mathbf{Q}_R^\dagger)_b{}^a (e^{-2V})_m{}^r{}_a{}^i \mathbf{Q}_R^m{}_r \\ & + \frac{y_2}{\Lambda^2} (\mathbf{L}^a{}_{bc} (\mathbf{L}^\dagger)_a{}^{bc})^2 \\ & + \frac{y_4}{\Lambda^5} \epsilon_{ijk} \epsilon^{lmn} \epsilon^{opq} \mathbf{L}^i{}_{lo} \left[ (\tilde{\Delta}_L)^j{}_a \mathbf{L}^a{}_{mp} (\tilde{\Delta}_R)^e{}_n \mathbf{L}^k{}_{eq} + (\tilde{\Delta}_L)^j{}_a \mathbf{L}^a{}_{mp} (\tilde{\Delta}_F)^f{}_q \mathbf{L}^k{}_{nf} + (\tilde{\Delta}_R)^b{}_m \mathbf{L}^j{}_{bp} (\tilde{\Delta}_F)^f{}_q \mathbf{L}^k{}_{nf} \right] \\ & + \epsilon^{ijk} \left[ \left( \frac{y_7}{\Lambda^3} + \frac{y_9}{\Lambda^3} \right) \mathbf{L}^l{}_{ni} \mathbf{Q}_R^n{}_j \mathbf{Q}_{Lpk} (\Delta_L)^p{}_l + \left( \frac{y_7}{\Lambda^3} + \frac{y_8}{\Lambda^3} \right) \mathbf{L}^p{}_{mi} \mathbf{Q}_R^n{}_j \mathbf{Q}_{Lpk} (\Delta_R)^m{}_n \right. \\ & \quad \left. + \frac{y_7}{\Lambda^3} \mathbf{L}^p{}_{na} \mathbf{Q}_R^n{}_j \mathbf{Q}_{Lpk} (\Delta_F)^a{}_i + \frac{y_8}{\Lambda^3} \mathbf{L}^p{}_{mi} \mathbf{Q}_R^m{}_b \mathbf{Q}_{Lpk} (\Delta_F)^b{}_j + \frac{y_9}{\Lambda^3} \mathbf{L}^l{}_{ni} \mathbf{Q}_R^n{}_j \mathbf{Q}_{Llc} (\Delta_F)^c{}_k \right] \\ & + \text{h.c.}, \end{aligned} \quad (\text{E7})$$

where the  $y_{10,11,12}$  terms may be ignored as they are subleading corrections to the  $y_{7,8,9}$  ones. In the same way, the  $\mathcal{H}$  low-energy relevant superpotential can be truncated as

$$\begin{aligned} \mathcal{H}'^a{}_l{}^b{}_m{}^c{}_n{}^d{}_o{}^e{}_p{}^f{}_q = & \delta_o^a \delta_p^b \delta_q^c \delta_l^d \delta_m^e \delta_n^f \\ & + \frac{y_{13}}{\Lambda^3} \epsilon_{ilo} \epsilon^{rbe} \epsilon^{gcf} \mathbf{L}^i{}_{rg} \mathbf{L}^a{}_{mn} \mathbf{L}^d{}_{pq} \\ & + \epsilon^{icf} \left[ \frac{y_{16}}{\Lambda^3} \mathbf{L}^a{}_{mi} \mathbf{Q}_R^b{}_p \mathbf{Q}_{Loq} \delta_l^d \delta_n^e + \frac{y_{17}}{\Lambda^3} \mathbf{L}^a{}_{mn} \mathbf{Q}_R^b{}_q \mathbf{Q}_{Loi} \delta_l^d \delta_p^e + \frac{y_{18}}{\Lambda^3} \mathbf{L}^a{}_{mn} \mathbf{Q}_R^e{}_i \mathbf{Q}_{Loq} \delta_l^d \delta_p^b \right] \\ & + \text{h.c.} \end{aligned} \quad (\text{E8})$$

These potentials generate the Lagrangian to be studied in the remainder of this article.

The SUSY breaking contributions, which are proportional to  $\langle \mathcal{D} \rangle$ , can be written in terms of three different effective adjoint VEVs

$$\begin{aligned} \langle (\tilde{\Delta}_L)^i{}_j \rangle &= \langle \mathbf{L}^i{}_{mn} (\mathbf{L}^\dagger)_j{}^{mn} \rangle - \langle \mathbf{L}^l{}_{mn} (\mathbf{L}^\dagger)_l{}^{mn} \rangle \delta_j^i / 3 \\ &= \mathbf{w}^2 (\delta_j^i \delta_j^3 - \delta_j^i / 3), \\ \langle (\tilde{\Delta}_R)^i{}_j \rangle &= \langle (\mathbf{L}^\dagger)_m{}^{in} \mathbf{L}^m{}_{jn} \rangle - \langle \mathbf{L}^l{}_{mn} (\mathbf{L}^\dagger)_l{}^{mn} \rangle \delta_j^i / 3 \\ &= \delta_1^i \delta_j^1 \langle \tilde{\nu}^{c\dagger k} \tilde{\nu}_k^c \rangle + \delta_1^i \delta_j^3 \langle \tilde{\nu}^{c\dagger k} \varphi_k \rangle + \delta_3^i \delta_j^1 \langle \varphi^{\dagger k} \tilde{\nu}_k^c \rangle + \delta_3^i \delta_j^3 \langle \varphi^{\dagger k} \varphi_k \rangle - \mathbf{w}^2 \delta_j^i / 3, \\ \langle (\tilde{\Delta}_F)^i{}_j \rangle &= \langle (\mathbf{L}^\dagger)_m{}^{ni} \mathbf{L}^m{}_{nj} \rangle - \langle \mathbf{L}^l{}_{mn} (\mathbf{L}^\dagger)_l{}^{mn} \rangle \delta_j^i / 3 \\ &= \mathbf{v}^i{}_j - \mathbf{v} \delta_j^i / 3, \end{aligned} \quad (\text{E9})$$

The SUSY breaking Wilson lines also break the gauge symmetry. They generate the broken gaugino mass matrix

$$\lambda_A M_A^\dagger M_B \lambda_B = \lambda_A \lambda_B \left( \langle \mathbf{L}^\dagger \rangle t_A t_B \langle \mathbf{L} \rangle \right), \quad (\text{E10})$$

where  $t_{\tilde{a}}$  with  $\tilde{a} = 1, \dots, 8$  are the Gell-Mann matrices which can belong to any  $\text{SU}(3)_{\text{C,L,R,F}}$ . Their product can be defined as

$$[t_{\tilde{a}}, t_{\tilde{b}}] = 2if_{\tilde{a}\tilde{b}}^{\tilde{c}} t_{\tilde{c}}, \quad \{t_{\tilde{a}}, t_{\tilde{b}}\} = \frac{4}{3}\delta_{\tilde{a}\tilde{b}} + 2d_{\tilde{a}\tilde{b}}^{\tilde{c}} t_{\tilde{c}}. \quad (\text{E11})$$

The squared broken gaugino mass matrix can then be written as

$$\begin{aligned} \lambda_A M_A^\dagger M_B \lambda_B = & \lambda_a^F \lambda_b^F \left[ \frac{2}{3} \mathbf{w}^2 \delta_{\tilde{a}\tilde{b}} + d_{\tilde{a}\tilde{b}}^{\tilde{c}} (\langle \tilde{\nu}^{c\dagger i} \rangle t_{\tilde{c}i}^j \langle \tilde{\nu}_j^c \rangle + \langle \varphi^{\dagger i} \rangle t_{\tilde{c}i}^j \langle \varphi_j \rangle) \right] \\ & + \lambda_a^R \lambda_b^R \left[ \langle \varphi^{\dagger i} \varphi_i \rangle \left( \delta_a^4 \delta_b^4 + \delta_a^5 \delta_b^5 + \delta_a^6 \delta_b^6 + \delta_a^7 \delta_b^7 + \frac{4}{3} \delta_a^8 \delta_b^8 \right) \right. \\ & + \langle \tilde{\nu}^{c\dagger i} \tilde{\nu}_i^c \rangle \left( \delta_a^1 \delta_b^1 + \delta_a^2 \delta_b^2 + \delta_a^3 \delta_b^3 + \delta_a^4 \delta_b^4 + \delta_a^5 \delta_b^5 + \frac{2}{3} \delta_a^8 \delta_b^8 + \frac{2}{\sqrt{3}} \delta_a^{(3)} \delta_b^{(8)} \right) \\ & + \langle \tilde{\nu}^{c\dagger i} \varphi_i \rangle \left( \delta_a^{(1)} \delta_b^{(6)} + i \delta_a^{(1)} \delta_b^{(7)} + i \delta_a^{(2)} \delta_b^{(6)} + \delta_a^{(2)} \delta_b^{(7)} + \delta_a^{(3)} \delta_b^{(4)} + i \delta_a^{(3)} \delta_b^{(5)} - \frac{1}{\sqrt{3}} \delta_a^{(4)} \delta_b^{(8)} - i \frac{1}{\sqrt{3}} \delta_a^{(5)} \delta_b^{(8)} \right) \\ & + \langle \varphi^{\dagger i} \tilde{\nu}_i^c \rangle \left( \delta_a^{(1)} \delta_b^{(6)} - i \delta_a^{(1)} \delta_b^{(7)} - i \delta_a^{(2)} \delta_b^{(6)} + \delta_a^{(2)} \delta_b^{(7)} + \delta_a^{(3)} \delta_b^{(4)} - i \delta_a^{(3)} \delta_b^{(5)} - \frac{1}{\sqrt{3}} \delta_a^{(4)} \delta_b^{(8)} + i \frac{1}{\sqrt{3}} \delta_a^{(5)} \delta_b^{(8)} \right) \Big] \\ & + \lambda_a^L \lambda_b^L \left[ \mathbf{w}^2 \left( \delta_a^4 \delta_b^4 + \delta_a^5 \delta_b^5 + \delta_a^6 \delta_b^6 + \delta_a^7 \delta_b^7 + \frac{4}{3} \delta_a^8 \delta_b^8 \right) \right] \\ & + \lambda_a^L \lambda_b^R \left[ \langle \tilde{\nu}^{c\dagger i} \tilde{\nu}_i^c \rangle \frac{4}{3} \delta_a^8 \delta_b^8 - \frac{2}{\sqrt{3}} \langle \varphi^{\dagger i} \varphi_i \rangle \left( \delta_b^3 + \frac{1}{\sqrt{3}} \delta_b^8 \right) \right. \\ & \quad \left. - \langle \varphi^{\dagger i} \tilde{\nu}_i^c \rangle \frac{2}{\sqrt{3}} \delta_a^8 (\delta_a^4 + i \delta_a^5) - \langle \tilde{\nu}^{c\dagger i} \varphi_i \rangle \frac{2}{\sqrt{3}} \delta_a^8 (\delta_a^4 - i \delta_a^5) \right] \\ & + \lambda_a^L \lambda_b^F \left[ -\frac{2}{\sqrt{3}} \delta_a^8 \left( \langle \tilde{\nu}^{c\dagger i} \rangle t_{\tilde{b}i}^j \langle \tilde{\nu}_j^c \rangle + \langle \varphi^{\dagger i} \rangle t_{\tilde{b}i}^j \langle \varphi_j \rangle \right) \right] \\ & + \lambda_a^R \lambda_b^F \left[ \langle \tilde{\nu}^{c\dagger i} \rangle \left( \delta_a^3 + \frac{1}{\sqrt{3}} \delta_a^8 \right) t_{\tilde{b}i}^j \langle \tilde{\nu}_j^c \rangle - \frac{2}{\sqrt{3}} \langle \varphi^{\dagger i} \rangle \delta_a^8 t_{\tilde{b}i}^j \langle \varphi_j \rangle \right. \\ & \quad \left. + \langle \varphi^{\dagger i} \rangle (\delta_a^4 - i \delta_a^5) t_{\tilde{b}i}^j \langle \tilde{\nu}_j^c \rangle + \langle \tilde{\nu}^{c\dagger i} \rangle (\delta_a^4 + i \delta_a^5) t_{\tilde{b}i}^j \langle \varphi_j \rangle \right]. \end{aligned} \quad (\text{E12})$$

This matrix  $M_A^\dagger M_B$  is supersymmetric, therefore this is also the mass matrix for the broken gauge vectors.



## Appendix F: Partial compactification

This model is built on the orbifold  $\mathbb{T}^6/(\mathbb{Z}_3^C \times \mathbb{Z}_3^F)$  acting as

$$\begin{aligned}\mathbb{Z}_3^F : (x, z_1, z_2, z_3) &\sim (x, \omega^2 z_1, \omega^2 z_2, \omega^2 z_3), \\ \mathbb{Z}_3^C : (x, z_1, z_2, z_3) &\sim (x, \omega^3 z_1, \omega z_2, \omega^2 z_3),\end{aligned}\tag{F1}$$

where  $\omega = e^{2i\pi/3}$ , where one can note that the second  $\mathbb{Z}_3^C$  does not affect the first coordinate. This second  $\mathbb{Z}_3^C$  orbifolding generates a splitting of eigenstates  $\sim M_{2,3}$ . As they both appear together, the mass splitting is proportional to the largest of them. If one assumes that  $M_1 \ll M_{2,3}$  then, there is a splitting of the KK modes.

One can obtain an effective partial compactification  $10d \rightarrow 6d$  of the orbifold  $\mathbb{T}^4/(\mathbb{Z}_3^C)$  acting as

$$(x, z_1, z_2, z_3) \sim (x, z_1, \omega z_2, \omega^2 z_3),\tag{F2}$$

with  $\mathcal{V} \rightarrow e^{2i\pi q_s^C} \mathcal{V}$ . This gives to each field the second charge of table Tab. VII, leaving a 6d space with massless fields from that table

$$\begin{aligned}V : & (\mathbf{8}, \mathbf{1}, \mathbf{1}, \mathbf{1}) + (\mathbf{1}, \mathbf{8}, \mathbf{1}, \mathbf{1}) + (\mathbf{1}, \mathbf{1}, \mathbf{8}, \mathbf{1}) + (\mathbf{1}, \mathbf{1}, \mathbf{1}, \mathbf{8}) + (\mathbf{1}, \bar{\mathbf{3}}, \mathbf{3}, \mathbf{3}) + (\mathbf{1}, \mathbf{3}, \bar{\mathbf{3}}, \bar{\mathbf{3}}), \\ \phi_1 : & (\mathbf{8}, \mathbf{1}, \mathbf{1}, \mathbf{1}) + (\mathbf{1}, \mathbf{8}, \mathbf{1}, \mathbf{1}) + (\mathbf{1}, \mathbf{1}, \mathbf{8}, \mathbf{1}) + (\mathbf{1}, \mathbf{1}, \mathbf{1}, \mathbf{8}) + (\mathbf{1}, \bar{\mathbf{3}}, \mathbf{3}, \mathbf{3}) + (\mathbf{1}, \mathbf{3}, \bar{\mathbf{3}}, \bar{\mathbf{3}}), \\ \phi_2 : & (\bar{\mathbf{3}}, \mathbf{3}, \mathbf{3}, \mathbf{1}) + (\bar{\mathbf{3}}, \bar{\mathbf{3}}, \mathbf{1}, \bar{\mathbf{3}}) + (\bar{\mathbf{3}}, \mathbf{1}, \bar{\mathbf{3}}, \mathbf{3}), \\ \phi_3 : & (\mathbf{3}, \bar{\mathbf{3}}, \bar{\mathbf{3}}, \mathbf{1}) + (\mathbf{3}, \mathbf{3}, \mathbf{1}, \mathbf{3}) + (\mathbf{3}, \mathbf{1}, \mathbf{3}, \bar{\mathbf{3}}).\end{aligned}\tag{F3}$$

It can be seen that the actual unbroken symmetry is  $\text{SU}(3)_C \times \text{E}_6$ . The supermultiplets  $(V, \phi_1)$  in the adjoint representation  $(\mathbf{8}, \mathbf{1}) + (\mathbf{1}, \mathbf{78})$  form a 6d  $\mathcal{N} = 1$  gauge superfield, which can be decomposed into an 4d  $\mathcal{N} = 2$  gauge superfield [101]. The supermultiplets  $(\phi_2, \phi_3)$  in the representation  $(\mathbf{3}, \mathbf{27}) + (\bar{\mathbf{3}}, \bar{\mathbf{27}})$  form a 6d  $\mathcal{N} = 1$  chiral superfield, which can be decomposed into an 4d  $\mathcal{N} = 2$  matter hypermultiplet [101].

## Appendix G: Effective field content at each different scale

In what follows, the coefficients of the beta-functions for each of the regimes in Eq. (5.8) will be determined.

### Running between $\Lambda_6$ and $\Lambda_5$ - Region I

Starting with the lowest-scale theory, denoted as region-I, and according to Tab. XIV, the field content features a SM extension with  $n_H = 1, 2, 3$  the number of Higgs doublet pairs in the low-scale spectrum. Knowing that for  $\text{SU}(3)$

$$T(\mathbf{8}) = C_2(\mathbf{8}) = 3, \quad T(\mathbf{3}) = \frac{1}{2},\tag{G1}$$

SO(1, 3)	SU(3) <sub>C</sub> × SU(2) <sub>L</sub> × U(1) <sub>Y</sub>
Massless complex scalars	$n_H \times (\mathbf{1}, \bar{\mathbf{2}}, 3) + n_H \times (\mathbf{1}, \bar{\mathbf{2}}, -3)$
Massless Weyl fermions	$3 \times (\mathbf{1}, \mathbf{2}, -3) + 3 \times (\mathbf{3}, \mathbf{2}, 1) + 3 \times (\bar{\mathbf{3}}, \mathbf{1}, -4) + 3 \times (\bar{\mathbf{3}}, \mathbf{1}, 2) + 3 \times (\mathbf{1}, \mathbf{1}, 6)$
Massless real vectors	$(\mathbf{8}, \mathbf{1}, 0) + (\mathbf{1}, \mathbf{3}, 0) + (\mathbf{1}, \mathbf{1}, 0)$

TABLE XIV: Field content in Region I

for SU(2)

$$T(\mathbf{3}) = C_2(\mathbf{3}) = 2, \quad T(\mathbf{2}) = \frac{1}{2}, \quad (\text{G2})$$

and considering the Abelian charges and respective multiplicities in Tab. XIV, one obtains

$$b_3^{\text{I}} = -7, \quad b_2^{\text{I}} = -\frac{10}{3} + \frac{n_H}{3}, \quad b_1^{\text{I}} = \frac{3}{5} \left( \frac{20}{3} + \frac{n_H}{3} \right). \quad (\text{G3})$$

### Running between $\Lambda_5$ and $\Lambda_4$ - Region II

Above the  $\Lambda_5$  scale, region-II, gauginos and Higgsinos, which can also be denoted as vector-like fermions (VLFs), contribute to the running such that, according to Tab. XV, modify the beta-function coefficients to

$$b_3^{\text{II}} = -5, \quad b_2^{\text{II}} = \frac{n_H}{3}, \quad b_1^{\text{II}} = \frac{3}{5} \left( \frac{26}{3} + \frac{n_H}{3} \right). \quad (\text{G4})$$

Notice that the presence of SU(2)<sub>L</sub> doublet and triplet vector-like fermions changes the sign

SO(1, 3)	SU(3) <sub>C</sub> × SU(2) <sub>L</sub> × U(1) <sub>Y</sub>
Massless complex scalars	$n_H \times (\mathbf{1}, \bar{\mathbf{2}}, 3) + n_H \times (\mathbf{1}, \bar{\mathbf{2}}, -3)$
Massless Weyl fermions	$(\mathbf{8}, \mathbf{1}, 0) + (\mathbf{1}, \mathbf{3}, 0) + (\mathbf{1}, \mathbf{1}, 0) + 3 \times (\mathbf{1}, \bar{\mathbf{2}}, 3) + 3 \times (\mathbf{1}, \bar{\mathbf{2}}, -3) + 6 \times (\mathbf{1}, \bar{\mathbf{1}}, 0)$ $+ 3 \times (\mathbf{1}, \mathbf{2}, -3) + 3 \times (\mathbf{3}, \mathbf{2}, 1) + 3 \times (\bar{\mathbf{3}}, \mathbf{1}, -4) + 3 \times (\bar{\mathbf{3}}, \mathbf{1}, 2) + 3 \times (\mathbf{1}, \mathbf{1}, 6)$
Massless real vectors	$(\mathbf{8}, \mathbf{1}, 0) + (\mathbf{1}, \mathbf{3}, 0) + (\mathbf{1}, \mathbf{1}, 0)$

TABLE XV: Field content in Region II

of the SU(2)<sub>L</sub> beta-function coefficient in Eq. (G4), which is necessary for the unification of the EW and family groups at the  $\Lambda_2$  scale. As discussed above, such an intermediate unifying picture is described by the flipped E<sub>6</sub> embedding of the trinification SU(3)<sub>F</sub> × SU(3)<sub>L</sub> × SU(3)<sub>R</sub> group such that  $g_{\text{family}} = g_2 = g_1 \equiv g_6$ . At that stage the tree-level matching condition of the U(1)<sub>Y</sub> inverse structure constant with those of the U(1) factors inside SU(3)<sub>L</sub> × SU(3)<sub>R</sub> reads as

$$\alpha_Y^{-1} = \frac{1}{3} \alpha_L^{-1} + \frac{4}{3} \alpha_R^{-1}. \quad (\text{G5})$$

Furthermore, the  $E_6$  embedding implies that  $\alpha_L^{-1} = \alpha_R^{-1}$ , which fixes the usual GUT normalization as

$$\frac{3}{5}\alpha_Y^{-1} \equiv \alpha_1^{-1} \quad \text{or equivalently} \quad \sqrt{\frac{5}{3}}g_Y = g_1, \quad (\text{G6})$$

and explains the  $\frac{3}{5}$  factors in  $b_1^{\text{I,II}}$ .

### Running between $\Lambda_4$ and $\Lambda_3$ - Region III

The next threshold scale,  $\Lambda_4$ , introduces the lightest KK modes in the physical particle spectrum. Taking into account the particle content and number of compact dimensions in

SO(1, 3)	SU(3) <sub>C</sub> × SU(2) <sub>L</sub> × U(1) <sub>Y</sub>
Weyl fermion KK tower	$(\mathbf{8}, \mathbf{1}, 0) + (\mathbf{1}, \mathbf{3}, 0) + (\mathbf{1}, \mathbf{1}, 0) + 3 \times (\mathbf{1}, \bar{\mathbf{2}}, 3) + 3 \times (\mathbf{1}, \bar{\mathbf{2}}, -3) + 6 \times (\mathbf{1}, \bar{\mathbf{1}}, 0)$
$\delta = 2$	$+3 \times (\mathbf{1}, \mathbf{2}, -3) + 3 \times (\mathbf{3}, \mathbf{2}, 1) + 3 \times (\bar{\mathbf{3}}, \mathbf{1}, -4) + 3 \times (\bar{\mathbf{3}}, \mathbf{1}, 2) + 3 \times (\mathbf{1}, \mathbf{1}, 6)$
Real vector KK tower	$(\mathbf{8}, \mathbf{1}, 0) + (\mathbf{1}, \mathbf{3}, 0) + (\mathbf{1}, \mathbf{1}, 0)$
$\delta = 2$	
Massless complex scalars	$n_H \times (\mathbf{1}, \bar{\mathbf{2}}, 3) + n_H \times (\mathbf{1}, \bar{\mathbf{2}}, -3)$
Massless Weyl fermions	$(\mathbf{8}, \mathbf{1}, 0) + (\mathbf{1}, \mathbf{3}, 0) + (\mathbf{1}, \mathbf{1}, 0) + 3 \times (\mathbf{1}, \bar{\mathbf{2}}, 3) + 3 \times (\mathbf{1}, \bar{\mathbf{2}}, -3) + 6 \times (\mathbf{1}, \bar{\mathbf{1}}, 0)$
	$+3 \times (\mathbf{1}, \mathbf{2}, -3) + 3 \times (\mathbf{3}, \mathbf{2}, 1) + 3 \times (\bar{\mathbf{3}}, \mathbf{1}, -4) + 3 \times (\bar{\mathbf{3}}, \mathbf{1}, 2) + 3 \times (\mathbf{1}, \mathbf{1}, 6)$
Massless real vectors	$(\mathbf{8}, \mathbf{1}, 0) + (\mathbf{1}, \mathbf{3}, 0) + (\mathbf{1}, \mathbf{1}, 0)$

TABLE XVI: Field content in Region III

Tab. XVI, one obtains the following coefficients

$$\tilde{b}_3^{\text{III}} = -5, \quad \tilde{b}_2^{\text{III}} = 0, \quad \tilde{b}_1^{\text{III}} = \frac{26}{5}. \quad (\text{G7})$$

### RG evolution between $\Lambda_3$ and $\Lambda_2$ - Region IV

In region IV the effect of heavier KK modes from the trinification and  $E_6$ -phases is considered. Their effect should be included after the SUSY and trinification breaking scales wearing out before the lightest KK models referred in region III are included.

At this stage, and for the field content in Tab. XVII, the coefficients governing the logarithmic evolution of the gauge couplings read as

$$b_3^{\text{IV}} = 0, \quad b_2^{\text{IV}} = 0, \quad b_1^{\text{IV}} = \frac{18}{5}, \quad (\text{G8})$$

whereas those of the power-law contributions, whose effect is dominates the running, are given by

$$\tilde{b}_3^{\text{IV}} = \frac{41}{2}, \quad \tilde{b}_2^{\text{IV}} = -8, \quad \tilde{b}_1^{\text{IV}} = -\frac{99}{40}. \quad (\text{G9})$$

$SO(1, 3)$	$SU(3)_C \times SU(2)_L \times U(1)_Y$
Real scalar KK tower	$(\mathbf{8}, \mathbf{1}, 0) + (\mathbf{1}, \mathbf{3}, 0) + 10 \times (\mathbf{1}, \mathbf{2}, 3) + 10 \times (\mathbf{1}, \mathbf{2}, -3)$
$\delta = 2$	$+4 \times (\mathbf{1}, \mathbf{1}, 6) + 4 \times (\mathbf{1}, \mathbf{1}, -6) + 27 \times (\mathbf{1}, \mathbf{1}, 0)$
Complex scalar KK tower	$5 \times (\mathbf{3}, \mathbf{2}, 1) + 5 \times (\bar{\mathbf{3}}, \mathbf{1}, -4) + 10 \times (\bar{\mathbf{3}}, \mathbf{1}, 2) + (\bar{\mathbf{3}}, \mathbf{2}, 5)$
$\delta = 2$	$+5 \times (\bar{\mathbf{3}}, \mathbf{2}, -1) + 5 \times (\mathbf{3}, \mathbf{1}, 4) + 10 \times (\mathbf{3}, \mathbf{1}, -2) + (\mathbf{3}, \mathbf{2}, -5)$
Weyl fermion KK tower	$2 \times (\mathbf{8}, \mathbf{1}, 0) + 2 \times (\mathbf{1}, \mathbf{3}, 0) + 20 \times (\mathbf{1}, \mathbf{2}, 3) + 20 \times (\mathbf{1}, \mathbf{2}, -3)$
$\delta = 2$	$+8 \times (\mathbf{1}, \mathbf{1}, 6) + 8 \times (\mathbf{1}, \mathbf{1}, -6) + 54 \times (\mathbf{1}, \mathbf{1}, 0)$
	$5 \times (\mathbf{3}, \mathbf{2}, 1) + 5 \times (\bar{\mathbf{3}}, \mathbf{1}, -4) + 10 \times (\bar{\mathbf{3}}, \mathbf{1}, 2) + (\bar{\mathbf{3}}, \mathbf{2}, 5)$
$\delta = 2$	$+5 \times (\bar{\mathbf{3}}, \mathbf{2}, -1) + 5 \times (\mathbf{3}, \mathbf{1}, 4) + 10 \times (\mathbf{3}, \mathbf{1}, -2) + (\mathbf{3}, \mathbf{2}, -5)$
Real vector KK tower	$(\mathbf{8}, \mathbf{1}, 0) + (\mathbf{1}, \mathbf{3}, 0) + 10 \times (\mathbf{1}, \mathbf{2}, 3) + 10 \times (\mathbf{1}, \mathbf{2}, -3)$
$\delta = 2$	$+4 \times (\mathbf{1}, \mathbf{1}, 6) + 4 \times (\mathbf{1}, \mathbf{1}, -6) + 27 \times (\mathbf{1}, \mathbf{1}, 0)$
Massless complex scalars	$3 \times (\mathbf{1}, \mathbf{2}, 3) + 6 \times (\mathbf{1}, \mathbf{2}, -3) + 3 \times (\mathbf{1}, \mathbf{1}, 6) + 6 \times (\mathbf{1}, \mathbf{1}, 0)$
	$+3 \times (\mathbf{3}, \mathbf{2}, 1) + 3 \times (\bar{\mathbf{3}}, \mathbf{1}, -4) + 6 \times (\bar{\mathbf{3}}, \mathbf{1}, 2) + 3 \times (\mathbf{3}, \mathbf{1}, -2)$
Massless Weyl fermions	$3 \times (\mathbf{1}, \mathbf{2}, 3) + 6 \times (\mathbf{1}, \mathbf{2}, -3) + 3 \times (\mathbf{1}, \mathbf{1}, 6) + 6 \times (\mathbf{1}, \mathbf{1}, 0)$
	$+3 \times (\mathbf{3}, \mathbf{2}, 1) + 3 \times (\bar{\mathbf{3}}, \mathbf{1}, -4) + 6 \times (\bar{\mathbf{3}}, \mathbf{1}, 2) + 3 \times (\mathbf{3}, \mathbf{1}, -2)$
	$+(\mathbf{8}, \mathbf{1}, 0) + (\mathbf{1}, \mathbf{3}, 0) + (\mathbf{1}, \mathbf{2}, 3) + (\mathbf{1}, \mathbf{2}, -3) + 15 \times (\mathbf{1}, \mathbf{1}, 0) + (\mathbf{1}, \mathbf{1}, 6) + (\mathbf{1}, \mathbf{1}, -6)$
Massless real vectors	$(\mathbf{8}, \mathbf{1}, 0) + (\mathbf{1}, \mathbf{3}, 0) + (\mathbf{1}, \mathbf{2}, 3) + (\mathbf{1}, \mathbf{2}, -3) + 15 \times (\mathbf{1}, \mathbf{1}, 0) + (\mathbf{1}, \mathbf{1}, 6) + (\mathbf{1}, \mathbf{1}, -6)$

TABLE XVII: Field content in Region IV

### Running between $\Lambda_2$ and $\Lambda_1$ - Region V

Above the energy scale  $\Lambda_2$ , and below  $\Lambda_0$ , the theory becomes six-dimensional. In particular, for the sub-range of energies smaller than  $\Lambda_1$ , denoted as region V, there are only 6d zero modes contributing to the evolution of the gauge couplings, as shown in Tab. XVIII. However, since there are six dimensions present, the running behaves as a power-law with

$SO(1, 3)$	$SU(3)_C \times E_6$
Complex Scalar KK tower $\delta = 2$	$(\mathbf{8}, \mathbf{1}) + (\mathbf{1}, \mathbf{78}) + (\mathbf{3}, \mathbf{27}) + (\bar{\mathbf{3}}, \mathbf{27})$
Weyl fermion KK tower $\delta = 2$	$2 \times (\mathbf{8}, \mathbf{1}) + 2 \times (\mathbf{1}, \mathbf{78}) + (\mathbf{3}, \mathbf{27}) + (\bar{\mathbf{3}}, \mathbf{27})$
Real vector KK tower $\delta = 2$	$(\mathbf{8}, \mathbf{1}) + (\mathbf{1}, \mathbf{78})$

TABLE XVIII: Field content in Region V

two EDs,  $\delta = 2$ , whose dominant contribution is governed by the last term in Eq. (5.5). Taking into account the  $E_6$  group factors,

$$T(\mathbf{78}) = C_2(\mathbf{78}) = 12, \quad T(\mathbf{27}) = 3, \quad (\text{G10})$$

and the representations in Tab. XVIII, the coefficients of the RGEs read as

$$b_3^V = 21, \quad b_6^V = -6. \quad (\text{G11})$$

### Running between $\Lambda_1$ and $\Lambda_0$ - Region VI

As one passes the  $\Lambda_1$  scale, contributions from KK modes resulting from the compactification of the  $E_8$  ten-dimensional theory need to be taken into account. Using the field

SO(1,3)	SU(3) <sub>C</sub> × E <sub>6</sub>
Complex Scalar KK tower $\delta = 6$	$2 \times (\mathbf{8}, \mathbf{1}) + 2 \times (\mathbf{1}, \mathbf{78}) + 2 \times (\mathbf{3}, \mathbf{27}) + 2 \times (\overline{\mathbf{3}}, \overline{\mathbf{27}})$
Real scalar KK tower $\delta = 6$	$(\mathbf{8}, \mathbf{1}) + (\mathbf{1}, \mathbf{78}) + (\mathbf{3}, \mathbf{27}) + (\overline{\mathbf{3}}, \overline{\mathbf{27}})$
Weyl fermion KK tower $\delta = 6$	$4 \times (\mathbf{8}, \mathbf{1}) + 4 \times (\mathbf{1}, \mathbf{78}) + 4 \times (\mathbf{3}, \mathbf{27}) + 4 \times (\overline{\mathbf{3}}, \overline{\mathbf{27}})$
Real vector KK tower $\delta = 6$	$(\mathbf{8}, \mathbf{1}) + (\mathbf{1}, \mathbf{78}) + (\mathbf{3}, \mathbf{27}) + (\overline{\mathbf{3}}, \overline{\mathbf{27}})$
Complex Scalar KK tower $\delta = 2$	$(\mathbf{8}, \mathbf{1}) + (\mathbf{1}, \mathbf{78}) + (\mathbf{3}, \mathbf{27}) + (\overline{\mathbf{3}}, \overline{\mathbf{27}})$
Weyl fermion KK tower $\delta = 2$	$2 \times (\mathbf{8}, \mathbf{1}) + 2 \times (\mathbf{1}, \mathbf{78}) + (\mathbf{3}, \mathbf{27}) + (\overline{\mathbf{3}}, \overline{\mathbf{27}})$
Real vector KK tower $\delta = 2$	$(\mathbf{8}, \mathbf{1}) + (\mathbf{1}, \mathbf{78})$

TABLE XIX: Field content in Region VI

content in Tab. XIX, one obtains the following coefficients for what we denote as region VI

$$\tilde{b}_3^{\text{VI}} = -5, \quad \tilde{b}_6^{\text{VI}} = -5. \quad (\text{G12})$$

Note the sign inversion for the SU(3)<sub>C</sub> beta-functions. This is due to the presence of the vector fields  $(\mathbf{3}, \mathbf{27}) + (\overline{\mathbf{3}}, \overline{\mathbf{27}})$  that contribute with a large negative factor equal to  $-\frac{11}{3}T(\mathbf{3}) \times 2 \times 27 = -99$ , resulting in a positive contribution to the running. Also, the equality  $\tilde{b}_3^{\text{VI}} = \tilde{b}_6^{\text{VI}}$  will have profound implications as we discuss below.

### Running above $\Lambda_0$ - Region VII

Finally above the largest energy  $\Lambda_0$ , there is only a single  $E_8$  vector superfield, which is decomposed into KK modes as in Tab. XX. The field content has an effective  $\mathcal{N} = 4$  SUSY

SO(1,3)	E <sub>8</sub>
Complex Scalar KK tower $\delta = 6$	$3 \times \mathbf{248}$
Weyl fermion KK tower $\delta = 6$	$4 \times \mathbf{248}$
Real vector KK tower $\delta = 6$	$\mathbf{248}$

TABLE XX: Field content in Region VII

and the single gauge coupling beta-function vanishes [101] i.e.,  $\beta_{g_s}^{(n)} = 0$ , thus no longer evolving with the energy-scale.

### Appendix H: RG equations for the SU(3)<sub>C</sub> × SU(2)<sub>L</sub> × U(1)<sub>Y</sub> phase

In this appendix, the RGEs for the vector-like fermion are presented for the extended version of the type-II 2HDM EFT-limit. The Yukawa couplings run according to the following

beta-functions:

$$\begin{aligned}
\kappa\beta_{y_{\bar{b}1}}^{(1)} &= y_{\bar{b}1} \left( 3y_b^2 + \frac{9}{4}y_{\bar{w}1}^2 + \frac{5}{2}y_{\bar{b}1}^2 + y_{\bar{b}2}^2 - \frac{9}{20}g_1^2 - \frac{9}{4}g_2^2 \right), \\
\kappa\tilde{\beta}_{y_{\bar{b}1}}^{(1)} &= y_{\bar{b}1} \left( 6y_b^2 + \frac{9}{2}y_{\bar{w}1}^2 + 5y_{\bar{b}1}^2 + 2y_{\bar{b}2}^2 - \frac{9}{20}g_1^2 - \frac{9}{4}g_2^2 \right), \\
\kappa\beta_{y_{\bar{b}2}}^{(1)} &= \beta_{y_{\bar{b}1}}^{(1)} \quad \text{and} \quad \tilde{\beta}_{y_{\bar{b}2}}^{(1)} = \tilde{\beta}_{y_{\bar{b}1}}^{(1)} \quad \text{replacing} \quad (y_b \rightarrow y_t, y_{\bar{b}1} \leftrightarrow y_{\bar{b}2}, y_{\bar{w}1} \rightarrow y_{\bar{w}2}), \\
\beta_{y_{\bar{w}1}}^{(1)} &= y_{\bar{w}1} \left( 3y_b^2 + \frac{11}{4}y_{\bar{w}1}^2 + \frac{3}{2}y_{\bar{b}1}^2 + \frac{1}{2}y_{\bar{w}2}^2 - \frac{9}{20}g_1^2 - \frac{33}{4}g_2^2 \right), \\
\kappa\tilde{\beta}_{y_{\bar{w}1}}^{(1)} &= y_{\bar{w}1} \left( 6y_b^2 + \frac{11}{2}y_{\bar{w}1}^2 + 3y_{\bar{b}1}^2 + y_{\bar{w}2}^2 - \frac{9}{20}g_1^2 - \frac{33}{4}g_2^2 \right), \\
\beta_{y_{\bar{w}2}}^{(1)} &= \beta_{y_{\bar{w}1}}^{(1)} \quad \text{and} \quad \tilde{\beta}_{y_{\bar{w}2}}^{(1)} = \tilde{\beta}_{y_{\bar{w}1}}^{(1)} \quad \text{replacing} \quad (y_b \rightarrow y_t, y_{\bar{w}1} \leftrightarrow y_{\bar{w}2}, y_{\bar{b}1} \rightarrow y_{\bar{b}2}), \\
\beta_{y_t}^{(1)} &= y_t \left( \frac{9}{2}y_t^2 + \frac{1}{2}y_b^2 + \frac{3}{2}y_{\bar{w}2}^2 + y_{\bar{b}2}^2 - 8g_3^2 - \frac{9}{4}g_2^2 - \frac{17}{20}g_1^2 \right), \\
\kappa\tilde{\beta}_{y_t}^{(1)} &= y_t \left( \frac{15}{2}y_t^2 + \frac{1}{2}y_b^2 + 3y_{\bar{w}2}^2 + 2y_{\bar{b}2}^2 - 8g_3^2 - \frac{9}{4}g_2^2 - \frac{17}{20}g_1^2 \right), \\
\kappa\beta_{y_b}^{(1)} &= y_b \left( \frac{9}{2}y_b^2 + \frac{1}{2}y_t^2 + \frac{3}{2}y_{\bar{w}1}^2 + y_{\bar{b}1}^2 - 8g_3^2 - \frac{9}{4}g_2^2 - \frac{1}{4}g_1^2 \right), \\
\kappa\tilde{\beta}_{y_b}^{(1)} &= y_b \left( \frac{15}{2}y_b^2 + \frac{1}{2}y_t^2 + 3y_{\bar{w}1}^2 + 2y_{\bar{b}1}^2 - 8g_3^2 - \frac{9}{4}g_2^2 - \frac{1}{4}g_1^2 \right),
\end{aligned} \tag{H1}$$

with  $\kappa = 16\pi^2$ .

The scalar quartic couplings beta-functions read as

$$\begin{aligned}
\kappa\beta_{\lambda_1}^{(1)} &= \frac{27}{200}g_1^4 + \frac{9}{20}g_1^2g_2^2 + \frac{9}{8}g_2^4 - \frac{9}{5}g_1^2\lambda_1 - 9g_2\lambda_1 + 24\lambda_1^2 + 2\lambda_3^2 + 2\lambda_3\lambda_4 + \lambda_4^2 + |\lambda_5|^2 \\
&\quad + 12\lambda_1y_b^2 - 6y_b^4 + 4\lambda_1y_{\bar{b}1}^2 - 2y_{\bar{b}1}^4 - 2y_{\bar{b}1}^2y_{\bar{w}1}^2 + 6\lambda_1y_{\bar{w}1}^2 - \frac{5}{2}y_{\bar{w}1}^4 \\
\kappa\tilde{\beta}_{\lambda_1}^{(1)} &= \frac{27}{200}g_1^4 + \frac{9}{20}g_1^2g_2^2 + \frac{9}{8}g_2^4 - \frac{9}{5}g_1^2\lambda_1 - 9g_2\lambda_1 + 24\lambda_1^2 + 2\lambda_3^2 + 2\lambda_3\lambda_4 + \lambda_4^2 + |\lambda_5|^2 \\
&\quad + 24\lambda_1y_b^2 - 12y_b^4 + 8\lambda_1y_{\bar{b}1}^2 - 4y_{\bar{b}1}^4 - 4y_{\bar{b}1}^2y_{\bar{w}1}^2 + 12\lambda_1y_{\bar{w}1}^2 - 5y_{\bar{w}1}^4 \\
\kappa\beta_{\lambda_2}^{(1)} &= \frac{27}{200}g_1^4 + \frac{9}{20}g_1^2g_2^2 + \frac{9}{8}g_2^4 - \frac{9}{5}g_1^2\lambda_2 - 9g_2\lambda_2 + 24\lambda_2^2 + 2\lambda_4^2 + 2\lambda_3\lambda_4 + \lambda_4^2 + |\lambda_5|^2 \\
&\quad + 12\lambda_2y_t^2 - 6y_t^4 + 4\lambda_2y_{\bar{b}2}^2 - 2y_{\bar{b}2}^4 - 2y_{\bar{b}2}^2y_{\bar{w}2}^2 + 6\lambda_2y_{\bar{w}2}^2 - \frac{5}{2}y_{\bar{w}2}^4 \\
\kappa\tilde{\beta}_{\lambda_2}^{(1)} &= \frac{27}{200}g_1^4 + \frac{9}{20}g_1^2g_2^2 + \frac{9}{8}g_2^4 - \frac{9}{5}g_1^2\lambda_2 - 9g_2\lambda_2 + 24\lambda_2^2 + 2\lambda_4^2 + 2\lambda_3\lambda_4 + \lambda_4^2 + |\lambda_5|^2 \\
&\quad + 24\lambda_2y_t^2 - 12y_t^4 + 8\lambda_2y_{\bar{b}2}^2 - 4y_{\bar{b}2}^4 - 4y_{\bar{b}2}^2y_{\bar{w}2}^2 + 12\lambda_2y_{\bar{w}2}^2 - 5y_{\bar{w}2}^4,
\end{aligned} \tag{H2}$$

$$\begin{aligned}
\kappa\beta_{\lambda_3}^{(1)} &= \frac{27}{100}g_1^4 + \frac{9}{10}g_1^2g_2^2 + \frac{9}{4}g_2^4 - \frac{9}{5}g_1^2\lambda_3 - 9g_2\lambda_3 + 12(\lambda_1 + \lambda_2)\lambda_3 + 4\lambda_3^2 \\
&\quad + 4(\lambda_1 + \lambda_2)\lambda_4 + 2\lambda_4^2 + 2|\lambda_5|^2 + 6(y_b^2 + y_t^2)\lambda_3 - 12y_b^2y_t^2 - 4y_{b1}^2y_{b2}^2 \\
&\quad + 2(y_{b1}^2 + y_{b2}^2)\lambda_3 + 3(y_{\bar{w}1}^2 + y_{\bar{w}2}^2)\lambda_3 - 5y_{\bar{w}1}^2y_{\bar{w}2}^2 + 4y_{b1}y_{b2}y_{\bar{w}1}y_{\bar{w}2} \\
\kappa\tilde{\beta}_{\lambda_3}^{(1)} &= \frac{27}{100}g_1^4 + \frac{9}{10}g_1^2g_2^2 + \frac{9}{4}g_2^4 - \frac{9}{5}g_1^2\lambda_3 - 9g_2\lambda_3 + 12(\lambda_1 + \lambda_2)\lambda_3 + 4\lambda_3^2 \\
&\quad + 4(\lambda_1 + \lambda_2)\lambda_4 + 2\lambda_4^2 + 2|\lambda_5|^2 + 12(y_b^2 + y_t^2)\lambda_3 - 24y_b^2y_t^2 - 8y_{b1}^2y_{b2}^2 \\
&\quad + 4(y_{b1}^2 + y_{b2}^2)\lambda_3 + 6(y_{\bar{w}1}^2 + y_{\bar{w}2}^2)\lambda_3 - 10y_{\bar{w}1}^2y_{\bar{w}2}^2 + 8y_{b1}y_{b2}y_{\bar{w}1}y_{\bar{w}2} \\
\kappa\beta_{\lambda_4}^{(1)} &= \frac{9}{5}g_1^2g_2^2 - \frac{9}{5}g_1^2\lambda_4 - 9g_2^2\lambda_4 + 4(\lambda_1 + \lambda_2)\lambda_4 + 8\lambda_3\lambda_4 + 4\lambda_4^2 + 8|\lambda_5|^2 \\
&\quad + 6(y_b^2 + y_t^2)\lambda_4 + 12y_b^2y_t^2 + 2\lambda_4y_{b2}^2 + 3(y_{\bar{w}1}^2 + y_{\bar{w}2}^2)\lambda_4 + 4y_{\bar{w}1}^2y_{\bar{w}2}^2 \\
&\quad - 8y_{b1}y_{b2}y_{\bar{w}1}y_{\bar{w}2} \\
\kappa\tilde{\beta}_{\lambda_4}^{(1)} &= \frac{9}{5}g_1^2g_2^2 - \frac{9}{5}g_1^2\lambda_4 - 9g_2^2\lambda_4 + 4(\lambda_1 + \lambda_2)\lambda_4 + 8\lambda_3\lambda_4 + 4\lambda_4^2 + 8|\lambda_5|^2 \\
&\quad + 12(y_b^2 + y_t^2)\lambda_4 + 24y_b^2y_t^2 + 4\lambda_4y_{b2}^2 + 6(y_{\bar{w}1}^2 + y_{\bar{w}2}^2)\lambda_4 + 8y_{\bar{w}1}^2y_{\bar{w}2}^2 \\
&\quad - 16y_{b1}y_{b2}y_{\bar{w}1}y_{\bar{w}2} \\
\kappa\beta_{\lambda_5}^{(1)} &= \lambda_5 \left[ -\frac{9}{5}g_1^2 - 9g_2^2 + 4(\lambda_1 + \lambda_2 + 2\lambda_3 + 3\lambda_4) + 2(y_{b1}^2 + y_{b2}^2) \right. \\
&\quad \left. + 3(y_{\bar{w}1}^2 + y_{\bar{w}2}^2) + 6(y_b^2 + y_t^2) \right] \\
\kappa\tilde{\beta}_{\lambda_5}^{(1)} &= \lambda_5 \left[ -\frac{9}{5}g_1^2 - 9g_2^2 + 4(\lambda_1 + \lambda_2 + 2\lambda_3 + 3\lambda_4) + 4(y_{b1}^2 + y_{b2}^2) \right. \\
&\quad \left. + 6(y_{\bar{w}1}^2 + y_{\bar{w}2}^2) + 12(y_b^2 + y_t^2) \right] .
\end{aligned} \tag{H3}$$

Finally, the Higgsino mass parameters beta-functions are given by

$$\begin{aligned}
\kappa\beta_{M_E}^{(1)} &= M_E \left[ -\frac{9}{10}(5g_2^2 + g_1^2) + \frac{1}{2}(y_{b1}^2 + y_{b2}^2) + \frac{3}{4}(y_{\bar{w}1}^2 + y_{\bar{w}2}^2) \right] \\
\tilde{\beta}_{M_E}^{(1)} &= \beta_{M_E}^{(1)} \\
\kappa\beta_{M_{LE}}^{(1)} &= M_{LE} \left[ -\frac{9}{10}(5g_2^2 + g_1^2) + \frac{1}{2}y_{b2}^2 + \frac{3}{4}y_{\bar{w}2}^2 \right] \\
\tilde{\beta}_{M_{LE}}^{(1)} &= \beta_{M_{LE}}^{(1)} .
\end{aligned} \tag{H4}$$

- 
- [1] G. Aad *et al.* (ATLAS), *Phys. Lett. B* **716**, 1 (2012), [arXiv:1207.7214 \[hep-ex\]](#).
  - [2] S. Chatrchyan *et al.* (CMS), *Phys. Lett. B* **716**, 30 (2012), [arXiv:1207.7235 \[hep-ex\]](#).
  - [3] G. Arnison *et al.* (UA1), *Phys. Lett. B* **122**, 103 (1983).
  - [4] F. J. Hasert *et al.* (Gargamelle Neutrino), *Phys. Lett. B* **46**, 138 (1973).
  - [5] F. J. Hasert *et al.*, *Phys. Lett. B* **46**, 121 (1973).
  - [6] F. Abe *et al.* (CDF), *Phys. Rev. Lett.* **74**, 2626 (1995), [arXiv:hep-ex/9503002](#).



- [7] R. H. Parker, C. Yu, W. Zhong, B. Estey, and H. Müller, *Science* **360**, 191 (2018), [arXiv:1812.04130 \[physics.atom-ph\]](#).
- [8] Y. Fukuda *et al.* (Super-Kamiokande), *Phys. Rev. Lett.* **81**, 1562 (1998), [arXiv:hep-ex/9807003](#).
- [9] G. Bertone, D. Hooper, and J. Silk, *Phys. Rept.* **405**, 279 (2005), [arXiv:hep-ph/0404175](#).
- [10] H. Georgi and S. L. Glashow, *Phys. Rev. Lett.* **32**, 438 (1974).
- [11] N. Sakai, *Z. Phys. C* **11**, 153 (1981).
- [12] H. Fritzsch and P. Minkowski, *Annals Phys.* **93**, 193 (1975).
- [13] F. Gurse, P. Ramond, and P. Sikivie, *Phys. Lett. B* **60**, 177 (1976).
- [14] S. F. King, S. Moretti, and R. Nevzorov, *Phys. Lett. B* **634**, 278 (2006), [arXiv:hep-ph/0511256](#).
- [15] W. Buchmüller and O. Napoly, *Phys. Lett. B* **163**, 161 (1985).
- [16] M. Koca, *Lect. Notes Phys.* **180**, 356 (2005).
- [17] R. Slansky, *Phys. Rept.* **79**, 1 (1981).
- [18] J. E. Camargo-Molina, A. P. Morais, A. Ordell, R. Pasechnik, M. O. P. Sampaio, and J. Wessén, *Phys. Rev. D* **95**, 075031 (2017), [arXiv:1610.03642 \[hep-ph\]](#).
- [19] J. E. Camargo-Molina, A. P. Morais, A. Ordell, R. Pasechnik, and J. Wessén, *Phys. Rev. D* **99**, 035041 (2019), [arXiv:1711.05199 \[hep-ph\]](#).
- [20] A. P. Morais, R. Pasechnik, and W. Porod, *Eur. Phys. J. C* **80**, 1162 (2020), [arXiv:2001.06383 \[hep-ph\]](#).
- [21] S. F. King and G. G. Ross, *Phys. Lett. B* **520**, 243 (2001), [arXiv:hep-ph/0108112](#).
- [22] S. F. King, *Prog. Part. Nucl. Phys.* **94**, 217 (2017), [arXiv:1701.04413 \[hep-ph\]](#).
- [23] C. Hagedorn, S. F. King, and C. Luhn, *JHEP* **06**, 048 (2010), [arXiv:1003.4249 \[hep-ph\]](#).
- [24] S. Antusch, I. de Medeiros Varzielas, V. Maurer, C. Sluka, and M. Spinrath, *JHEP* **09**, 141 (2014), [arXiv:1405.6962 \[hep-ph\]](#).
- [25] F. Björkeröth, F. J. de Anda, I. de Medeiros Varzielas, and S. F. King, *JHEP* **06**, 141 (2015), [arXiv:1503.03306 \[hep-ph\]](#).
- [26] F. Björkeröth, F. J. de Anda, I. de Medeiros Varzielas, and S. F. King, *Phys. Rev. D* **94**, 016006 (2016), [arXiv:1512.00850 \[hep-ph\]](#).
- [27] F. Björkeröth, F. J. de Anda, S. F. King, and E. Perdomo, *JHEP* **10**, 148 (2017), [arXiv:1705.01555 \[hep-ph\]](#).
- [28] F. J. de Anda, S. F. King, and E. Perdomo, *JHEP* **12**, 075 (2017), [Erratum: *JHEP* **04**, 069 (2019)], [arXiv:1710.03229 \[hep-ph\]](#).
- [29] A. E. Cárcamo Hernández, D. T. Huong, S. Kovalenko, A. P. Morais, R. Pasechnik, and I. Schmidt, *Phys. Rev. D* **102**, 095003 (2020), [arXiv:2004.11450 \[hep-ph\]](#).
- [30] A. P. Morais, R. Pasechnik, and W. Porod, (2020), [arXiv:2001.04804 \[hep-ph\]](#).
- [31] J. E. Camargo-Molina, A. P. Morais, R. Pasechnik, and J. Wessén, *JHEP* **09**, 129 (2016), [arXiv:1606.03492 \[hep-ph\]](#).
- [32] M. Reig, J. W. F. Valle, C. A. Vaquera-Araujo, and F. Wilczek, *Phys. Lett. B* **774**, 667 (2017), [arXiv:1706.03116 \[hep-ph\]](#).
- [33] G. Altarelli, F. Feruglio, and C. Hagedorn, *JHEP* **03**, 052 (2008), [arXiv:0802.0090 \[hep-ph\]](#).
- [34] T. J. Burrows and S. F. King, *Nucl. Phys. B* **835**, 174 (2010), [arXiv:0909.1433 \[hep-ph\]](#).
- [35] T. J. Burrows and S. F. King, *Nucl. Phys. B* **842**, 107 (2011), [arXiv:1007.2310 \[hep-ph\]](#).

- [36] F. J. de Anda and S. F. King, *JHEP* **07**, 057 (2018), [arXiv:1803.04978 \[hep-ph\]](#).
- [37] G. Altarelli, F. Feruglio, and Y. Lin, *Nucl. Phys. B* **775**, 31 (2007), [arXiv:hep-ph/0610165](#).
- [38] A. Adulpravitchai and M. A. Schmidt, *JHEP* **01**, 106 (2011), [arXiv:1001.3172 \[hep-ph\]](#).
- [39] A. Adulpravitchai, A. Blum, and M. Lindner, *JHEP* **07**, 053 (2009), [arXiv:0906.0468 \[hep-ph\]](#).
- [40] T. Asaka, W. Buchmuller, and L. Covi, *Phys. Lett. B* **523**, 199 (2001), [arXiv:hep-ph/0108021](#).
- [41] F. J. de Anda, J. W. F. Valle, and C. A. Vaquera-Araujo, *Phys. Lett. B* **801**, 135195 (2020), [arXiv:1910.05605 \[hep-ph\]](#).
- [42] F. J. de Anda, S. F. King, and E. Perdomo, *Phys. Rev. D* **101**, 015028 (2020), [arXiv:1812.05620 \[hep-ph\]](#).
- [43] F. J. de Anda and S. F. King, *JHEP* **10**, 128 (2018), [arXiv:1807.07078 \[hep-ph\]](#).
- [44] L. E. Ibanez, J. Mas, H.-P. Nilles, and F. Quevedo, *Nucl. Phys. B* **301**, 157 (1988).
- [45] E. Parr, P. K. S. Vaudrevange, and M. Wimmer, *Fortsch. Phys.* **68**, 2000032 (2020), [arXiv:2003.01732 \[hep-th\]](#).
- [46] S. L. Adler, *Phys. Lett. B* **533**, 121 (2002), [arXiv:hep-ph/0201009](#).
- [47] S. L. Adler, (2004), [arXiv:hep-ph/0401212](#).
- [48] S. Garibaldi, *Bull. Am. Math. Soc.* **53**, 643 (2016), [arXiv:1605.01721 \[math.RA\]](#).
- [49] S. Thomas, *J. Phys. A* **19**, 1141 (1986).
- [50] S. E. Konshtein and E. S. Fradkin, *Pisma Zh. Eksp. Teor. Fiz.* **32**, 575 (1980).
- [51] N. S. Baaklini, *Phys. Rev. D* **22**, 3118 (1980).
- [52] N. S. Baaklini, *Phys. Lett. B* **91**, 376 (1980).
- [53] S. M. Barr, *Phys. Rev. D* **37**, 204 (1988).
- [54] I. Bars and M. Gunaydin, *Phys. Rev. Lett.* **45**, 859 (1980).
- [55] M. Koca, *Phys. Lett. B* **107**, 73 (1981).
- [56] S. Mahapatra and B. B. Deo, *Phys. Rev. D* **38**, 3554 (1988).
- [57] C.-L. Ong, *Phys. Rev. D* **31**, 3271 (1985).
- [58] D. I. Olive and P. C. West, *Nucl. Phys. B* **217**, 248 (1983).
- [59] N. Arkani-Hamed, T. Gregoire, and J. G. Wacker, *JHEP* **03**, 055 (2002), [arXiv:hep-th/0101233](#).
- [60] L. Brink, J. H. Schwarz, and J. Scherk, *Nucl. Phys. B* **121**, 77 (1977).
- [61] P. Candelas, G. T. Horowitz, A. Strominger, and E. Witten, *Nucl. Phys. B* **258**, 46 (1985).
- [62] A. Aranda, F. J. de Anda, and S. F. King, *Nucl. Phys. B* **960**, 115209 (2020), [arXiv:2005.03048 \[hep-ph\]](#).
- [63] F. J. de Anda, A. Aranda, A. P. Morais, and R. Pasechnik, (2020), [arXiv:2011.13902 \[hep-ph\]](#).
- [64] A. Aranda and F. J. de Anda, *Int. J. Mod. Phys. A* **36**, 15 (2021), [arXiv:2007.13248 \[hep-ph\]](#).
- [65] C. A. Scrucca and M. Serone, *Int. J. Mod. Phys. A* **19**, 2579 (2004), [arXiv:hep-th/0403163](#).
- [66] L. E. Ibanez, in *Latin American School of Physics (ELAF 87): Contacts among Particle Physics, Nuclear Physics, Statistical Mechanics and Condensed Matter* (1987).
- [67] M. B. Green and J. H. Schwarz, *Phys. Lett. B* **149**, 117 (1984).
- [68] F. J. De Anda, *Class. Quant. Grav.* **37**, 195012 (2020), [arXiv:1910.03599 \[hep-th\]](#).
- [69] N. S. Linnemann and M. R. Visser, *Stud. Hist. Phil. Sci. B* **64**, 1 (2018), [arXiv:1711.10503 \[physics.hist-ph\]](#).
- [70] C. Barcelo, S. Liberati, and M. Visser, *Class. Quant. Grav.* **18**, 3595 (2001), [arXiv:gr-qc/0104001](#).

- [71] H. K. Dreiner, *Adv. Ser. Direct. High Energy Phys.* **21**, 565 (2010), [arXiv:hep-ph/9707435](#).
- [72] R. Barbier *et al.*, *Phys. Rept.* **420**, 1 (2005), [arXiv:hep-ph/0406039](#).
- [73] F. Burnell and G. D. Kribs, *Phys. Rev. D* **73**, 015001 (2006), [arXiv:hep-ph/0509118](#).
- [74] S. Arrenberg, L. Baudis, K. Kong, K. T. Matchev, and J. Yoo, *Phys. Rev. D* **78**, 056002 (2008), [arXiv:0805.4210 \[hep-ph\]](#).
- [75] K. Kong and K. T. Matchev, *JHEP* **01**, 038 (2006), [arXiv:hep-ph/0509119](#).
- [76] G. Servant and T. M. P. Tait, *Nucl. Phys. B* **650**, 391 (2003), [arXiv:hep-ph/0206071](#).
- [77] D. Hooper and S. Profumo, *Phys. Rept.* **453**, 29 (2007), [arXiv:hep-ph/0701197](#).
- [78] A. B. Kobakhidze, *Phys. Lett. B* **514**, 131 (2001), [arXiv:hep-ph/0102323](#).
- [79] W. de Boer, *Prog. Part. Nucl. Phys.* **33**, 201 (1994), [arXiv:hep-ph/9402266](#).
- [80] H. Murayama and D. B. Kaplan, *Phys. Lett. B* **336**, 221 (1994), [arXiv:hep-ph/9406423](#).
- [81] P. A. Zyla *et al.* (Particle Data Group), *PTEP* **2020**, 083C01 (2020).
- [82] V. Takhistov (Super-Kamiokande), in *51st Rencontres de Moriond on EW Interactions and Unified Theories* (2016) [arXiv:1605.03235 \[hep-ex\]](#).
- [83] T. Bandyopadhyay, B. Brahmachari, and A. Raychaudhuri, *JHEP* **02**, 023 (2016), [arXiv:1509.03232 \[hep-ph\]](#).
- [84] K. R. Dienes, E. Dudas, and T. Gherghetta, *Nucl. Phys. B* **537**, 47 (1999), [arXiv:hep-ph/9806292](#).
- [85] K. R. Dienes, E. Dudas, and T. Gherghetta, *Phys. Lett. B* **436**, 55 (1998), [arXiv:hep-ph/9803466](#).
- [86] L.-X. Liu and A. Cornell, *Phys. Rev. D* **86**, 056002 (2012), [arXiv:1204.0532 \[hep-ph\]](#).
- [87] “Computing resources,” <http://gravitation.web.ua.pt/computing>.
- [88] M. Aaboud *et al.* (ATLAS), *Phys. Rev. D* **96**, 052004 (2017), [arXiv:1703.09127 \[hep-ex\]](#).
- [89] K.-m. Cheung and G. L. Landsberg, *Phys. Rev. D* **65**, 076003 (2002), [arXiv:hep-ph/0110346](#).
- [90] R. Barbieri, A. Pomarol, R. Rattazzi, and A. Strumia, *Nucl. Phys. B* **703**, 127 (2004), [arXiv:hep-ph/0405040](#).
- [91] F. Staub, *Comput. Phys. Commun.* **185**, 1773 (2014), [arXiv:1309.7223 \[hep-ph\]](#).
- [92] G. Bhattacharyya, A. Datta, S. K. Majee, and A. Raychaudhuri, *Nucl. Phys. B* **760**, 117 (2007), [arXiv:hep-ph/0608208](#).
- [93] G. C. Branco, P. M. Ferreira, L. Lavoura, M. N. Rebelo, M. Sher, and J. P. Silva, *Phys. Rept.* **516**, 1 (2012), [arXiv:1106.0034 \[hep-ph\]](#).
- [94] F. F. Freitas, J. a. Gonçalves, A. P. Moraes, and R. Pasechnik, *JHEP* **01**, 076 (2021), [arXiv:2010.01307 \[hep-ph\]](#).
- [95] B. Abi *et al.* (Muon g-2), *Phys. Rev. Lett.* **126**, 141801 (2021), [arXiv:2104.03281 \[hep-ex\]](#).
- [96] P. Athron, C. Balázs, D. H. Jacob, W. Kotlarski, D. Stöckinger, and H. Stöckinger-Kim, (2021), [arXiv:2104.03691 \[hep-ph\]](#).
- [97] G.-Y. Huang, S. Jana, F. S. Queiroz, and W. Rodejohann, (2021), [arXiv:2103.01617 \[hep-ph\]](#).
- [98] I. Doršner, S. Fajfer, and O. Sumensari, *JHEP* **06**, 089 (2020), [arXiv:1910.03877 \[hep-ph\]](#).
- [99] A. Angelescu, D. Bečirević, D. A. Faroughy, and O. Sumensari, *JHEP* **10**, 183 (2018), [arXiv:1808.08179 \[hep-ph\]](#).
- [100] R. Aaij *et al.* (LHCb), (2021), [arXiv:2103.11769 \[hep-ex\]](#).
- [101] M. F. Sohnius, *Phys. Rept.* **128**, 39 (1985).
- [102] L. J. Dixon, J. A. Harvey, C. Vafa, and E. Witten, *Nucl. Phys. B* **261**, 678 (1985).

- [103] L. J. Dixon, J. A. Harvey, C. Vafa, and E. Witten, [Nucl. Phys. B \*\*274\*\*, 285 \(1986\)](#).
- [104] F. J. De Anda, S. F. King, E. Perdomo, and P. K. S. Vaudrevange, [JHEP \*\*12\*\*, 055 \(2019\)](#), [arXiv:1910.04175 \[hep-ph\]](#).
- [105] M. Fischer, M. Ratz, J. Torrado, and P. K. S. Vaudrevange, [JHEP \*\*01\*\*, 084 \(2013\)](#), [arXiv:1209.3906 \[hep-th\]](#).
- [106] S. Groot Nibbelink, O. Loukas, A. Mütter, E. Parr, and P. K. S. Vaudrevange, [Fortsch. Phys. \*\*68\*\*, 2000044 \(2020\)](#), [arXiv:1710.09237 \[hep-th\]](#).
- [107] S. Forste, H. P. Nilles, and A. Wingerter, [Phys. Rev. D \*\*72\*\*, 026001 \(2005\)](#), [arXiv:hep-th/0504117](#).
- [108] N. Marcus, A. Sagnotti, and W. Siegel, [Nucl. Phys. B \*\*224\*\*, 159 \(1983\)](#).
- [109] S. Weinberg, *The quantum theory of fields. Vol. 3: Supersymmetry* (Cambridge University Press, 2013).
- [110] M. Koca, [Phys. Rev. D \*\*24\*\*, 2645 \(1981\)](#).